Travel Choices under Pandemic Federalism

Daniel Kaffine* Lucas Ladenburger† Alessandro Peri‡

September 18, 2025

Abstract

We develop a quantitative theory to study disease dynamics and the welfare consequences of endogenous travel choices. Travel responds to and influences disease dynamics, serving as an infection avoidance strategy and a vector for pandemic transmission. We integrate a metapopulation SIRD epidemiological framework with an economic model to recover consistent travel choices. We analytically characterize the role of travel as an infection avoidance mechanism, distinct from and in addition to home isolation. We then quantify its relative importance during a pandemic. We show local pandemic policies lead to suboptimal Nash equilibrium outcomes and train surrogate models to assess parameter impacts.

Keywords: epi-econ metapopulation model, endogenous travel, pandemic federalism, travel bans, surrogate models.

JEL Classification: C6, C7, E6, H7, I1, Z3.

*Department of Economics, Renewable and Sustainable Energy Institute, University of Colorado Boulder, daniel.kaffine@colorado.edu.

†Department of Economics, University of Colorado Boulder, Lucas.Ladenburger@colorado.edu. Corresponding author.

‡Department of Economics, University of Colorado Boulder, alessandro.peri@colorado.edu.

1 Introduction

The interconnection of regions via travel is a crucial component in the emergence of pandemics. Dating back to the Plague of Justinian in the 6th Century, it is travel that ultimately puts the "pan" in pandemics. While travel constitutes a small fraction of a typical household's time and budget, its key role in disease spread makes it a primary policy concern. Household travel choices, responding to differences in infection rates, may lead to intermixing of populations and will likely influence the trajectory of a pandemic, especially in the presence of uncoordinated, unilateral, public policy interventions across different locales ("pandemic federalism").

In this paper, we develop a coupled epidemiological-economic (epi-econ) metapopulation model to examine how individuals' travel decisions interact with the spread of disease. Our quantitative theory comprises two heterogeneous populations connected through interregional travel. At its core, our framework integrates a standard SIRD epidemiological system, capturing individuals' transitions through disease states (Susceptible, Infectious, Recovered, Deceased), with an economic model, where the SIRD compositions of each population segment influence agents' decisions regarding travel, consumption, labor, and home isolation. Central to our approach is establishing the connection between epidemiological dynamics and economic behavior through the probability of disease transmission. These infection probabilities dictate the pandemic's course, shaping individual activity and travel decisions, which in turn affect transmission probabilities, creating a feedback loop. Our theoretical framework leads to sharp analytical results, which we use to cleanly calibrate parameters and interpret our quantitative findings.

We analytically characterize travel and home isolation choices during a pandemic. In our metapopulation model, susceptible individuals (those at risk of becoming sick) can either isolate at home or travel in response to disease progression in their region. We show travel can act as either an infection avoidance asset or liability, depending on whether traveling to a foreign region reduces or increases the likelihood of getting infected.[1] We further identify the conditions under which

[1]Residents choosing to travel specifically to avoid high infection rates and risk of death—and not for other reasons, such as work or leisure—has a long history, from the Black Death of Europe in the 16th and 17th Century ("...the poorer sort of people that have no friends nor place to flee

travel is preferred over home isolation as an avoidance strategy. In this context, we highlight key drivers, including activity-specific contact rates with infected individuals and the relative share of infectious in home and foreign populations. We also demonstrate that travel is preferred to home isolation when infection rates are low.

We calibrate our metapopulation model to the U.S. economy. In order to conduct positive and normative analysis for regions of different size, we focus on a two-region version of our model. This environment leads to a fast solution algorithm that allows us to explore over one million epidemiological-economic parameter configurations. Our quantitative analysis is conducted in two policy-relevant scenarios: (*i*) one with regions of similar size (symmetric), meant to capture travel across roughly similar-sized countries (e.g. Germany and France) or U.S. regions (e.g. 'blue' and 'red' states); and *(ii)* another where one region is significantly smaller than the other (asymmetric), intended to capture travel into a small country (e.g. Cayman Islands) or an individual U.S. county.

Our positive analysis focuses on the feedback loop between the economic and epidemiological modules. We first study how susceptible individuals respond to the evolution of the pandemic. In the symmetric case, susceptible individuals prefer travel to isolation at the onset and ending of a pandemic. Our theory shows that in these circumstances, isolation is less effective than travel due to both low infection rates and the high utility cost of foregone travel. In the asymmetric case, susceptibles in the small region use travel and susceptibles in the large region use isolation for avoidance throughout the pandemic. In both environments, the role of travel as infectious avoidance asset or liability evolves over time and is quantitatively driven by both relative contact rates and differential rates of exposure at home and abroad. Using regression analysis on PlaceIQ cellphone data and Coronavirus Resource Center data from the recent COVID-19 pandemic, we empirically validate our model's prediction that travel responds to relative infection rates between regions, but this effect is muted when infection rates are high. We then investigate how the disease dynamics are affected by these behavioral responses. To

unto..." - Bishop Hooper of Gloucester and Worcester) to the 1793 outbreak of yellow fever in the then-capital Philadelphia, which led the U.S. government and 20,000 citizens to leave the city. More recently, similar behavior was observed in Wuhan, New York, and other coronavirus outbreak epicenters.

isolate the connectivity role of travel, we compare a metapopulation model without travel against different specifications of the model incorporating exogenous and endogenous travel choices. Both exogenous and endogenous travel synchronizes peak infectious across regions. When regions are asymmetric, endogenous traveling behavior leads to a nearly threefold increase in peak infectious in the small region.

Our normative analysis of pandemic federalism reveals that the Nash game between local planners leads to the classic Prisoner's Dilemma outcome. Local policymakers' best responses are to impose the most stringent travel restrictions on incoming travelers (to mitigate the externality effect), while at the same time impose no restrictions on their own citizens' outgoing travel, such that they can take advantage of the avoidance and utility benefits of travel. With both policymakers following this strategy, the resulting equilibrium is very close to that under travel autarky (effectively a travel ban), leading to significant welfare losses relative to the optimal coordinated policy by a centralized authority.

The scope of our quantitative results are inherently constrained by the specific parameterization of our model. To cope with this challenge, we perform a comprehensive sensitivity analysis over one million combinations of structural parameters governing epidemiological and economic characteristics. Across the parameter space, we confirm travel to be an effective infection avoidance asset for low infection rates (that is, at the beginning and ending of the pandemic) and the Prisoner's Dilemma outcome to be a Nash equilibrium in 99% of economies. We find endogenous travel reduces peak infection rates, uncovering a more relevant role of endogenous travel for mitigating the heat of the pandemic than that indicated by our benchmark (COVID-19) calibration. Unlike our benchmark, we also find socially optimal policy to involve positive restrictions on travel for 32% of economies. These last findings caution against drawing general conclusions from a single parametrization.

Finally, we use Deep Neural Networks to estimate surrogate models of the unknown mapping from epidemiological-economic parameters to model outcomes. We identify the basic reproductive number, R_0, as the primary driver of: *(i)* disease dynamics, which, in turn, govern the effectiveness of travel as an avoidance mechanism; *(ii)* welfare losses associated with the Prisoner's Dilemma outcome. Travel is preferred more often to isolation for highly contagious diseases (R_0 greater than

6). For several prominent diseases with lower reproductive numbers, such as Ebola, H1N1, the seasonal flu, SARS, and COVID-19, we find the effectiveness of travel choices to be highly sensitive to the value of R_0, making early accurate estimates of transmissibility a primary priority for determining travel policies.

The rest of the paper is organized as follows: Section 2 summarizes the contribution of this work to the related literature, Section 3 describes the model and theoretical results, Section 4 lays out the calibration, Section 5 presents the quantitative results, Section 6 discusses the parameters space exploration, Section 7 empirically tests model predictions, and Section 8 concludes. Additional results are presented in the Online Appendix.

2 Contributions

The incorporation of behavioral considerations into epidemiological models (e.g. the classic SIR model of Kermack and McKendrick (1927)) has been an important advance in the literature in recent years. Building on influential groundwork by Kremer (1996) and Fenichel et al. (2011), the COVID-19 pandemic produced a flurry of coupled epidemiological-economic models (e.g. Eichenbaum, Rebelo, and Trabandt, 2021, Farboodi, Jarosch, and Shimer, 2021, Ash et al., 2022, Boppart et al., 2025). Although these models differ in their quantitative and qualitative features, a key component is that disease dynamics both influence and respond to the behavioral choices made by individuals. We contribute to this literature by endogenizing travel decisions between regions in a quantitative epi-econ metapopulation model.[2]

Our paper contributes in several ways to a recent strand of the literature which considers endogenous travel in multi-region metapopulation models (Antràs, Redding, and Rossi-Hansberg, 2023; Chen et al., 2024). First, we isolate the infectious avoidance role of travel vis-á-vis home isolation, a channel missing from both studies. We show analytically in a two-region metapopulation model that traveling is preferred to home isolation for infectious avoidance reasons when infection

[2]Metapopulation models with endogenous choices by economic agents have also been considered in natural resource contexts (e.g. Sanchirico and Wilen, 2001; Kaffine and Costello, 2011; Fabbri, Faggian, and Freni, 2024).

rates are low and home isolation is ineffective due to the high utility cost of foregone travel. By contrast, high infection rates reduce agents willingness to travel, a point we corroborate empirically using US data during the COVID-19 pandemic. Moreover, we show quantitatively that abstracting from home isolation can dramatically overestimate the reliance on travel for infectious avoidance purposes. Second, we study a Nash pandemic-federalism game among local planners, which implement uncoordinated, unilateral, public policy interventions to maximize welfare in their locales. This analysis introduces strategic policy-relevant considerations, which are missing in both Antràs, Redding, and Rossi-Hansberg (2023) and Chen et al. (2024). The resulting Nash equilibrium features asymmetric travel restrictions across regions with different size and yields prisoner dilemma outcomes, underscoring the value of stronger coordination across policy-makers during pandemics. Finally, we go beyond the COVID-19 calibration considered in previous work, and conduct an extensive sensitivity analysis to test the robustness of our quantitative findings over *one million* unique epidemiological-economic parameter combinations and using novel techniques discussed below.[3]

We contribute methodologically to the quantitative epi-econ literature by proposing surrogate models to explore the robustness of our results across the parameter space. Surrogate models combine sampling, fitting, and validation techniques to create a simplified representation of complex systems, like the epi-econ model at the heart of our analysis.[4] More precisely our work extends the regression approach in Iverson, Karp, and Peri (2022), by applying recent techniques developed in Chen, Didisheim, and Scheidegger (2023) to study how the relevance of travel for disease transmission and welfare costs varies with different policy- (and time-) invariant aspects of disease transmission and individual behavioral responses.

[3] As noted in Antràs, Redding, and Rossi-Hansberg (2023), the feedback between disease dynamics and agent choices increases the numerical complexity of the problem and makes it difficult to solve the model for many parameter variations. This will be true of this class of epi-econ models in general, such as Boppart et al. (2025), whose multi-generation, single-region epi-econ model conducts sensitivity analysis on a few selected parameter calibrations.

[4] From the seminal work by Box and Wilson (1951) surrogate models (also known as response surface models or metamodels) have been routinely used in chemistry (McBride and Sundmacher, 2019), physics (Tripathy and Bilionis, 2018), engineering (Alizadeh, Allen, and Mistree, 2020), econometrics (Bai and Perron, 2003), climate (Friedl et al., 2023) and finance (Scheidegger and Treccani, 2021, Chen, Didisheim, and Scheidegger, 2023).

Our framework provides theoretical support for empirical findings that people both avoid traveling to areas with high disease burdens (Fenichel, Kuminoff, and Chowell, 2013; Brinkman and Mangum, 2022; Ojo et al., 2023) and travel away from areas with high disease burdens (Gibbs et al., 2020; Coven, Gupta, and Yao, 2023). Travel is also linked to increases in cases in the receiving destination (Kraemer et al., 2020; Julliard, Shi, and Yuan, 2023; Boto-García, 2023). Given these travel responses and the potential for jurisdictional spillovers, our paper also contributes to the literature on policy responses to pandemics (Gersovitz and Hammer, 2004; Rowthorn, Laxminarayan, and Gilligan, 2009; Kraemer et al., 2020; Boppart et al., 2025), geographic implications (Bisin and Moro, 2022), and pandemic federalism (Graff Zivin and Sanders, 2020; Renne, Roussellet, and Schwenkler, 2020; Iverson and Barbier, 2021). Our findings on decentralized policymaking related to pandemic travel are consistent with the general literature on environmental federalism, whereby externalities between regions generally leads decentralized planning to be suboptimal (Eichner and Runkel, 2012; Fell and Kaffine, 2014), except in certain circumstances (Landry, 2021).

3 Model

Our epi-econ model is organized in three modules. The epidemiological module in Section 3.1 dictates the evolution of the aggregate disease states; this framework expands the canonical compartmental modeling structure to multiple regions (a metapopulation model). The economic module in Section 3.2 describes individuals' behavioral responses to the state of the pandemic; the economy consists of $\mathscr{I}$ distinct regions populated by atomistic agents who optimize over consumption, labor, travel, and isolation choices, and interact with one another both within and across regional boundaries. The infection probability module in Section 3.3 establishes the connection between the epidemiological and economic modules. Subsection 3.4 describes the equilibrium. Subsection 3.5 concludes by analytically characterizing the equilibrium.

3.1 Epidemiological Module

We use an SIRD metapopulation model to describe the evolution across regions and over time of the aggregate measure of individuals over the disease states: susceptible, infectious, recovered, and deceased, $\mathscr{T}_t = \{S_{i,t}, I_{i,t}, R_{i,t}, D_{i,t}\}_{i=1}^{\mathscr{I}}$ (also referred to as compartments). Interaction and transitions across compartments in our metapopulation model are governed by the following system of equations:

$$S_{i,t+1} = \left(1 - \mathscr{P}_i^{SI}(\mathscr{A}_t, \mathscr{T}_t) - P^{D^*}\right) S_{i,t} + \gamma\left(S_{i,t} + I_{i,t} + R_{i,t}\right), \tag{1}$$

$$I_{i,t+1} = \left(1 - P^{D^*} - P^R - P^D\right) I_{i,t} + \mathscr{P}_i^{SI}(\mathscr{A}_t, \mathscr{T}_t) S_{i,t}, \tag{2}$$

$$R_{i,t+1} = \left(1 - P^{D^*}\right) R_{i,t} + P^R I_{i,t}, \tag{3}$$

$$D_{i,t+1} = D_{i,t} + P^D I_{i,t} + P^{D^*}\left(S_{i,t} + I_{i,t} + R_{i,t}\right), \tag{4}$$

where S_i, I_i, R_i, D_i are the population in each disease state for region i, γ is the population growth rate, P^R is the probability of transition from infectious to recovered, P^D is the probability of transition from infectious to deceased, and P^{D^*} is the probability of death from all other outside causes.

The force of infection $\mathscr{P}_i^{SI}(\mathscr{A}_t, \mathscr{T}_t)$ denotes the endogenous share of susceptibles that become infectious. This function depends on the share of the population in each of the disease states, $\mathscr{T}_t$, and economic activities, $\mathscr{A}_t$ (regional aggregate consumption, labor, and travel flows in and out of regions).[5] The force of infection plays the key role of connecting the epidemiological module with the economic module discussed in the following section. Section 3.3 formalizes this link.

3.2 Economic Module

The economy consists of a continuum of agents of measure one who live in one of $\mathscr{I} = 2$ home and foreign regions with competitive firms that hire labor to produce a homogeneous consumption good. The population share of region i is given by

[5] In the classic SIR framework, new infections at time t are equal to $\beta I_t S_t$ where β is the average number of contacts multiplied by the probability of infection per contact. In our framework, $\mathscr{P}_i^{SI}(\mathscr{A}_t, \mathscr{T}_t)$ corresponds to βI_t while allowing the number of contacts and probability of infection to vary over the course of the pandemic due to choices.

λ_i for $i \in \{1,2\}$. Although individuals may temporarily travel from one region to another, citizens of region i remain so forever.

3.2.1 Individuals

Agents make choices over consumption, labor, travel, and isolation to maximize their lifetime utility. As in Antràs, Redding, and Rossi-Hansberg (2023) and Boppart et al. (2025), we abstract from saving and borrowing decisions, due to the short time horizon. The flow utility, $u_i(c,m)$, is an increasing and concave function of a numeraire consumption good, c, and the share of time spent traveling for leisure, m.[6] The utility satisfies the Inada conditions $\lim_{c\to 0} \partial u_i(c,m)/\partial c = \infty$, $\lim_{c\to\infty} \partial u_i(c,m)/\partial c = 0$, $\lim_{m\to 0} \partial u_i(c,m)/\partial m = \infty$, $\lim_{m\to\infty} \partial u_i(c,m)/\partial m = 0$. Additionally, we allow the utility to depend on region i to reflect different preferences for travel.[7]

Before the start of (and after the end of) the pandemic, an agent in region i solves:

$$
\begin{aligned}
U_{i,t}^{pre} = \max_{\{c_t^{pre}, l_t^{pre}, m_t^{pre}\}} & \; u_i(c_t^{pre}, m_t^{pre}) + \delta \left[(1 - P^{D^*}) U_{i,t+1}^{pre} + P^{D^*} U_{i,t+1}^{D} \right] \qquad (5) \\
\text{s.t.} \quad & c_t^{pre} = w_t \bar{l} l_t^{pre}, \\
& m_t^{pre} + l_t^{pre} = 1,
\end{aligned}
$$

where w_t is the wage rate, l_t^{pre} is the labor share choice, $\bar{l}$ is the time endowment, $U_{i,t+1}^{D}$ is the value function of being deceased in the next period, where the individual exogenous probability of dying for natural causes P^{D*} coincides with the share of individuals that die for natural causes in (1)-(4). We model the start of the pandemic ($t = 0$) as an unanticipated MIT shock. We assume the pandemic ends deterministically at $t = T$. Thus, $U_{i,t}^{pre} = \bar{U}_i^{pre}$ for all $t < 0$ and $t > T$.

During the pandemic, agents observe their *individual* disease states, $z \in \{S, I, R, D\}$,

[6] Travel for leisure accounts for around 80% of observed travel time in the American Travel Survey. Accordingly, we conceptualize and quantitatively discipline $u(c,\cdot)$ as capturing utility from leisure travel.

[7] To establish uniqueness of optimal travel choices, we further require q-complementarity between consumption and travel choices, $\partial^2 u_i(c,m)/\partial c \partial m \geq 0$. This assumption is satisfied by the utility function utilized in our quantitative analysis.

the aggregate distribution of individuals over regions and disease states $\mathscr{T}_t$, and aggregate economic activities, including inflows and outflows for traveling reasons, $\mathscr{A}_t$. Susceptible agents $z = S$ solve

$$
\begin{aligned}
U^S_{i,t} \equiv U^S_i(\mathscr{A}_t, \mathscr{T}_t) = \max_{\{c^S_t, l^S_t, m^S_t, h^S_t\}} & u_i(c^S_t, m^S_t) + \delta \Big[P^I_i(m^S_t, l^S_t, h^S_t; \mathscr{A}_t, \mathscr{T}_t) U^I_{i,t+1} \\
& + (1 - P^I_i(m^S_t, l^S_t, h^S_t; \mathscr{A}_t, \mathscr{T}_t) - P^{D^*}) U^S_{i,t+1} + P^{D^*} U^D_{i,t+1} \Big] \qquad (6) \\
\text{s.t.} \quad & c^S_t = w_t \bar{l} l^S_t, \\
& m^S_t + l^S_t + h^S_t = (1 - \theta_i), \\
& m^S_t \in [0, \min\{1 - \bar{m}^{in}_j, 1 - \bar{m}^{out}_i\}], \\
& h^S_t \in [0, \bar{h}],
\end{aligned}
$$

where h^S_t denotes their voluntary home isolation choice, θ_i imposes an exogenously determined limit on time spent on total economic activities involving contacts (e.g., zero-contact local social distancing restrictions) and $\bar{m}^{out}_i, \bar{m}^{in}_j$ are restrictions on outbound travel from region i and inbound travel to region j respectively. To account for essential workers, home isolation is bounded by $\bar{h}$, though it is not binding in equilibrium in our benchmark model (Section 5.1).

Crucially, in our model agents know their disease state and respond accordingly when making choices. Specifically, a key feature of our framework is that susceptibles internalize how their labor, l^S_t, travel, m^S_t, and home isolation choices, h^S_t, affect their probability of infection $P^I_i(m^S_t, l^S_t, h^S_t; \mathscr{A}_t, \mathscr{T}_t)$.[8] Note that during a pandemic, agents can also choose to isolate at home, in which case they can reduce the likelihood of getting infected, but do not receive any direct utility benefits. Section 3.3 describes the probability of infection $P^I_i(m^S_t, l^S_t, h^S_t; \mathscr{A}_t, \mathscr{T}_t)$ and its dependence on the alternative infection channels.[9]

[8] This is in contrast to the assumption in Farboodi, Jarosch, and Shimer (2021) and Antràs, Redding, and Rossi-Hansberg (2023), where agents are uncertain and probabilistically infer their type and make decisions based on *S, I, R* type shares in the population.

[9] Alternatively, one could complicate the model and assume that after exposure to the virus, susceptible agents transition to an "exposed" type. If these exposed agents are pre-symptomatic and do not realize they have become exposed, they would make the same choices as susceptible agents. Following an incubation period, exposed individuals will then develop symptoms and become infectious. As shown in Online Appendix F.1, the presence of exposed agents introduces delays in

Unlike susceptible agents, the decision of infectious and recovered individuals do not depend on the aggregate states, $\mathscr{T}_t$ and $\mathscr{A}_t$. Infectious individuals $z = I$ solve:

$$
\begin{aligned}
U^I_{i,t} = \max_{\{c^I_t, l^I_t, m^I_t, h^I_t\}} & u^I_i(c^I_t, m^I_t) + \delta \Big[(1 - P^R - P^D - P^{D^*}) U^I_{i,t+1} + P^R U^R_{i,t+1} \\
& + (P^D + P^{D^*}) U^D_{i,t+1} \Big] \qquad (7) \\
\text{s.t.} \quad & c^I_t = \phi w_t \bar{l} l^I_t, \\
& m^I_t + l^I_t + h^I_t = 1 - \theta_i, \\
& m^I_t \in [0, \min\{1 - \bar{m}^{in}_j, 1 - \bar{m}^{out}_i\}], \\
& h^I_t \in [0, \bar{h}],
\end{aligned}
$$

where ϕ is a productivity penalty associated with being sick. In addition, we allow for a different utility function for infectious $u^I_i(\cdot)$ to accommodate a reduced preference for travel while sick. Infectious individuals eventually transition to either recovered or deceased.

The recovered problem $z = R$ is

$$
\begin{aligned}
U^R_{i,t} = \max_{\{c^R_t, l^R_t, m^R_t, h^R_t\}} & u_i(c^R_t, m^R_t) + \delta \Big[(1 - P^{D^*}) U^R_{i,t+1} + P^{D^*} U^D_{i,t+1} \Big] \qquad (8) \\
\text{s.t.} \quad & c^R_t = w_t \bar{l} l^R_t, \\
& m^R_t + l^R_t + h^R_t = 1 - \theta_i, \\
& m^R_t \in [0, \min\{1 - \bar{m}^{in}_j, 1 - \bar{m}^{out}_i\}], \\
& h^R_t \in [0, \bar{h}].
\end{aligned}
$$

Infectious and recovered individuals take the transition probabilities as given. Furthermore, they do not internalize the externality associated with their choices and the effect on the infection probability $P^I_i(\cdot)$ in the susceptible problem in (6). Accordingly, the decisions that solve their dynamic problem are static.[10] Absent direct utility benefits from isolation, infectious and recovered individuals choose zero iso-

peak infectious due to disease-specific incubation periods that yield more realistic disease dynamics, but does not alter the fundamental insights of the analysis.

[10] The model does not feature general equilibrium price effects from the pandemic, implying that infectious and recovered choose a constant travel share.

lation, $h_t^I = h_t^R = 0$.

Those that die, either from the virus or other causes, receive a one time payoff of Ω_i, so that the value for the deceased is

$$U_{i,t}^D = \Omega_i. \tag{9}$$

3.2.2 Production

Individuals supply labor to perfectly competitive firms which use labor to produce an homogeneous consumption good (the numeraire) with a linear production technology $Y_t = AL_t$. We do not distinguish between the production technologies of different regions. Instead, we assume that the markets are sufficiently integrated such that all firms operate with identical technology and marginal products are equalized across regions.

3.3 Infection Probability Module

The epidemiological module describes the evolution of the aggregate disease states given the behavior of individuals, while the economic module captures the behavioral response of individuals to the aggregate disease state of the economy. Connecting these two modules is the force of infection $\mathscr{P}_i^{SI}(\mathscr{A}_t, \mathscr{T}_t)$ and the infection probability $P_i^I(m_t^S, l_t^S, h_t^S; \mathscr{A}_t, \mathscr{T}_t)$.[11] In equilibrium, the coupled modules' consistency requires that

$$\mathscr{P}_i^{SI}(\mathscr{A}_t, \mathscr{T}_t) = P_i^I(m_t^S(\mathscr{A}_t, \mathscr{T}_t), l_t^S(\mathscr{A}_t, \mathscr{T}_t), h_t^S(\mathscr{A}_t, \mathscr{T}_t); \mathscr{A}_t, \mathscr{T}_t). \tag{10}$$

The previous equation formalizes the handshake between the epidemiological and economic module, and determines the channel through which agents' behavioral responses affect the course of the pandemic and vice-versa. To connect economic activities with contacts and ultimately infection probabilities, we extend Ash et al. (2022) and Boppart et al. (2025)'s linear random meeting technology to multiple regions to account for travel activities and their corresponding contacts.

[11] Because all region i susceptible individuals are ex ante identical, all make the same choices, and the infection probability $P_i^I(m_t^S, l_t^S, h_t^S; \mathscr{A}_t, \mathscr{T}_t)$ is the same for all susceptible individuals in i.

The general formulation for the probability of infection given $\mathscr{C}$ contacts and the epidemiological probability τ that a contact with an infectious person leads to infection is

$$P(\text{infection}) = 1 - \left(1 - \tau \cdot \frac{I}{N}\right)^{\mathscr{C}}.$$ [12]

We extend this logic to a model with multiple regions and endogenous choices over activities. The probability that a susceptible is infected depends on the share of time the susceptible spend in each activity, the likelihood that a contact during that activity leads to infection, and the number of contacts during the activity,

$$P_i^I(m_t^S, l_t^S, h_t^S; \mathscr{A}_t, \mathscr{T}_t) \equiv 1 - \Bigg[\underbrace{\left(\frac{l_t^S}{1-\theta_i}\right)}_{\text{Work share}} \left(1 - \underbrace{\tau \cdot \frac{(I_{i,t} - M_{i,t}^I + M_{j,t}^I)}{N_{i,t}}}_{\text{Home Exposure}}\right)^{\mathscr{C}_{i,t}^l} \tag{11}$$

$$+ \underbrace{\left(\frac{m_t^S}{1-\theta_i}\right)}_{\text{Travel share}} \left(1 - \underbrace{\tau \cdot \frac{(I_{j,t} - M_{j,t}^I + M_{i,t}^I)}{N_{j,t}}}_{\text{Foreign Exposure}}\right)^{\mathscr{C}_{i,t}^m} + \underbrace{\left(\frac{h_t^S}{1-\theta_i}\right)}_{\text{Isolation share}} \left(1 - \underbrace{\tau \cdot \frac{(I_{i,t} - M_{i,t}^I + M_{j,t}^I)}{N_{i,t}}}_{\text{Home Exposure}}\right)^{\mathscr{C}_{i,t}^h} \Bigg].$$

The three infection channels isolate the probability of getting infected per contact while working, isolating, or traveling. Agents allocate their time endowment accounting for the fact that each activity (l_t^S, m_t^S, h_t^S) leads to a differential activity-and-region specific likelihood of not getting infected, denoted by the terms $(\cdot)^{\mathscr{C}^z}$, $z \in \{l, m, h\}$. Crucially agent takes the latter as given, introducing a key behavioral externality into the disease dynamics.

In a metapopulation model, the infectious population share in i depends on the infectious residents of i who leave and travel to the other regions, $M_{i,t}^I = I_{i,t} m_{i,t}^I$, as well as the infectious residents of other regions who travel to region i, $M_{j,t}^I = I_{j,t} m_{j,t}^I$ (recall in equilibrium infectious do not isolate). The total population engaged in

[12] Given n independent draws (contacts), the probability of getting infected is the probability of at least one success, $P(\text{at least one success}) = 1 - P(\text{failure})^n$. The probability that a contact does not lead to infection is $P(\text{failure}) = 1 - P(\text{infection from a contact}) = 1 - P(\text{Infectious Contact}) \cdot P(\text{contact with Infectious leads to infection})$. Thus, the probability that a contact is infectious, $P(\text{Infectious Contact})$, corresponds to the share of the relevant population that belongs to I, while the probability that a contact with an infectious person leads to infection is τ.

economic activities in region i at time t, $N_{i,t}$, includes the residents of i, less those traveling to the other region, plus residents of j traveling into i:

$$N_{i,t} = \sum_{Z \in \{S,I,R\}} Z_{i,t} - M^Z_{i,t} + M^Z_{j,t}, \tag{12}$$

where $M^Z_{i,t}$ are type Z travelers.[13]

The number of contacts an agent has depends on the activities they participate in. The contacts of an agent who chooses to work (and consume) are given by

$$\mathscr{C}^l_{i,t} = \underbrace{\rho^C w_t \bar{l}(1-\theta_i) C^*_{i,t}}_{\text{Consumption contacts}} + \underbrace{\rho^L \bar{l}(1-\theta_i) L^*_{i,t}}_{\text{Work contacts}} + \underbrace{\mathscr{C}^u}_{\text{Unavoidable contacts}}. \tag{13}$$

The unavoidable contacts can be thought of primarily as contacts occurring at home, but could also include things such as religious activities. Consumption contacts are determined by the dollar amount spent by the individual for consumption activities, $w_t \bar{l}(1-\theta_i)$, the average dollar value of consumption activities by others in region i, $C^*_{i,t}$, and the parameter ρ^C which converts individual and average consumption into contacts. Likewise, work contacts depend on the number of hours the individual works, $\bar{l}(1-\theta_i)$, the average number of hours others in region i work, $L^*_{i,t}$, and ρ^L which converts individual and average labor into contacts.[14]

The aggregate distribution of individuals over regions and disease states $\mathscr{T}_t$, as well as aggregate economic activities including travel, $\mathscr{A}_t$, together determine the average dollar value of consumption and average number of work hours in i. These

[13] In Online Appendix F.2, we consider an alternative specification for the infection probability where isolating agents are removed from the relevant local population. We show quantitatively that this leads to higher peak infectious, but otherwise similar dynamics.

[14] From the budget and time constraints in (6), if the agent chooses zero travel and isolation $m^S_{i,t} = h^S_{i,t} = 0$, then labor hours are $\bar{l}(1-\theta_i)$ and consumption is $w_t \bar{l}(1-\theta_i)$ as in (13).

quantities are given by

$$C^*_{i,t} \equiv C^*_i(\mathscr{A}_t, \mathscr{T}_t) = \sum_{Z\in\{S,I,R\}} \left(\underbrace{c^Z_{i,t} \frac{Z_{i,t} - M^Z_{i,t}}{N_{i,t}}}_{\text{Consumption by } i \text{ agents}} + \underbrace{\kappa \frac{M^Z_{j,t}}{N_{i,t}}}_{\text{Consumption by } j \text{ agents}} \right), \quad (14)$$

$$L^*_{i,t} \equiv L^*_i(\mathscr{A}_t, \mathscr{T}_t) = \sum_{Z\in\{S,I,R\}} \bar{l} \cdot l^Z_{i,t} \frac{Z_{i,t}}{S_{i,t} + I_{i,t} + R_{i,t}}. \quad (15)$$

$C^*_{i,t}$ is a weighted average of the consumption by those individuals the susceptible agent may encounter in region i (i.e. those in each disease state in i less those that are traveling or isolating) and consumption dollars spent by those traveling from j into i, where κ converts travel shares into dollars.[15] $L^*_{i,t}$ is the weighted average labor hours by agents in region i. We do not adjust $L^*_{i,t}$ for those traveling because this is already captured by the time share spent on work $l^Z_{i,t}$.

When traveling the agent has contacts from consumption activities in the foreign region as well as unavoidable contacts,

$$\mathscr{C}^m_{i,t} = \underbrace{\rho^M \bar{l}(1-\theta_i) C^*_{j,t}}_{\text{Travel contacts}} + \underbrace{\mathscr{C}^u}_{\text{Unavoidable contacts}}, \quad (16)$$

where $C^*_{j,t}$ is defined as in (14), and ρ^M converts the dollars-hours product into contacts. Finally, if the susceptible individual chooses to isolate, they have only the unavoidable contacts,

$$\mathscr{C}^h_{i,t} = \mathscr{C}^u. \quad (17)$$

Notice that the choices of individual agents affect the probability of infection both directly through the work, travel, and isolation activity shares in (11), and indirectly through the contacts associated with those activities (12) - (17). Because agents are atomistic, they take contacts $\mathscr{C}^l_{i,t}, \mathscr{C}^m_{i,t}$ and population shares $N_{i,t}$ as given when making their choices. Our solution algorithm in Online Appendix B recovers

[15] The parameter κ allows for the possibility that people spend more on consumption activities when traveling than at home.

the individual choices consistent with these aggregates.

3.4 Equilibrium

An equilibrium is defined as a set of individual agents' choices $(c^z_{i,t}, l^z_{i,t}, m^z_{i,t}, h^z_{i,t})$ and associated value functions $U^z_{i,t}$ for all regions i, time t, and agents disease state $z \in \{S, I, R, D\}$, an aggregate wage rate w_t, the time-varying regional disease states of the economy $\mathscr{T}_{i,t} = (S_{i,t}, I_{i,t}, R_{i,t}, D_{i,t})$, such that, in every period, t and region, i:

1. **Individual Choices:** Given the wage, aggregate disease states of the economy $\mathscr{T}_{i,t}$, agents' choices solve (6), (7), and (8);

2. **Firms' Zero-profit Condition:** Labor is paid its marginal product: $w_t = A$;

3. **Market Clearing:** Given the individual choices, aggregate disease states of the economy $\mathscr{T}_{i,t}$, aggregate labor supply equals labor demand:

$$\sum_i \left[l^S_{i,t} S_{i,t} + \phi l^I_{i,t} I_{i,t} + l^R_{i,t} R_{i,t} \right] = L_t$$

4. **Epidemiological Module:** The disease states $\mathscr{T}_t = \{S_{i,t}, I_{i,t}, R_{i,t}, D_{i,t}\}_{i=1}^{\mathscr{I}}$ follow the law of motion described by the system of equations in (1)-(4)

5. **Infection Probabilities' Module:** Given the wage, the individual choices, and the law of motion for the disease states, coupled models' consistency requires that equation (10) is satisfied in every period.

Online Appendix B describes the solution algorithm.

3.5 Equilibrium Characterization: Infection Avoidance and Arbitrage

What are the determinants of travel and isolation decisions during a pandemic? This section analytically characterizes the infection avoidance role of travel and the infection arbitrage opportunity provided by home isolation. To do so, we initially

shut down the home isolation channel in Proposition 1, and then later reintroduce it in Proposition 2 and 3. Online Appendix A contains all proofs.

In the pre-pandemic period, agents choose travel by comparing their marginal utility benefits and opportunity costs,

$$\frac{\partial u_i}{\partial m} = \frac{\partial u_i}{\partial c} w_t \bar{l}.$$

The pandemic introduces new considerations in the susceptible agents' travel decisions,

$$\underbrace{\frac{\partial u_i}{\partial m}}_{\text{Direct Benefit}} \underbrace{- \delta (U^S_{i,t+1} - U^I_{i,t+1}) \frac{\partial P^I_i}{\partial m}}_{\text{Pandemic Considerations}} = \underbrace{\frac{\partial u_i}{\partial c} w_t \bar{l}}_{\text{Opportunity Cost of Travel}} .$$

which account for the extent by which traveling to a region with different infectiousness levels affects their likelihood of becoming infected,

$$\frac{\partial P^I_i}{\partial m} \equiv \frac{1}{1-\theta_i} \left[\left(1 - \tau \cdot \underbrace{\frac{(I_{i,t} - M^I_{i,t} + M^I_{j,t})}{N_{i,t}}}_{\text{Home Exposure}} \right)^{\mathscr{C}^l_{i,t}} - \left(1 - \tau \cdot \underbrace{\frac{(I_{j,t} - M^I_{j,t} + M^I_{i,t})}{N_{j,t}}}_{\text{Foreign Exposure}} \right)^{\mathscr{C}^m_{i,t}} \right] \quad (18)$$

and the associated discounted payoff of moving from a susceptible to an infectious state in the next period, $\delta(U^S_{i,t+1} - U^I_{i,t+1})$. Crucially, pandemic considerations are absent among infectious and recovered agents, whose traveling decisions have no bearing on their continuation value.

We focus our analysis on the policy-relevant case where the pandemic is deadly or costly enough that agents do not want to *strategically* contract the virus, $U^S_{i,t} - U^I_{i,t} > 0$. Lemma 1 in Online Appendix A.1 shows that the following condition eliminates these *selfish incentives for herd immunity*, and implies $U^R_{i,t} > U^I_{i,t}$, $U^R_{i,t} \geq U^S_{i,t}$.[16]

[16] This condition is intuitively satisfied when the infectious state productivity loss is large enough (ϕ small) or the probability of death due to the virus, P^D is large enough.

Assumption 1. ***No selfish incentives for herd immunity.*** *For all m,t,*

$$\Big(u_i(c^R(m),m) - u_i^I(c^I(m),m)\Big) - \delta(1-P^D)(U_{i,t}^R - \Omega_i) \geq 0,$$

where $c^R(m) \equiv w_t\bar{l}(1-\theta_i-m)$ and $c^I(m) \equiv \phi w_t\bar{l}(1-\theta_i-m)$.

In the presence of endogenous travel choices, traveling acts not only as a pathway for the virus to spread, but also an insurance mechanism by which susceptible people may avoid infection. When the case rate is high (low) in their home region susceptibles have an additional incentive (disincentive) to travel. This mechanism is absent in models with exogenous travel choices. Proposition 1 formalizes the conditions under which travel provide an infection avoidance asset or liability.

Proposition 1. ***The Infection Avoidance Role of Travel.*** *Under Assumption 1 and absent home isolation, $h = 0$, endogenous travel choices provide susceptibles with:*

(a) ***an infection avoidance asset*** *if the likelihood of contracting the virus in the foreign region while traveling is lower than the likelihood of contracting the virus in the home region while working, $\frac{\partial P_i^I}{\partial m} < 0$. In this case, susceptible agents travel strictly more than if they were recovered. In the absence of direct benefits from travel, susceptible travel weakly more than if they were recovered.*[17]

(b) ***an infection avoidance liability*** *if the likelihood of contracting the virus in the foreign region while traveling is higher than the likelihood of contracting the virus in the home region while working, $\frac{\partial P_i^I}{\partial m} > 0$. In this case, susceptible agents travel less than if they were recovered. Absent direct benefits from travel, susceptible choose not to travel.*

Next, consider the case where susceptibles have access to an additional infection avoidance asset: isolation at home, $h^S > 0$. Home isolation yields lower contact rates than travel ($\mathscr{C}^h \leq \mathscr{C}^m$) but does not offer direct utility benefits. Crucially, the

[17] Distinct from Antràs, Redding, and Rossi-Hansberg (2023), in our metapopulation model, the avoidance role of travel emerges even in the absence of direct benefits from travel, which in their model arise due to gains from trade.

presence of both traveling and home isolation provide susceptibles with an infection avoidance arbitrage opportunity, which we formalize in Proposition 2.

Proposition 2. ***Avoidance Channels and Infection Arbitrage.*** ***(a)*** *Under Assumption 1, in the absence of utility benefits from travel, $u(c,m) = u(c)$, susceptibles will choose the infection avoidance asset (travel or home isolation) that yields the greater reduction in the likelihood of infection. Susceptibles weakly prefer travel if home isolation is less effective in reducing the exposure risk,*

$$\underbrace{\left(1 - \underbrace{\tau \cdot \frac{(I_{i,t} - M^I_{i,t} + M^I_{j,t})}{N_{i,t}}}_{\text{Home Exposure}}\right)^{\mathscr{C}^h_{i,t}} - \left(1 - \underbrace{\tau \cdot \frac{(I_{j,t} - M^I_{j,t} + M^I_{i,t})}{N_{j,t}}}_{\text{Foreign Exposure}}\right)^{\mathscr{C}^m_{i,t}} \leq 0.}_{\text{Effectiveness of home isolation in reducing infection exposure } (+/-)} \tag{19}$$

This is true when

$$\frac{\partial P^I_i}{\partial m} \leq \frac{\partial P^I_i}{\partial h} = \frac{1}{1-\theta_i} \underbrace{\left[\left(1 - \underbrace{\tau \cdot \frac{(I_{i,t} - M^I_{i,t} + M^I_{j,t})}{N_{i,t}}}_{\text{Home Exposure}}\right)^{\mathscr{C}^l_{i,t}} - \left(1 - \underbrace{\tau \cdot \frac{(I_{i,t} - M^I_{i,t} + M^I_{j,t})}{N_{i,t}}}_{\text{Home Exposure}}\right)^{\mathscr{C}^h_{i,t}}\right] \leq 0,}_{\text{Effectiveness of home isolation in reducing home-infection exposure } (-)}$$

which depends on the number of contacts associated with each activity given by equations (16) and (17), as well as the share of infectious in the home and foreign populations. Conversely, susceptibles weakly prefer home isolation if the previous inequality is flipped ($\geq$). ***(b)*** *Under Assumption 1, independent of whether agents receive direct utility from travel, susceptibles will not isolate ($h = 0$) if infection rates in the home region are sufficiently low that isolation's opportunity cost (in terms of consumption) is too high. Susceptibles will also not isolate and instead travel for avoidance purposes if these conditions hold: (i) travel is more effective than home isolation in reducing the likelihood of infection or home and foreign infection rates are sufficiently small; (ii) the marginal utility benefits of travel are sufficiently large, $\partial u/\partial m$; and (iii) travel is either an interior solution or the shadow value on its upper-bound constraint is not too large that isolating may become at-*

tractive.

Next, we use assumptions on the functional form of the utility function adopted in our quantitative analysis to provide closed-form solutions of traveling choices.

Proposition 3. ***Susceptible Travel Choices.*** *Let $u_i(c,m) = (1-\beta_i)\ln(c) + \beta_i \ln(m)$, then pre-pandemic agents, infectious and recovered types choose a region-specific constant share of time traveling*

$$m_{i,t}^{pre} = \beta_i, \qquad m_{i,t}^{I} = \beta_i^I(1-\theta_i), \qquad m_{i,t}^{R} = \beta_i(1-\theta_i). \tag{20}$$

Under Assumption 1, if susceptibles do not choose to isolate ($h=0$)—or absent isolation options—they travel more than recovered individuals when traveling reduces the likelihood of becoming infectious ($\partial P_{i,t}^I / \partial m_{i,t}^S < 0$) and less otherwise,[18]

$$\frac{m_{i,t}^S}{m_{i,t}^R} = 1 + \begin{cases} \underbrace{\frac{1-2\beta_i}{2\beta_i} + \frac{1}{2\beta_i\tilde{B}}\left(1+\sqrt{1+\tilde{B}(\tilde{B}+2(1-2\beta_i)}\right)}_{\geq 0}, & \frac{\partial P_{i,t}^I}{\partial m_{i,t}^S} < 0, \quad \textit{Inf. Avoid. Asset} \\ \underbrace{\frac{1-2\beta_i}{2\beta_i} + \frac{1}{2\beta_i\tilde{B}}\left(1-\sqrt{1+\tilde{B}(\tilde{B}+2(1-2\beta_i)}\right)}_{\leq 0}, & \frac{\partial P_{i,t}^I}{\partial m_{i,t}^S} > 0, \quad \textit{Inf. Avoid. Liability} \end{cases} \tag{21}$$

where $\tilde{B} \equiv (1-\theta_i)\delta(U_{i,t+1}^S - U_{i,t+1}^I)\partial P_{i,t}^I / \partial m$. If susceptibles isolate, $h>0$, this expression becomes

$$\frac{m_{i,t}^S}{m_{i,t}^R} = \frac{1}{\delta(U_{i,t+1}^S - U_{i,t+1}^I)\left[\underbrace{\left(1-\tau\cdot\frac{(I_{i,t}-M_{i,t}^I+M_{j,t}^I)}{N_{i,t}}\right)^{\mathscr{C}_{i,t}^h} - \left(1-\tau\cdot\frac{(I_{j,t}-M_{j,t}^I+M_{i,t}^I)}{N_{j,t}}\right)^{\mathscr{C}_{i,t}^m}}_{\textit{Effectiveness of home isolation in reducing infection exposure}(+,h>0)}\right]} \tag{22}$$

and susceptibles travel even less, relative to recovered individuals, when home isolation is increasingly effective at reducing the likelihood of becoming infected.

This section isolates the key considerations driving traveling choices during a pandemic, specifically, regional differences in relative contact rates and infectious population shares. Section 5 explores the quantitative relevance of these key trade-offs over the evolution of a pandemic.

[18] Susceptibles do not isolate, $h=0$, if $\hat{m}_{i,t}^S > \tilde{m}_{i,t}^S$ where $\hat{m}_{i,t}^S$ satisfies (21) and $\tilde{m}_{i,t}^S$ satisfies (22).

4 Model Calibration

We calibrate the model to match features of the U.S. economy (e.g. average share of time spent traveling) prior to the COVID-19 pandemic. We examine a two region version of the model, $i \in \{home, foreign\}$. A period in the model corresponds to one day and the pandemic lasts two years, $T = 730$, at which point a vaccine arrives and the pandemic ends with certainty.[19] Table 1 summarizes the parameter values used in our benchmark analysis.[20]

4.1 Preferences

We discipline the preferences of agents to capture pre-pandemic (long-run) traveling and consumption decisions. We follow Prescott (1986) and assume that agents have preferences

$$u_i(c,m) = \frac{\left(c^{1-\beta_i} \cdot m^{\beta_i}\right)^{1-\sigma} - 1}{1-\sigma} \qquad i \in \{home, foreign\}$$

over a composite good $c^{1-\beta_i} \cdot m^{\beta_i}$, where $\beta_i > 0$ is the travel share parameter, and $1/\sigma > 0$ is the elasticity of intertemporal substitution. As income and substitution effects tend to compensate each other in the long-run (e.g. Prescott, 1986, Kimball and Shapiro, 2008), we focus our quantitative analysis on the case where $\sigma \to 1$,

$$u_i(c,m) = (1-\beta_i)\ln(c) + \beta_i \ln(m) \qquad i \in \{home, foreign\}$$

The log-utility proves useful for two reasons. First, it provides unique closed-form solutions to the susceptible agent's problem, dispensing with the need for root-finding procedures and enhancing the interpretability of our quantitative re-

[19] In our exploration of the parameter space in Section 6, across over one million parameter combinations, the pandemic ends (infectious population less than one per million) after an average of 395 days.

[20] The values for pre-pandemic contacts during consumption $\mathscr{C}^{c^*}$ and travel $\mathscr{C}^{m^*}$, and the consumption and travel contacts conversion factors ρ^C, ρ^M, depend on the relative population of the home region (see Section 4.2). For these, Table 1 reports values for both symmetric ($\lambda_{home} = 0.5$) and asymmetric ($\lambda_{home} = 0.00001$) regions.

sults.[21] Second, it allows us to cleanly identify the travel preference parameters $\{\beta_{home}, \beta_{foreign}\}$ to match the pre-pandemic share of time residents travel. In particular, under this utility specification, agents display a constant share of time traveling, $m_{i,t}^{pre} = \beta_i$, with $i \in \{home, foreign\}$. We calculate these time shares with information from the Bureau of Transportation Statistics American Travel Survey (ATS). Using ATS, we calculate the share of time spent traveling from the average (across households) number of days spent on travel of at least 100 miles per year. Crucially, the prediction of a constant share of time traveling is consistent with recent evidence suggesting the absence of trends in traveling choices.[22]

Finally, to account for potential health effects of the disease on preferences for traveling activities, we allow infectious agents to receive different (lower) utility from travels, $\beta_i^I < \beta_i$. In particular, we choose β_i^I so that the time share spent traveling by infectious relative to that of recovered is adjusted by the share of infectious with severe symptoms, $m_i^I = (1 - \phi^{severe}) m_i^R$, where ϕ^{severe} is the share of infectious with severe symptoms.[23]

4.2 Contacts

We follow Ash et al. (2022) to calculate the parameters ρ^C, ρ^L, ρ^m which convert economic activities into contacts. Ash et al. (2022) use contact data from Prem, Cook, and Jit (2017) to calculate average daily contacts by activity. They separate contacts into those occurring during labor activities $\mathscr{C}^{l^*}$, contacts from home activities, which we assign to unavoidable contacts $\mathscr{C}^u$, and contacts from other activities, which we assign to consumption $\mathscr{C}^{c^*}$ and travel $\mathscr{C}^{m^*}$. We choose the

[21] This assumption eliminates the dependence of travel choices on exogenously fixed aspects of our economic environment, such as the opportunity costs of travel $(\phi, \bar{l})$ and the wage, which is set to A in equilibrium. Since our analysis abstracts from targeted labor market interventions (such as the Paycheck Protection Program in the U.S.) or the long-run effect of a pandemic on productivity, this assumption is not overly restrictive for our purposes.

[22] An annual survey from Expedia shows that travel behavior has remained relatively constant over time at ~ 11 (business) days per year. *Source:* Expedia - 2007, Expedia - 2024.

[23] Ash et al. (2022) calculate the share of infectious with severe symptoms ϕ^{severe} as a duration-weighted average of time spent in different states of infection severity, with major sufferers being those who become hospitalized weighted by their time spent symptomatic, giving a value of $\phi^{severe} = 0.1445$.

Table 1: Parameter Values

Parameter	Value	Description	Source
Epidemiological Parameters			
R_0	2.6	Initial reproduction number	Ash et al. (2022)
d	5.1	Duration of infectiousness	Ash et al. (2022)
μ	0.015	Case fatality rate	Ash et al. (2022)
$\mathscr{C}^{c^*}$	[3.984, 4.546]	Pre-pandemic contacts during consumption	Described in Section 4.2
$\mathscr{C}^{m^*}$	[1.183, 0.621]	Pre-pandemic contacts during travel	Described in Section 4.2
$\mathscr{C}^{l^*}$	7.513	Pre-pandemic contacts during labor	Prem, Cook, and Jit (2017)
$\mathscr{C}^{u}$	3.549	Unavoidable contacts	Prem, Cook, and Jit (2017)
τ	0.033	Infections per contact	Described in Section 4.3
P^R	0.193	Daily probability of recovery	$=(1/d)(1-\mu)$
P^D	0.003	Daily probability of death	$=(1/d)\mu$
P^{D^*}	3.6e-5	Daily probability of death (outside cause)	$=1/(76*365)$
γ	3.6e-5	Population growth rate	Set $\gamma = P^{D^*}$
Economic Parameters			
δ	$0.96^{1/365}$	Daily discount factor	Implied risk-free interest rate of $\sim$0.04
ϕ	0.8555	Share minor sufferers	Ash et al. (2022)
β_i	0.063	Travel share	Described in Section 4.1
β_i^I	0.054	Infectious travel share	Described in Section 4.1
$\bar{h}$	0.7	Share essential workers	Iverson, Karp, and Peri (2022)
κ	345.58	Daily travel cost	Described in Section 4.2
Ω_i	-33,420	Value for deceased	Described in Section 4.4
A	19.86	Technology	Implies pre-pandemic GDP per capita of $58,000
$\bar{l}$	8.54	Time endowment	Implies pre-pandemic individual labor supply = 8 hours
λ_{home}	[1e-5, 0.5]	Home population share	Set externally
ρ^C	[1.6e-4, 1.7e-4]	Consumption contacts conversion factor	Described in Section 4.2
ρ^M	[0.006, 0.007]	Travel contacts conversion factor	Described in Section 4.2
ρ^L	0.117	Labor contacts conversion factor	Described in Section 4.2

Note: For parameters in brackets, the first value corresponds to the case with asymmetric regions, and the second to symmetric regions.

contact parameters ρ^C, ρ^L, ρ^m so that average pre-pandemic contacts match these values,

$$\sum_i \lambda_i \rho^L \bar{l} l_i^{pre} L_i^{pre^*} = \mathscr{C}^{l^*},$$
$$\sum_i \lambda_i \left(\rho^C c_i^{pre} C_i^{pre^*} + \rho^M \bar{l} m_i^{pre} C_j^{pre^*} \right) = \mathscr{C}^{c^*} + \mathscr{C}^{m^*},$$

where λ_i are regional population shares and

$$C_i^{pre^*} = c_i^{pre} \frac{\lambda_i (1 - m_i^{pre})}{\lambda_i (1 - m_i^{pre}) + \lambda_j m_j^{pre}} + \kappa \frac{\lambda_j m_j^{pre}}{\lambda_i (1 - m_i^{pre}) + \lambda_j m_j^{pre}},$$
$$L_i^{pre^*} = \bar{l} l_i^{pre},$$

are the pre-pandemic average consumption and labor activities in region i.[24] We calculate the parameter κ, which converts time spent on travel into dollars using data from Business Travel News (BTN) and the Federal Highway Administration Next-Generation National Household Travel Survey (NHTS). We weight the total daily cost for travel to a given city in the BTN data by the annual total trips to the city in the NHTS data to arrive at an average daily cost of travel.

4.3 Transmissibility of the Virus

We calculate the transmissibility of the virus τ by backing it out from the formula for the reproductive number R_0. R_0 denotes the expected number of new cases caused by a single case in a population of entirely susceptibles. R_0 is given by

$$R_0 = \tau \mathscr{C}^* d,$$

where $\tau \in [0,1]$ is infections per contact, $\mathscr{C}^*$ is the number of contacts between the infectious person and susceptibles per day, and d is the number of days a person is infectious. For our two region model, we calculate contacts $\mathscr{C}^*$ as a weighted

[24] We compute the model-implied values for $\mathscr{C}^{c^*}$ and $\mathscr{C}^{m^*}$ individually as $\mathscr{C}^{c^*} = \sum_i \lambda_i \rho^C c_i^{pre} C_i^{pre^*}$ and $\mathscr{C}^{m^*} = \sum_i \lambda_i \rho^M \bar{l} m_i^{pre} C_j^{pre^*}$. These values are reported in Table 1.

average of contacts across regions,

$$\mathscr{C}^* = \sum_{i \in \{home, foreign\}} \lambda_i \left(\rho^C c_i^I C_i^{pre^*} + \rho^L l_i^I \bar{l} L_i^{pre^*} + \rho^M m_i^I \bar{l} C_j^{pre^*} + \mathscr{C}^u \right), \tag{23}$$

with $j \neq i$.[25] Given epidemiological estimates of R_0 and d we can compute the transmissibility τ implied by $R_0 = \tau \mathscr{C}^* d$.

4.4 Value of Being Deceased

We calibrate the value of deceased Ω_i to be consistent with a value of a statistical life (VSL) of \$10 million.[26] The VSL provides a measure of how much consumption individuals are willing to give up in order to reduce the likelihood of death. That is, for a marginal increase in the probability of dying of ΔP^{D^*}, agents require $VSL \cdot \Delta P^{D^*}$ additional wealth. Alternatively, for a marginal increase in wealth of Δa, individuals will accept an increase in the probability of death of $\Delta a / VSL$. Thus, we can find the implied Ω_i from the following equality:

$$U_{i,t}^{pre} = U_{i,t}^{VSL},$$

where $U_{i,t}^{pre}$ is pre-pandemic value given in (5), and $U_{i,t}^{VSL}$ is given by the solution to

$$U_{i,t}^{VSL} = \max_{\{c_t^{VSL}, l_t^{VSL}, m_t^{VSL}\}} \{u(c_t^{VSL}, m_t^{VSL}) + \delta((1 - P^{D^*} - \frac{\Delta a}{VSL}) U_{i,t+1}^{pre} + (P^{D^*} + \frac{\Delta a}{VSL}) U_{i,t+1}^{D})\},$$
$$\text{s.t. } c_t^{VSL} = w_t \bar{l} l_t^{VSL} + \Delta a, \qquad m_t^{VSL} + l_t^{VSL} = 1.$$

[25] When travel between regions is not permitted, $m_i^I = 0$, $c_i^I = \phi w \bar{l}$, $C_i^{pre^*} = w\bar{l}$, and $L_i^{pre^*} = \bar{l}$, which implies $\mathscr{C}^* = \sum_i \lambda_i \left(\rho^C \phi (w\bar{l})^2 + \rho^L \bar{l}^2 + \mathscr{C}^u \right)$, analogous to the single region contact model in Ash et al. (2022).

[26] Setting the value associated with death $\Omega_i = 0$, as is sometimes done in the literature, can lead to unintended individual behavior. As an illustrative example, take the case of CRRA preferences $u(c) = c^{1-\sigma}/(1-\sigma)$. For $\sigma > 1$, discounted lifetime utility is less than 0 implying death would *raise* lifetime utility, contrary to how we typically think people view dying. We follow Ash et al. (2022) in setting a positive disutility term associated with death. Equivalently, one could add a positive utility term to being alive as in Boppart et al. (2025) and calibrate accordingly.

In the pre-pandemic steady state, $U_{i,t}^{VSL} = \bar{U}_i^{VSL}$. To numerically implement this, we set the marginal increase in wealth Δa to be equivalent to a 10% increase in daily wage, $\Delta a = 0.1\bar{l}w$.

4.5 Initial Conditions of the Pandemic

The model requires an initial infectious seed to start the pandemic. Unless otherwise specified, we set the population of infectious at time zero to $I_{0,i} = 0.0001\%$ in both regions $i = \{H, F\}$.

5 Quantitative Analysis

This section examines the quantitative relevance of travel choices and disease containment strategies in the context of pandemic federalism. Section 5.1 studies the determinants of endogenous travel and isolation choices, while Section 5.2 analyzes the effect of behavioral responses on disease dynamics, both in a laissez-faire environment—in which travel restrictions $\bar{m}_i^{out}, \bar{m}_j^{in}$ and social distancing restrictions θ_i are set to zero. Section 5.3 examines pandemic federalism, the role of travel restrictions, and endogenous policy under a non-cooperative (Nash) game between two local policymakers. Additional results are provided in Online Appendix C.

5.1 Endogenous Travel and Isolation Choices

When is travel an asset or a liability for infection avoidance purposes? When do agents prefer travel to isolation? How do these incentives change over the evolution of a pandemic? We build on the theoretical results in Section 3.5 to explore these quantitative questions. We examine two economies, one where regions are identical in every aspect (symmetric economy), and another where the home-region is relatively small (asymmetric economy). The symmetric case is most relevant when considering policies and travel across roughly similar-sized countries (e.g. Germany and France) or U.S. regions (e.g. 'blue' and 'red' states). The asymmetric case is most relevant when we consider travel among very heterogeneous countries (e.g. U.S. and Cayman Islands) or U.S. regions (e.g. travel into a small U.S.

county) with different potentials to shape the course of the pandemic, to which we will return in Section 5.3.

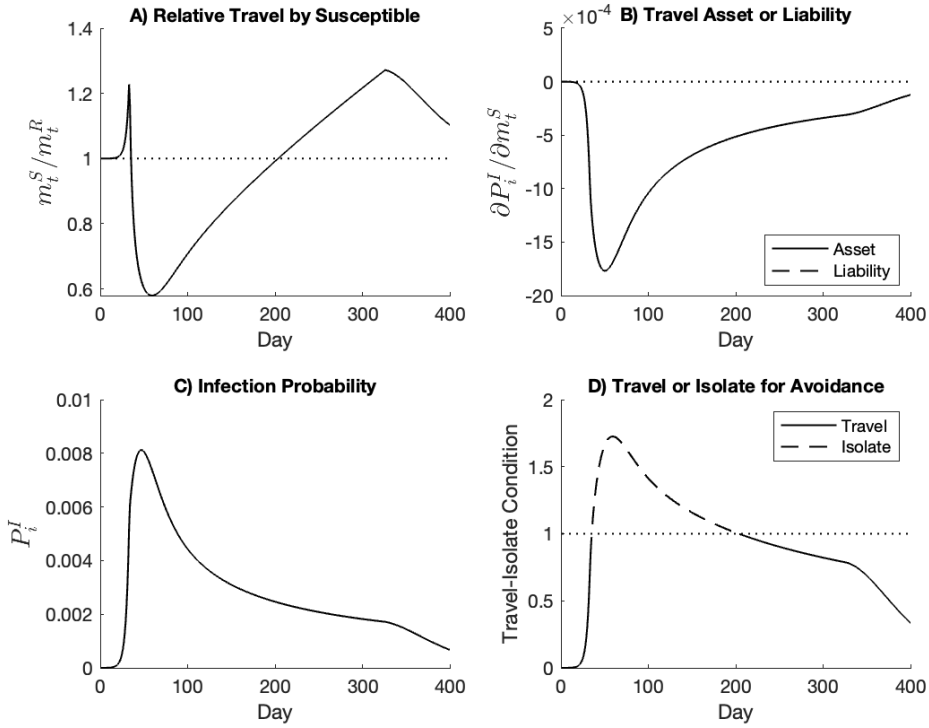

Figure 1: Determinants of travel choice with symmetric regions.

We begin by analyzing the endogenous travel decisions of susceptibles within a symmetric economy, illustrated in Figure 1. In this environment, home- and foreign- infection exposures are identical along the equilibrium path (Panel C), accordingly it may seem surprising to observe travel for avoidance purposes (Panel A). However, in this environment, the relative contact rates across activities are the key determinants of travel and isolation choices. Panel B shows that contact rates of traveling are lower than working, $\partial P_{i,t}^I/\partial m_{i,t}^S < 0$; therefore, even when infection rates are identical across regions, travel is an infection avoidance asset over the course of the entire pandemic (Proposition 1). Nonetheless, the relative effectiveness of travel and home isolation as infectious avoidance channels varies over the evolution of the pandemic.

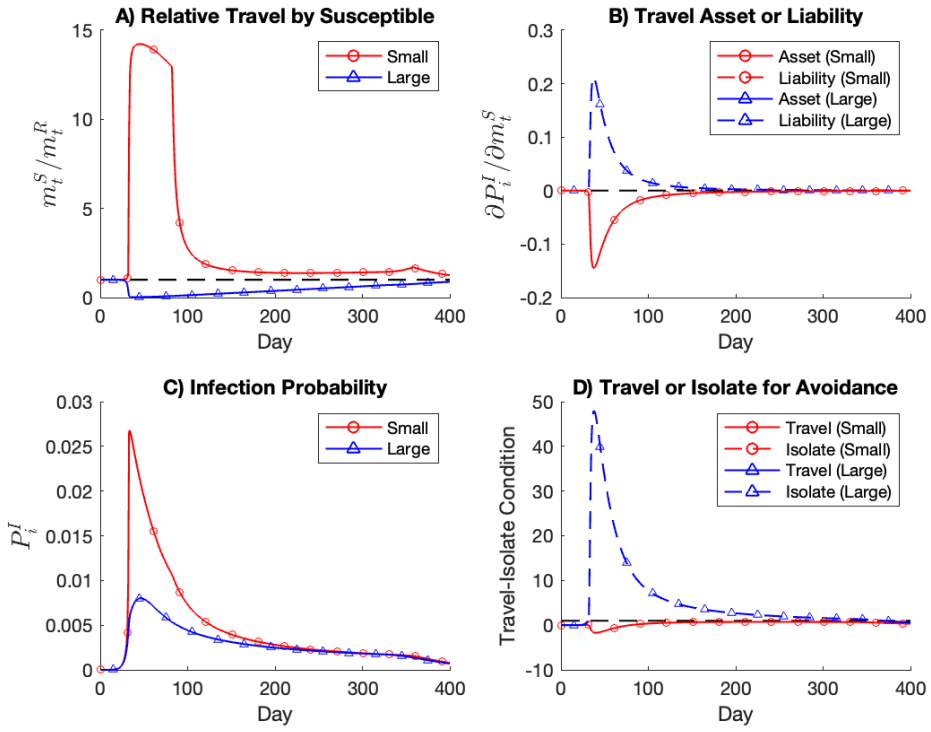

Figure 2: Determinants of travel choice with asymmetric regions.

Proposition 2 states that when the likelihood of infection in the home region is low, isolation is not an effective avoidance tool. Consistent with this insight, Panel D shows that at the beginning and end of the pandemic, agents do not isolate, and prefer to travel for infectious avoidance purposes.[27] Finally, Panel A shows that susceptible agents travel more than recovered agents when traveling is a more effective infectious avoidance mechanism than isolation (Proposition 3), which is particularly true when infection rates are low (Proposition 2), at the beginning and ending of the pandemic.[28]

Next, in Figure 2 we study the travel and isolation choices of susceptibles when

[27]The travel-isolate condition corresponds to the reciprocal of (22). When this quantity is smaller than one and $\partial P_{i,t}^I/\partial m_{i,t}^S < 0$, travel is an effective asset and susceptible agents increase travel relative to recovered.

[28]The sharp spike in travel as the initial infectious share rises is consistent with observed outflows of people from early hot spots such as Wuhan (Kraemer et al., 2020) and New York City (Coven, Gupta, and Yao, 2023) during the COVID-19 pandemic.

the home and foreign regions are asymmetric in population shares (home is small, foreign is large).[29] The role of travel as an asset or liability depends on whether the agent resides in the small or the large region. In particular, and in contrast to the symmetric case, travel becomes a liability ($\partial P^I_{i,t}/\partial m^S_{i,t} > 0$) for the agents in the large region when infection rates are high, shown in Panel B . Hence Panel A shows agents reduce their travel relative to the recovered (Proposition 1) beginning in the peak infection period and continuing throughout the pandemic. On the other hand, travel is an asset for agents in the small region even during the peak. Furthermore, travel remains an *effective* asset (Proposition 3), as shown in Panel D, such that susceptibles in the small region favor travel over isolation for avoidance over the entirety of the pandemic, unlike the symmetric case where agents switch to isolation during the peak. However, despite travel being a relatively more attractive avoidance mechanism than isolation, susceptibles in the small region are unable to meaningfully reduce their infection probability, as the evolution of the pandemic in *both* regions is driven by the behavior of agents in the large region. This illustrates one of our main quantitative results: As the relative size between the two economies increases, the effectiveness of travel as an avoidance mechanism (for susceptibles in both regions) drops.[30]

To sum up, in the symmetric environment, susceptibles prefer travel to isolation as an infectious avoidance tool for a significant (77%) portion of a two-year pandemic, especially at the beginning and the end, when isolation is very costly relative to the benefits due to low infection rates. By contrast, in the asymmetric environment, agents in the small region use travel and those in the large region use isolation for avoidance throughout the pandemic. Notably, the role of travel as an infection avoidance asset or liability evolves over time and is driven by both relative

[29] We set the home population share to 0.001% to illustrate a small nation facing travelers from the rest of the world.

[30] For completeness, Online Appendix C.1 replicates this analysis under the assumption that susceptibles do not receive utility benefits from travel. Here, susceptibles travel only if the foreign-exposure is lower than the home-exposure (Proposition 1). Accordingly, in the absence of any asymmetry between regions, agents do not travel. Additionally, Online Appendix C.2.2 illustrates susceptibles' travel response and disease dynamics under the assumption that agents cannot isolate at home. Therein, we show that absent home isolation options, susceptible agents' overrely on travel for infectious avoidance purposes when travel is an infection avoidance asset.

contact rates and the differential of exposure at home and abroad. Finally, travel for avoidance becomes less relevant as the size disparity between regions grows.

5.2 Disease Dynamics and Behavioral Responses

How do behavioral responses affect the disease dynamics in a metapopulation framework? In our metapopulation model, travel works as a pathway for the virus to spread. Here, we show how exogenous and endogenous travel choices affect these disease dynamics, accounting for the fact susceptibles can also isolate. Numerical results for all model comparisons are reported in Table 2.

Table 2: Peak Infectious and Days Between Peaks Across Different Model Specifications

	Peak Infectious - Home (%)		Days Between Peaks	
	$I_{0,H} = I_{0,F}$	$I_{0,H} < I_{0,F}$	$I_{0,H} = I_{0,F}$	$I_{0,H} < I_{0,F}$
Autarky				
No Behavioral Response	26.52	26.52	0	24
Home Isolation	**3.51**	3.51	0	**24**
Symmetric Size				
Exogenous Travel	3.68	3.71	0	**2**
Endogenous Travel	3.58	3.56	0	**5**
Asymmetric Size				
Exogenous Travel	**4.17**	4.18	2	**2**
Endogenous Travel	**9.44**	9.48	9	**9**

Note: No Behavioral Response model has no travel or endogenous avoidance. Home Isolation has no travel, but allows positive home isolation. Exogenous Travel enforces travel at the pre-pandemic rate, with endogenous home isolation response. Endogenous Travel allows both travel and home isolation choices to respond endogenously. The table reports the peak home infectious as percent of the home population and the number of days between the home and foreign peaks. Outcomes are shown for the case with home and foreign infectious seeds set to 0.0001% ($I_{0,H} = I_{0,F}$) and for the home seed set to 0.0001% and the foreign seed set to 0.1% ($I_{0,H} < I_{0,F}$).

To assess the role of home isolation, we first contrast an economy where agents cannot travel and isolate (first row),[31] with one where agents cannot travel but are

[31]The model with no isolation and traveling coincides with an SIRD model where the share of

able to isolate (second row).[32] Home isolation is an effective avoidance strategy, reducing peak infectious from more than 25% down to 3.51%, close to that under our baseline symmetric economy (3.58%).

Next, to understand the connectivity role of travel, we contrast the home isolation autarky model with four alternative specifications: models with either symmetric or asymmetric region sizes under exogenous or endogenous travel choices (the models with endogenous choices coincide with those presented in Section 5.1).[33] Under exogenous travel, the share of time spent traveling during the pandemic is set to its pre-pandemic period level, $m^{pre} = m^R = m^I = m^S$. This specification isolates the role of travel as a vector of pandemic transmission, by abstracting from endogenous pandemic considerations of susceptibles.

Travel synchronizes disease dynamics across regions relative to home isolation autarky, reducing the time between peak infections by three weeks under exogenous travel, and slightly less (two weeks) under endogenous travel, independently of relative region size. Accordingly, modeling travel as exogenous performs reasonably well in capturing its impact on the synchronization of disease dynamics under our benchmark calibration, a point we will revisit in our robustness analysis.

Although relative regional sizes do not affect the synchronicity of disease dynamics, they do affect the severity of the pandemic. When regions are symmetric in size, travel has little to no impact on the height of peak infectious relative to the home isolation autarky. In contrast, when regions are asymmetric, travel exacerbates the severity of the pandemic in the small region, particularly under endogenous travel, where peak infectious experience a *threefold* increase relative to home isolation autarky. This is due to the fact that, in the asymmetric case, the disease dynamics in the small region are dominated by those in the large region.

susceptibles becoming infected, $\mathscr{P}_i^{SI}(\mathscr{A}_t, \mathscr{T}_t)$ is consistent with the probability of getting infected implied by agents spending their entire time working in order to consume (equation (10)).

[32] The no behavioral response and home isolation autarky outcomes are reported for the case of symmetric regions. When regions are asymmetric, these outcomes change due to the updated transmissibility parameter τ (Section 4.3), though the differences are not economically significant. We report additional results in Online Appendix C.2.1.

[33] We assume under travel autarky that agents do not receive utility benefits from travel, $\beta_i = 0$. For comparison purposes, we also assume that agents do not receive utility from travel under exogenous travel.

While the time to peak infectious in the large region shifts minimally (by only 2 days) compared to autarky, inflows of infectious from the large region induce an earlier peak in the small region, occurring 24 (33) days earlier under exogenous (endogenous) travel. Notably, these dynamics reverse the effect of a reduction in the infectious seed of the small region that occurs under home isolation autarky, accelerating rather than delaying the peak of the pandemic in the small region (Appendix Figure 7). Taken together, these results indicate potential benefits for small regions to restrict incoming travel (such as, smaller and delayed onset of peak infectious), to which we turn in the next subsection.

To sum up: travel matters. When regions are similar in size, such as 'blue' and 'red' U.S. states, travel synchronizes peaks across regions. When regions differ in size, endogenous travel leads to severe outcomes for the small region (US county or small country), for which disease dynamics are dictated by the large travel inflows from the rest of the world. Clearly, these analyses hinge on initial assumptions over many important drivers of disease dynamics in a metapopulation model (e.g the reproductive number). Our parameter space exploration in Section 6, will check the robustness of these results across the parameter space.

5.3 Public Policy under Pandemic Federalism

What are the welfare consequences of travel bans and social distancing? In a pandemic federalism setting, local policies not only affect the strategic decisions of policymakers in other regions, but they are also influenced by them. We analyze the Nash equilibrium in a game between policymakers in the home and foreign regions who choose a fixed public intervention to begin at time $t \geq 1$. Given the relevance to our research question and space constraints, we focus our discussion on travel restrictions, a widely adopted yet less understood public intervention policy. Additional results on the Nash equilibria for social distancing policies, as well as outcomes under exogenous policy, are provided in Online Appendix C.3.

Consider a local policymaker who chooses fixed incoming and outgoing travel

restrictions $x_i \equiv \{\bar{m}_i^{in}, \bar{m}_i^{out}\}$ to maximize the welfare in its own region i

$$\max_{x_i \in [0,1)\times[0,1)} \sum_{Z_{i,1} \in \{S_{i,1}, I_{i,1}, R_{i,1}, D_{i,1}\}} \frac{Z_{i,1}}{\lambda_i} U_{i,1}^{Z}(x_i, x_j)$$

taking as given the other planner's policies, $x_j \equiv \{\bar{m}_j^{in}, \bar{m}_j^{out}\}$, and subject to the agents' optimization problems (6)-(9) and the transition equations (1)-(4).

Note that the region i policymaker can choose both a policy that restricts their own population $\bar{m}_i^{out}$, as well as one which restricts the j population $\bar{m}_i^{in}$. We restrict the feasible set of policies to 25%, 50%, 75%, or 99% reductions relative to pre-pandemic travel, or the planner can impose no restriction.[34] Online Appendix C.3.4 provides additional details about the local policymaker's problem.

Table 3: Nash Outcomes under Alternative Travel Policies

	Peak Infectious (%)		Welfare	
	Fixed	Infections-Guided	Fixed	Infections-Guided
Symmetric	3.58	[3.43, 3.58]	-23.30	[-23.30, -3.34]
Asymmetric Small	4.21	[4.08, 4.21]	-4.84	[-4.84, 4.85]
Asymmetric Large	3.52	[3.45, 3.52]	-21.30	[-21.30, -5.35]

Note: Peak Infectious is a percent of the region population. Welfare is the percent change from the economy with no travel restrictions. Under a Fixed policy rule, the Nash equilibrium outcome is unique for both symmetric and asymmetric regions. Under an Infections-Guided rule, there are multiple Nash equilibrium outcomes that fall within the range reported in brackets.

As in the previous sections, we study the Nash equilibria of the travel restric-

[34] We prefer a 99% over a 100% reduction due to the log-utility specification, which implies welfare is not defined in an economy with no travel. This assumption is also reasonable, as some leakage between regions is likely to occur when travel is fully banned. Also note that we implicitly assume full commitment on travel restrictions across time from policymakers, which is restrictive but reasonable given the relatively short-horizon of pandemics and the COVID-19 pandemic experience.

tions game for symmetric and asymmetric regions.[35] Table 3 summarizes the Nash equilibrium outcomes in each environment, considering both a benchmark where the travel bans are fixed in place for the entire pandemic and the case for which bans only become active when the infectious population share passes a threshold.

For both symmetric and asymmetric regions, there is a unique Nash equilibrium outcome under the fixed benchmark timing, where policymakers impose a 99% reduction in travel for both regions. It is always the best response of local policymakers to shut down incoming travel, leading to dynamics similar to those under the home isolation autarky specification presented in Section 5.2.

In the symmetric case, welfare losses relative to the benchmark with no travel restrictions are large, with a -23.30% change in welfare. These losses accrue due to both the direct loss in utility (agents like to travel) as well as the inability to utilize travel for avoidance (Proposition 1). Further, the symmetric environment implies both regions see identical welfare losses, and both could improve welfare by coordinating to achieve the no-restriction benchmark, similar to the textbook Prisoner's Dilemma.

Turning to the case where regions are asymmetric in size, the Nash equilibrium outcome once again leads to a Prisoner's Dilemma. However, unlike the symmetric case, welfare losses are not shared equally between the two regions. While the large region sees welfare losses similar to that under symmetric economies, the small region experiences much smaller losses. In the small region, Nash travel restrictions still reduce the utility benefits of traveling, but this loss is partially offset by beneficial reductions in peak infectious, down to 4.21% from 9.44% under the model with no travel restrictions (Table 2).[36]

We next study how the timing of policy interventions affect welfare outcomes in the Nash game. To do so, we allow for a policy decision rule under which travel bans are in place when the global infectious population share is above a threshold value ("Infections-Guided"). Each policymaker commits to both travel restric-

[35] Initial conditions for the two regions are identical for all results presented in this section. In Online Appendix C.3.4, we show results are similar when the foreign region begins with a higher infectious share than the home region.

[36] In Online Appendix C.3.3, we exogenously vary policies to identify those that maximize aggregate welfare.

tions (inbound and outbound) and the threshold at which restrictions become active, choosing a triple $x_i = \{\bar{m}_i^{in}, \bar{m}_i^{out}, I_i^{\text{thresh.}}\}$.[37] This enables policymakers to choose strategies for which travel restrictions do not bind during the beginning and end of the pandemic, when travel is most effective (Section 5.1).

When policymakers use infections to guide the imposition of travel bans, welfare losses are significantly reduced compared to those under a fixed policy rule. For symmetric economies, the equilibrium which maximizes welfare sees policymakers wait to enforce bans until the pandemic is well underway–each chooses a threshold value of 1%–leading to a 20 percentage point improvement in welfare from the fixed policy Nash equilibrium. Likewise for asymmetric regions, delayed policy can improve welfare in both regions. In fact, the small region can see welfare gains (relative to the case without policy restrictions) up to 4.85%. This is despite the equilibrium thresholds for asymmetric regions being quite low: in the welfare-maximizing equilibrium, travel bans are in place in the small region when the infectious population share is above 0.25% and in the large region at 0.5%.

We note that allowing policymakers to choose when to impose travel bans may still result in undesirable Nash equilibria. For symmetric and asymmetric regions, the 'worst' (aggregate welfare-minimizing) Nash equilibrium features full travel restrictions in place for the entire pandemic, equivalent to the fixed-policy economies.[38] Thus, coordination mechanisms would be needed to allow policymakers to achieve the welfare-maximizing Nash equilibrium. We leave the study of such mechanisms for future work.

In summary, local policy under pandemic federalism can lead to a suboptimal prisoners' dilemma for which all travel is banned. When regions are symmetric, fixed policy leads to large welfare losses relative to no restrictions. The effect is similar when regions are asymmetric in size and the disease dynamics are dominated by the large region. However, it is muted for the small region, which experiences a meaningful drop in peak infectious as a result of travel restrictions. In both cases, welfare can be improved by enforcing travel bans only when infection rates

[37] Policymakers choose a threshold from the set $I^{\text{thresh.}} \in X^{\text{thresh.}} \equiv \{0\%, 0.25\%, 0.5\%, ..., 3\%\}$.

[38] For context, Online Appendix Table 7 shows that while travel restrictions are never global welfare-maximizing when regions are symmetric, modest fixed or Infections-Guided restrictions can be globally optimal when regions are asymmetric.

are high. In Section 6, we use the surrogate model to study an intermediate case, where regions are asymmetric, but the small region is not so small that it is unable to influence aggregate dynamics.

6 Robustness

Is the quantitative relevance of travel choices a feature of our specific calibration to the COVID-19 pandemic or does it extend to alternative diseases? What are the key parameters driving the direction and magnitude of our positive and normative findings? To answer these questions, we conduct a comprehensive exploration of the parameter space, by solving our epi-econ model for *one million* unique epidemiological-economic parameter combinations.[39] We then use these model solutions to train surrogates of key features of our model in order to isolate the direction and magnitude of each parameter's influence on our results.[40]

We begin our parameter space exploration by documenting how often travel is effective across the one million economies. On average, susceptibles prefer travel to isolation for 37% of a pandemic period.[41] Consistent with Proposition 2, this percentage goes up to 50% if we restrict attention to the pandemic periods when the global infectious population share is low (below 1%).

We next use surrogate models to study what factors drive this result. The reproductive number R_0 emerges as the key parameter, underscoring the predominant role of disease contagiousness for endogenous avoidance strategies.[42] Figure 3 il-

[39] Online Appendix D.1 details how we use estimates of disease characteristics from the epidemiological literature to discipline the boundaries of our parameter space. We are not aware of any epidemiological studies that provide a specific distribution over this space. Accordingly, we appeal to the principle of insufficient reasons (e.g., Izhakian, 2020) and assume a uniform distribution within these boundaries.

[40] A surrogate model is an estimate $\hat{f}$ of an unknown mapping $f : \mathbb{X} \to \mathbb{R}^m$ from an input space $\mathbb{X}$ to outcomes $y = f(\underline{\mathbf{x}})$, $\underline{\mathbf{x}} \in \mathbb{X}$. In our case, $\mathbb{X}$ is the space of model parameters, while y represents a model outcome of interest (e.g. model-generated moments). We use deep neural networks to estimate the surrogate $\hat{f}$. Details concerning the surrogate model are provided in Online Appendix D. Throughout our surrogate analysis, we report results for the home (small) region.

[41] Online Appendix D.4 defines the statistic used to evaluate the share of days in which travel is an effective asset over the days in which global infections are larger than a small threshold (1e-6). This statistic ensures comparability among diseases with different contagiousness of transmission.

[42] We use the permutation feature importance methodology to determine which features (parameters)

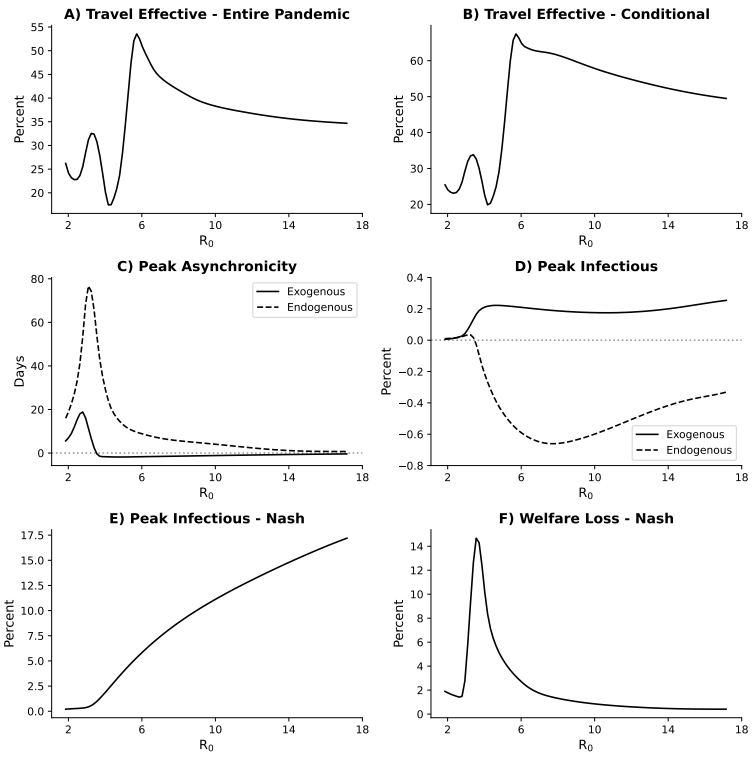

Figure 3: Partial dependence plot of model outcomes (vertical axis) on R_0 (horizontal axis). A) Average percent of days travel is an effective avoidance asset. B) Average percent of days travel is an effective avoidance asset when the infectious population share is above 1%. C) Change in the time between home and foreign peaks from a home isolation autarky model to models with exogenous (solid line) or endogenous (dashed line) travel. D) Percentage point change in peak infectious (percent of population) from a home isolation autarky model to models with exogenous (solid line) or endogenous (dashed line) travel. E) Peak infectious under the 'worst' (aggregate-welfare-minimizing) Prisoner's Dilemma. F) Change in welfare (consumption equivalent units) from the aggregate-welfare-maximizing coordinated solution to the aggregate-welfare-minimizing Prisoner's Dilemma.

lustrates how the share of time during which travel is effective varies with R_0 when we consider either the entire pandemic (Panel A) or periods when the infectious population share is below 1% (Panel B).[43] These panels offer two key insights. First, susceptibles are more likely to prefer travel to home isolation for higher values of the reproductive number, with a predicted average effectiveness of 30% when $R_0 \leq 6$ and 38% otherwise (average effectiveness increases to 34% for $R_0 \leq 6$ and 56% for $R_0 > 6$ when we restrict attention to only the periods where the infectious population is below 1%). Second, the effectiveness of travel is highly sensitive to R_0 for prominent diseases with reproductive numbers below 6, such as Ebola, H1N1, the seasonal flu, SARS, and COVID-19. This finding highlights the value of early accurate estimates of this key epidemiological parameter.[44]

Next, we study how characteristics of the virus and economy dictate disease dynamics, and the extent to which these are driven by endogenous vs. exogenous travel response. Section 5.2 shows both exogenous and endogenous travel significantly reduce the time to peak infectious in the home region compared to a home isolation autarky, by synchronizing infection rates across regions. This quantitative finding remains robust across our parameter space exploration for exogenous travel, though the reduction in time between peaks is far more modest (0.37 days on average). Conversely, we find endogenous travel reduces synchronization, by increasing the time between peaks by an average of 10.8 days. This result reveals a qualitatively and quantitatively distinct impact of endogenous compared to exogenous travel than indicated by our benchmark calibration.

Over our parameter space exploration, peak infectious is on average 9.13% under home isolation autarky. In contrast to our COVID-19 calibration in Section 5.2, endogenous travel reduces (instead of increases) peak infectious, but the effect is

drive the results. Details and results for all features are provided in Online Appendix D.5.

[43] Figure 3 is called a Partial Dependence (PD) plot. This graph reports the dependence of a model outcome on a parameter (horizontal axis), computed as the average of the predicted surrogate model outcomes across all occurrences of the other parameters in the training data. Online Appendix D.6 provides further details.

[44] Table 9 in the Online Appendix provides estimates from the literature of the R_0 for these and other diseases. We verified that this non-monotonicity is not the numerical feature of an overly sparse grid by confirming its persistence after we replicate the analysis for $R_0 \in [1.01, 6]$ (Online Appendix F.4).

modest (-6%). In line with our original calibration, exogenous travel increases the peak relative to the home isolation autarky, but by a smaller amount (9%).

Figure 3 shows how R_0 drives the impact of travel on disease dynamics through peak synchronization (Panel C) and peak infectious (Panel D). Panel C reports the absolute value of the time difference between peaks under endogenous and exogenous travel, minus the same statistic computed under home isolation autarky. A value above zero denotes a reduction in synchronicity. Under endogenous travel, marginal increases in R_0 significantly reduce synchronicity for low values of the reproductive number (up to 3.1), and increase synchronicity after that, though to a lesser degree for $R_0 > 6$. In the case of exogenous travel, low values of R_0 are associated with a reduction in synchronicity, but for $R_0 > 3.6$ exogenous travel is associated with stronger synchronicity between peaks, albeit modest, as noted above. Panel D shows infectious peaks vary with the reproductive number (relative to home isolation autarky). Endogenous travel is associated with a modest decrease (instead of a significant increase) in peak infectious for most values of R_0. This result suggests a qualitatively distinct role of travel for mitigating the heat of the pandemic, as opposed to that indicated by the COVID-19 calibration. These results underscore the implications of the avoidance role of endogenous travel choices vis-á-vis exogenous travel choices on disease dynamics.

We close our analysis by exploring the determinants of welfare effects under time-invariant travel restrictions.[45] In particular, we use the Nash equilibrium of the game between local policymakers (Section 5.3) to study how equilibrium welfare varies throughout the parameter space. Across the one million parameter combinations, we find 99% lead to a Nash equilibrium that is not Pareto optimal, consistent with the results in Section 5.3. However unlike under the COVID-19 calibration with fixed policy rules, we find the socially optimal policy involves positive restrictions on travel for 32% of economies. This suggests the implementation of globally-optimal travel bans necessitates consideration of the particular epidemiological and economic characteristics.[46]

[45] Solving for the Infections-Guided Nash equilibrium is computationally intensive for a single economy and infeasible for parameter space exploration.

[46] As in Section 5.3, when considering Pareto optimality, we restrict the feasible set of travel restrictions to those which limit travel to no more than 1%, 25%, 50%, or 75% of average pre-pandemic

We once again use the surrogate model to examine the impact of R_0–the primary driver of the results–on outcomes in the local policymakers' game.[47] Figure 3 Panel E shows home peak infectious population share under the 'worst' (aggregate welfare-minimizing) Nash equilibrium. Panel F displays the loss in aggregate welfare relative to the globally-optimal coordinated solution. As was the case in the absence of public policy, most variation in welfare losses associated with the Prisoner's Dilemma outcome arises for $R_0 < 6$, where we see non-monotonic effects on welfare. Interestingly, for R_0 higher than this, average welfare losses relative to the coordinated solution *decrease* with R_0, indicating a smaller role for coordinated policy with very infectious diseases.[48]

To sum up, this section explores the robustness of our COVID-19 calibrated-predictions of behavioral responses to disease dynamics, the response of disease dynamics to travel choices, and welfare outcomes under pandemic federalism across the parameter space. Our analysis reveals that several of the quantitative results of Section 5 depend on the particular disease under consideration. Critically, we find endogenous travel alleviates the severity of the pandemic, in contrast to what is suggested by the benchmark calibration to COVID-19. This highlights the importance of parameter space exploration of complex systems and sounds a note of caution against drawing general conclusions from a single parametrization.

7 Model Validation Exercise

Our model predicts that travel for infection avoidance crucially depends on relative infectious shares in the home and foreign region. This section uses smartphone movement data from PlaceIQ and the US spatial evolution of COVID-19 from Coronavirus Resource Center to empirically test whether travel choices were consistent with this prediction.

To operationalize our analysis, we proceed as follows. First, we compute a daily

travel, or no restrictions on travel.

[47] We drop the 1% of economies which do not have a Prisoner's Dilemma Nash equilibrium for our surrogate analysis of the local policymakers' game.

[48] While higher R_0 leads to a decline in *relative* welfare losses, the absolute change in welfare can be large, as suggested by the increasing peak infectious share in Figure 3 Panel E.

measure of inflows of people into county i, leveraging the county-level contact matrices constructed by Couture et al. (2021), using PlaceIQ data. We calculate travel inbound in county i, $Y_{i,t}$ as the share of phones that ping in county i on day t that did not ping in county i during the 14 days prior to t, multiplied by the yearly county-i population from the 2020 U.S. Census. Second, we merge this information with the number of daily cases in each county from the Coronavirus Resource Center at Johns Hopkins University. In this context, we use annual county population counts from the 2020 U.S. Census to compute the relative infectious rate, $X_{i,t}$, as the share of infectious population in i relative to the population-weighted average of infectious share across all other US counties ($j \neq i$).[49]

We assess the effect of relative infectious rates $X_{i,t}$ in a US county (small region) on inbound travel $Y_{i,t}$ from the rest of the US (large region) by estimating the following OLS regression:

$$\ln Y_{i,t} = \beta \ln X_{i,t} + \alpha_i + \lambda_t + \varepsilon_{i,t}, \tag{24}$$

The regression includes county fixed effects α_i to absorb any time invariant unobserved county characteristic that may affect travel decisions, such as local amenities and concentration of business activities. We also include daily fixed effects, λ_t, to flexibly control for any unobserved aggregate trends and seasonal fluctuations that may affect travel choices across all counties. The coefficient of interest β represents the elasticity of travel with respect to infection rates, identified off of within-county daily variation in infection rates. Results are shown in Column (1) of Table 4.

The estimate in Column (1) implies the elasticity of travel with respect to the relative infectious share in the destination county is 0.003. Therefore, a one-standard deviation (2.49) increase in the logarithm of relative infectious share in county i reduces daily travel to the i locale by roughly one percent ($\hat{\beta} \cdot s_{\ln X}/100 = -0.84\%$), or approximately 113 travelers per county per day on average.[50]

[49] Online Appendix E.1 provides more details, including the calculation to recover the stock of infectious from the flow of new infections.

[50] A one-standard deviation increase in $\ln X_{i,t}$ reduces travel inflows to county i by $Y_{i,t} - \bar{Y} = \bar{Y} \times (-0.84/100) = 113$ travelers per county per day, where $\bar{Y} = 13{,}458$ is the unconditional sample average of inbound travel, $Y_{i,t}$.

Table 4: The Avoidance Role of Travel in the Data and Model

	Data		Model	
	(1)	(2)	(3)	(4)
log relative infectious$_{i,t}$	-0.337^{***}	-0.489^{***}	-0.633^{***}	-0.681^{***}
	(0.027)	(0.034)	(0.033)	(0.031)
log relative infectious$_{i,t} \cdot d_t^{high}$		0.376^{***}		0.110^{***}
		(0.037)		(0.036)
County FE	Yes	Yes	No	No
Day FE	Yes	Yes	No	No
N	298,373	298,373	729	729
R^2	0.971	0.971	0.723	0.730

Note: OLS estimates of the effect of the log relative infectious share in county i on the log of inbound travel to region i, multiplied by 100. Columns (1)-(2) report estimates using the PlaceIQ cellphone data and Coronavirus Resource Center data, covering the period from March 11, 2020 to August 21, 2021. Columns (3)-(4) report estimates using model-generated data. Robust standard errors are in parenthesis.

We then estimate the same travel elasticity coefficient using data generated from our model.[51] Column (3) implies that a one standard deviation increase in the logarithm of relative infectious share reduces travel by approximately 123 travelers per day. Hence, the model successfully predicts a response of travel to relative infection rates comparable in magnitude to that in the observed data.

Next, we test an implication of Proposition 2: susceptibles' travel choices are less responsive to relative infection rates when *aggregate* infection rates are high, and travel is less effective than isolation for avoidance purposes. We allow the effect of the relative infectious share on travel to differ during periods of high infection by

[51] To replicate domestic travel into one of the three thousand US counties, we simulate data from a model with asymmetric population shares. In this context, we consider travel inbound into a fictitious average county with 1/3000 of the aggregate population. Since the model-generated dataset used in the regression only includes time-series daily observations for the average county (small region), county and day fixed effects are excluded. Online Appendix E.2 details the simulation and construction of the variables used for the regression analysis.

including an additional interaction term $(\ln X_{i,t} \cdot d_t^{high})$ in the regression specification

$$\ln Y_{i,t} = \beta_1 \ln X_{i,t} + \beta_2 \ln X_{i,t} \cdot d_t^{high} + \alpha_i + \lambda_t + \varepsilon_{i,t}. \tag{25}$$

where d_t^{high} is a dummy variable that equals one if the aggregate infectious share on day t is above its 75th percentile. Columns (2) and (4) of Table 4 show a positive and significant coefficient on the interaction term β_2 in both observed data and model data regressions. Consistent with Proposition 2, the positive sign on β_2 indicates that the avoidance response of inbound travel to relative high infection rates ($\beta_1 < 0$) is muted when aggregate infection rates are high ($\beta_1 < \beta_1 + \beta_2 < 0$).[52]

Overall, this empirical analysis lends credibility to our quantitative analysis.

8 Conclusions

We develop a coupled epidemiological-economic metapopulation model to examine the role of travel choices in a pandemic. Our analysis focuses on a two region model. This assumption yields analytical tractability, clean interpretability of our quantitative results, and allows us to study the Nash game between local social planners.

We highlight the role of travel as an infection avoidance strategy as well as a vector of pandemic transmission. Quantitatively, we find susceptible individuals are more likely to prefer travel to home isolation as an avoidance strategy during the early run-up and late-stages of a pandemic. We also find individuals rely less on travel during peak infection periods, a prediction we corroborate empirically in US data during the COVID-19 pandemic. We also find modeling endogenous travel decisions is particularly quantitatively important when considering regions of asymmetric size. Our normative analysis shows locally-chosen travel policies under pandemic federalism lead to a suboptimal Prisoner's Dilemma outcome whereby both regions implement strict travel bans on incoming travelers, to the detriment of overall welfare.

Finally, we study the robustness of our quantitative results by solving the model

[52] Online Appendix C.2.2 shows that a model without home isolation does not match the data.

for one million combinations of structural parameters. This analysis confirms the role of travel as an effective avoidance mechanism when infection rates are low, as well as the robustness of the Prisoner's Dilemma Nash equilibrium outcome across parametrizations. Crucially, we find endogenous travel mitigates the severity of the pandemic, contrary to the implications of our benchmark calibration. We use neural networks to estimate surrogates of the key model outcomes. This analysis shows the basic reproductive number R_0 is the most important parameter in driving disease dynamics and ultimately welfare consequences of pandemics.

References

Alizadeh, Reza, Janet K Allen, and Farrokh Mistree. 2020. "Managing computational complexity using surrogate models: a critical review." *Research in Engineering Design* 31 (3):275–298.

Antràs, Pol, Stephen J Redding, and Esteban Rossi-Hansberg. 2023. "Globalization and pandemics." *American Economic Review* 113 (4):939–981.

Ash, Thomas, Antonio M Bento, Daniel Kaffine, Akhil Rao, and Ana I Bento. 2022. "Disease-economy trade-offs under alternative epidemic control strategies." *Nature communications* 13 (1):3319.

Azinovic, Marlon, Luca Gaegauf, and Simon Scheidegger. 2022. "Deep equilibrium nets." *International Economic Review* 63 (4):1471–1525.

Bai, Jushan and Pierre Perron. 2003. "Critical values for multiple structural change tests." *The Econometrics Journal* 6 (1):72–78. URL https://doi.org/10.1111/1368-423X.00102.

Bengio, Yoshua. 2012. "Practical recommendations for gradient-based training of deep architectures." In *Neural networks: Tricks of the trade: Second edition*. Springer, 437–478.

Bisin, Alberto and Andrea Moro. 2022. "JUE insight: Learning epidemiology by doing: The empirical implications of a Spatial-SIR model with behavioral responses." *Journal of Urban Economics* 127:103368.

Boppart, Timo, Karl Harmenberg, John Hassler, Per Krusell, and Jonna Olsson. 2025. "Integrated epi-econ assessment: Quantitative theory." *Quantitative Economics* 16 (1):89–131.

Boto-García, David. 2023. "Investigating the two-way relationship between mobility flows and COVID-19 cases." *Economic modelling* 118:106083.

Box, George E. P. and Kenneth B. Wilson. 1951. "On the Experimental Attainment of Optimum Conditions." *Journal of the royal statistical society series b-methodological* 13:1–38. URL https://api.semanticscholar.org/CorpusID:124869750.

Brinkman, Jeffrey and Kyle Mangum. 2022. "JUE insight: The geography of travel behavior in the early phase of the COVID-19 pandemic." *Journal of urban economics* 127:103384.

Chen, Hui, Antoine Didisheim, and Simon Scheidegger. 2023. "Deep surrogates for finance: With an application to option pricing." *Available at SSRN 3782722* .

Chen, Xiaoguang, Hanwei Huang, Jiandong Ju, Ruoyan Sun, and Jialiang Zhang. 2024. "Endogenous mobility in pandemics: Theory and evidence from the United States." .

Couture, Victor, Jonathan I. Dingel, Allison Green, Jessie Handbury, and Kevin R. Williams. 2021. "JUE Insight: Measuring movement and social contact with smartphone data: a real-time application to COVID-19." *Journal of Urban Economics* URL https://www.sciencedirect.com/science/article/pii/S0094119021000103.

Coven, Joshua, Arpit Gupta, and Iris Yao. 2023. "JUE Insight: Urban flight seeded the COVID-19 pandemic across the United States." *Journal of urban economics* 133:103489.

De Serres, Gaston, Isabelle Rouleau, Marie-Eve Hamelin, Caroline Quach, Danuta Skowronski, Louis Flamand, Nicole Boulianne, Yan Li, Julie Carbonneau, Anne-Marie Bourgault et al. 2010. "Contagious period for pandemic (H1N1) 2009." *Emerging infectious diseases* 16 (5):783.

Eichenbaum, Martin S, Sergio Rebelo, and Mathias Trabandt. 2021. "The macroeconomics of epidemics." *The Review of Financial Studies* 34 (11):5149–5187.

Eichner, Thomas and Marco Runkel. 2012. "Interjurisdictional spillovers, decentralized policymaking, and the elasticity of capital supply." *American Economic Review* 102 (5):2349–2357.

Fabbri, Giorgio, Silvia Faggian, and Giuseppe Freni. 2024. "On competition for spatially distributed resources in networks." *Theoretical Economics* 19 (2):743–781.

Farboodi, Maryam, Gregor Jarosch, and Robert Shimer. 2021. "Internal and external effects of social distancing in a pandemic." *Journal of Economic Theory* 196:105293.

Fell, Harrison and Daniel T Kaffine. 2014. "Can decentralized planning really achieve first-best in the presence of environmental spillovers?" *Journal of Envi-*

ronmental Economics and Management 68 (1):46–53.

Fenichel, Eli P, Carlos Castillo-Chavez, M Graziano Ceddia, Gerardo Chowell, Paula A Gonzalez Parra, Graham J Hickling, Garth Holloway, Richard Horan, Benjamin Morin, Charles Perrings et al. 2011. "Adaptive human behavior in epidemiological models." *Proceedings of the National Academy of Sciences* 108 (15):6306–6311.

Fenichel, Eli P, Nicolai V Kuminoff, and Gerardo Chowell. 2013. "Skip the trip: Air Travelers' behavioral responses to pandemic influenza." *PloS one* 8 (3).

Friedl, Aleksandra, Felix Kübler, Simon Scheidegger, and Takafumi Usui. 2023. "Deep uncertainty quantification: with an application to integrated assessment models." Tech. rep., Working Paper University of Lausanne.

Gersovitz, Mark and Jeffrey S Hammer. 2004. "The economical control of infectious diseases." *The Economic Journal* 114 (492):1–27.

Gibbs, Hamish, Yang Liu, Carl AB Pearson, Christopher I Jarvis, Chris Grundy, Billy J Quilty, Charlie Diamond, and Rosalind M Eggo. 2020. "Changing travel patterns in China during the early stages of the COVID-19 pandemic." *Nature communications* 11 (1):5012.

Graff Zivin, Joshua and Nicholas Sanders. 2020. "The spread of COVID-19 shows the importance of policy coordination." *Proceedings of the National Academy of Sciences* 117 (52):32842–32844.

Hastie, Trevor, Robert Tibshirani, Jerome H Friedman, and Jerome H Friedman. 2009. *The elements of statistical learning: data mining, inference, and prediction*, vol. 2. Springer.

Iverson, Terrence and Edward Barbier. 2021. "National and sub-national social distancing responses to COVID-19." *Economies* 9 (2):69.

Iverson, Terrence, Larry Karp, and Alessandro Peri. 2022. "Optimal Social Distancing and the Economics of Uncertain Vaccine Arrival." *Journal of Public Economic Theory* :1–30URL https://onlinelibrary.wiley.com/doi/abs/10.1111/jpet.12606.

Izhakian, Yehuda. 2020. "A theoretical foundation of ambiguity measurement." *Journal of Economic Theory* 187:105001.

Julliard, Christian, Ran Shi, and Kathy Yuan. 2023. "The spread of covid-19 in London: Network effects and optimal lockdowns." *Journal of Econometrics* 235 (2):2125–2154.

Kaffine, Daniel T and Christopher Costello. 2011. "Unitization of spatially connected renewable resources." *The BE Journal of Economic Analysis & Policy* 11 (1).

Kermack, William Ogilvy and Anderson G McKendrick. 1927. "A contribution to the mathematical theory of epidemics." *Proceedings of the royal society of london* 115 (772):700–721.

Kimball, Miles S and Matthew D Shapiro. 2008. "Labor supply: Are the income and substitution effects both large or both small?" Tech. rep., National Bureau of Economic Research.

Kingma, Diederik P. 2014. "Adam: A method for stochastic optimization." *arXiv preprint arXiv:1412.6980* .

Kraemer, Moritz UG, Chia-Hung Yang, Bernardo Gutierrez, Chieh-Hsi Wu, Brennan Klein, David M Pigott, Open COVID-19 Data Working Group†, Louis Du Plessis, Nuno R Faria, Ruoran Li et al. 2020. "The effect of human mobility and control measures on the COVID-19 epidemic in China." *Science* 368 (6490):493–497.

Kremer, Michael. 1996. "Integrating behavioral choice into epidemiological models of AIDS." *The Quarterly Journal of Economics* 111 (2):549–573.

Kucherenko, Sergei and Yury Sytsko. 2005. "Application of deterministic low-discrepancy sequences in global optimization." *Computational Optimization and Applications* 30:297–318.

Landry, Joel R. 2021. "Think globally, cap locally, and trade widely: efficient decentralized policy making in the presence of spillovers." *Journal of the Association of Environmental and Resource Economists* 8 (1):91–124.

Maliar, Lilia, Serguei Maliar, and Pablo Winant. 2021. "Deep learning for solving dynamic economic models." *Journal of Monetary Economics* 122:76–101.

McBride, Kevin and Kai Sundmacher. 2019. "Overview of surrogate modeling in chemical process engineering." *Chemie Ingenieur Technik* 91 (3):228–239.

Ojo, Kehinde E, Susana Ferreira, John Salazar, John Bergstrom, and Kyle Maurice Woosnam. 2023. "Recreational travel behavior and COVID-19: Insights from expected utility and the theory of planned behavior." *Tourism Economics* 29 (3):643–663.

Prem, Kiesha, Alex Cook, and Mark Jit. 2017. "Projecting social contact matrices in 152 countries using contact surveys and demographic data." *PLOS Computational Biology* 13 (9).

Prescott, Edward C. 1986. "Theory ahead of business-cycle measurement." In *Carnegie-Rochester conference series on public policy*, vol. 25. Elsevier, 11–44.

Qureshi, Adnan I, Morad Chughtai, Elhadj Ibrahima Bah, Moumié Barry, Kézély Béavogui, Tokpagnan Oscar Loua, and Ahmed A Malik. 2015. "High survival rates and associated factors among Ebola virus disease patients hospitalized at

Donka National Hospital, Conakry, Guinea." *Journal of Vascular and Interventional Neurology* 8 (1.5):S4.

Renne, Jean-Paul, Guillaume Roussellet, and Gustavo Schwenkler. 2020. "Preventing COVID-19 fatalities: State versus federal policies." *arXiv preprint arXiv:2010.15263* .

Robbins, Herbert and Sutton Monro. 1951. "A stochastic approximation method." *The annals of mathematical statistics* :400–407.

Rowthorn, Robert E, Ramanan Laxminarayan, and Christopher A Gilligan. 2009. "Optimal control of epidemics in metapopulations." *Journal of the Royal Society Interface* 6 (41):1135–1144.

Sanchirico, James N and James E Wilen. 2001. "A bioeconomic model of marine reserve creation." *Journal of Environmental Economics and Management* 42 (3):257–276.

Scheidegger, Simon and Adrien Treccani. 2021. "Pricing American options under high-dimensional models with recursive adaptive sparse expectations." *Journal of Financial Econometrics* 19 (2):258–290.

Sobol', Il'ya Meerovich. 1967. "On the distribution of points in a cube and the approximate evaluation of integrals." *Zhurnal Vychislitel'noi Matematiki i Matematicheskoi Fiziki* 7 (4):784–802.

Tripathy, R. K. and I. Bilionis. 2018. "Deep UQ: Learning deep neural network surrogate models for high dimensional uncertainty quantification." *Journal of Computational Physics* 375:565–588.

Online Appendix

A Equilibrium Characterization

This section collects the proofs of the propositions in the paper. We start by deriving/describing objects and listing assumptions that will be useful in the next subsections.

Pre-pandemic value function. The first order condition for the pre-pandemic agent's problem (5) is

$$\frac{\beta_i}{m_t^{pre}} = \frac{(1-\beta_i)}{1-m_t^{pre}},$$

which implies $m_t^{pre} = \beta_i$. Since the pre-pandemic problem is stationary with $U_{i,t}^{pre} = U_{i,t+1}^{pre} = U_i^{pre}$, we can rewrite the pre-pandemic value function in (5) as

$$U_i^{pre} = \frac{1}{1-\delta(1-P^{D^*})}\left[(1-\beta_i)\ln(w\bar{l}(1-\beta_i)) + \beta_i \ln(\beta_i) + \delta P^{D^*}\Omega_i\right].$$

Recovered value function. The first order condition for the recovered agent's problem (8) is

$$\frac{\beta_i}{m_t^R} = \frac{(1-\beta_i)}{(1-\theta_i)-m_t^R},$$

which implies $m_t^R = (1-\theta_i)\beta_i$. In the final period of the pandemic $t = T$, the recovered value function in (8) is

$$\begin{aligned} U_{i,T}^R &= (1-\beta_i)\ln(w\bar{l}(1-\theta_i)(1-\beta_i)) + \beta_i \ln((1-\theta_i)\beta_i) + \delta\left((1-P^{D^*})U_{i,T+1}^R + P^{D^*}\Omega_i\right) \\ &= (1-\beta_i)\ln(w\bar{l}(1-\theta_i)(1-\beta_i)) + \beta_i \ln((1-\theta_i)\beta_i) + \delta\left((1-P^{D^*})U_i^{pre} + P^{D^*}\Omega_i\right), \end{aligned}$$

since $U_{i,t}^R = U_i^{pre}$ for $t > T$ after the arrival of a vaccine. Likewise in period $t =$

$T-1$, the recovered value function is,

$$\begin{aligned}
U^R_{i,T-1} &= (1-\beta_i)\ln(w\bar{l}(1-\theta_i)(1-\beta_i)) + \beta_i \ln((1-\theta_i)\beta_i) + \delta\left((1-P^{D^*})U^R_{i,T} + P^{D^*}\Omega_i\right) \\
&= (1-\beta_i)\ln(w\bar{l}(1-\theta_i)(1-\beta_i)) + \beta_i \ln((1-\theta_i)\beta_i) \\
&+ \delta\Bigg[(1-P^{D^*})\Big((1-\beta_i)\ln(w\bar{l}(1-\theta_i)(1-\beta_i)) + \beta_i \ln((1-\theta_i)\beta_i) \\
&+ \delta\left((1-P^{D^*})U^{pre}_i + P^{D^*}\Omega_i\right)\Big) + P^{D^*}\Omega_i\Bigg].
\end{aligned}$$

For general $U^R_{i,T-j}$ with $j \in \{0,...,T-1\}$, we have

$$\begin{aligned}
U^R_{i,T-j} &= \sum_{t=0}^{j}\left(\delta(1-P^{D^*})\right)^t\left[(1-\beta_i)\ln(w\bar{l}(1-\theta_i)(1-\beta_i)) + \beta_i\ln((1-\theta_i)\beta_i)\right] \\
&+ \sum_{t=0}^{j}\left(\delta P^{D^*}\right)^{t+1}\Omega_i + \left(\delta(1-P^{D^*})\right)^{j+1}U^{pre}_i. \qquad (26)
\end{aligned}$$

Infectious value function. The first order condition for the infectious agent's problem (7) is

$$\frac{\beta^I_i}{m^I_t} = \frac{(1-\beta^I_i)}{(1-\theta_i)-m^I_t},$$

which implies $m^I_t = (1-\theta_i)\beta^I_i$. In the final period of the pandemic $t=T$, the infectious value function in (7) is

$$\begin{aligned}
U^I_{i,T} &= (1-\beta^I_i)\ln(\phi w\bar{l}(1-\theta_i)(1-\beta^I_i)) + \beta^I_i\ln((1-\theta_i)\beta^I_i) \\
&+ \delta[(1-P^R-P^D-P^{D^*})U^I_{i,T+1} + P^R U^R_{i,T+1} + (P^D+P^{D^*})\Omega_i] \\
&= (1-\beta^I_i)\ln(\phi w\bar{l}(1-\theta_i)(1-\beta^I_i)) + \beta^I_i\ln((1-\theta_i)\beta^I_i) + \delta[(1-P^D-P^{D^*})U^{pre}_i \\
&+ (P^D+P^{D^*})\Omega_i],
\end{aligned}$$

since $U^R_{i,t} = U^I_{i,t} = U^{pre}_i$ for $t > T$ after the arrival of a vaccine. Likewise in period

$t = T-1$, the infectious value function is,

$$
\begin{aligned}
U^I_{i,T-1} &= (1-\beta^I_i)\ln(\phi w \bar{l}(1-\theta_i)(1-\beta^I_i)) + \beta^I_i \ln((1-\theta_i)\beta^I_i) + \delta[(1-P^R-P^D-P^{D^*})U^I_{i,T} \\
&\quad + P^R U^R_{i,T} + (P^D + P^{D^*})\Omega_i] \\
&= (1-\beta^I_i)\ln(\phi w \bar{l}(1-\theta_i)(1-\beta^I_i)) + \beta^I_i \ln((1-\theta_i)\beta^I_i) + \delta\Big[(1-P^R-P^D-P^{D^*}) \\
&\quad \Big((1-\beta^I_i)\ln(\phi w \bar{l}(1-\theta_i)(1-\beta^I_i)) + \beta^I_i \ln((1-\theta_i)\beta^I_i) + \delta[(1-P^D-P^{D^*})U^{pre}_i \\
&\quad + (P^D + P^{D^*})\Omega_i]\Big) + P^R U^R_{i,T} + (P^D + P^{D^*})\Omega_i\Big].
\end{aligned}
$$

For general $U^I_{i,T-j}$ with $j \in \{0,...,T-1\}$, we have

$$
\begin{aligned}
U^I_{i,T-j} &= \sum_{t=0}^{j} \Big(\delta(1-P^R-P^D-P^{D^*})\Big)^t \Big[(1-\beta^I_i)\ln(\phi w \bar{l}(1-\theta_i)(1-\beta^I_i)) + \beta^I_i \ln((1-\theta_i)\beta^I_i)\Big] \\
&\quad + \sum_{t=0}^{j} \Big(\delta P^R\Big)^{t+1} U^R_{T+1-j+t} + \sum_{t=0}^{j} \Big(\delta(P^D + P^{D^*})\Big)^{t+1} \Omega_i + \Big(\delta(1-P^R-P^D-P^{D^*})\Big)^{j+1} U^{pre}_i,
\end{aligned}
$$

with $U^R_{T+1} = U^{pre}_i$ and U^R_t given by (26) for $t \in \{1,...T\}$.

Assumption 2. ***Restrictions on*** θ_i. *We focus on the interesting case where social distancing is low enough,* $\theta_i \in [0, \bar{\theta})$, *such that* $U^R_{i,t}, U^S_{i,t}, U^I_{i,t} \geq \Omega_i$. *We define* $0 < \bar{\theta} \leq 1$ *as the upper bound to the social distancing restriction such that* $U^I_{i,1} = \Omega_i$. *Under the conditions of Lemma 1,* $\theta_i \in [0, \bar{\theta})$ *is a sufficient condition for* $U^I_{i,t} > \Omega_i$ $\forall t$.

This is a quantitative assumption that rules out drastic social policy interventions where agents prefer to be dead than alive. The parameter $\bar{\theta}$ can be derived analytically and it is available upon request.

A.1 No selfish incentives for herd immunity

The following lemma establishes a sufficient condition that eliminates the *selfish incentives for herd immunity*.

Lemma 1. *The value function of being recovered is always larger than the value function of being infectious or susceptible,* $U^R_{i,t} > U^I_{i,t}$, $U^R_{i,t} \geq U^S_{i,t}$. *The value of*

being susceptible is larger than the one of being infectious, $U^R_{i,t} \geq U^S_{i,t} > U^I_{i,t}$, when catching the disease is costly enough, that is

$$\Big(u_i(c^R(m),m) - u^I_i(c^I(m),m)\Big) - \delta(1-P^D)(U^R_{i,t} - \Omega_i) \geq 0, \qquad \forall m,t$$

where $c^R(m) \equiv w\bar{l}(1-\theta_i - m)$ and $c^I(m) \equiv \phi w\bar{l}(1-\theta_i - m)$. That is, when the infectious state productivity loss is large enough (ϕ small) or the probability of death due to the virus, P^D is large enough.

We prove the value functions ordering presented in Lemma 1

$$U^R_{i,t} \geq U^S_{i,t} > U^I_{i,t} > \Omega_i \qquad \forall t \in \{1,2,\ldots,T\}$$

by backward induction. First, use the budget constraint for each disease type S, I, R to define functions:

$$\begin{aligned} c^S(m) &\equiv w\bar{l}(1-\theta_i - m), \\ c^I(m) &\equiv \phi w\bar{l}(1-\theta_i - m), \\ c^R(m) &\equiv w\bar{l}(1-\theta_i - m), \end{aligned}$$

The proof proceeds in three steps.

Step 1. We show that $U^R_{i,t} > U^I_{i,t}$ $\forall t \in \{1,2,\ldots,T\}$. In the last period of the pandemic, T,

$$\begin{aligned} U^R_{i,T} &= \max_{m_T}\{u_i(c^R(m_T),m_T) + \delta\Big((1-P^{D^*})U^R_{i,T+1} + P^{D^*}\Omega_i\Big)\} \\ &= \max_{m_T}\{u_i(c^R(m_T),m_T) + \delta\Big((1-P^{D^*})U^{pre}_{i,T+1} + P^{D^*}\Omega_i\Big)\} \\ &> \max_{m_T}\{u_i(c^R(m_T),m_T) + \delta\Big((1-P^D-P^{D^*})U^{pre}_{i,T+1} + (P^D+P^{D^*})\Omega_i\Big)\} \\ &= \max_{m_T}\{u_i(c^R(m_T),m_T) + \delta\Big((1-P^R-P^D-P^{D^*})U^{pre}_{i,T+1} + P^R U^{pre}_{i,T+1} + (P^D+P^{D^*})\Omega_i\Big)\} \\ &> \max_{m_T}\{u_i(c^I(m_T),m_T) + \delta\Big((1-P^R-P^D-P^{D^*})U^{pre}_{i,T+1} + P^R U^{pre}_{i,T+1} + (P^D+P^{D^*})\Omega_i\Big)\} \\ &= \max_{m_T}\{u_i(c^I(m_T),m_T) + \delta\Big((1-P^R-P^D-P^{D^*})U^I_{i,T+1} + P^R U^I_{i,T+1} + (P^D+P^{D^*})\Omega_i\Big)\} \\ &= U^I_{i,T}, \end{aligned}$$

where the first inequality follows because $U_{i,t}^{pre} > \Omega_i$ as explained in Section 4, and the second inequality uses the fact that $c^R(m) = w\bar{l}((1-\theta_i)-m) > \phi w\bar{l}((1-\theta_i)-m) = c^I(m)$ for all $m \in [0, 1-\theta]$, $\phi < 1$. Now, let $t = T-1$

$$
\begin{aligned}
U_{i,t}^R &= \max_{m_t}\{u_i(c^R(m_t), m_t) + \delta\left((1-P^{D^*})U_{i,t+1}^R + P^{D^*}\Omega_i\right)\} \\
&> \max_{m_t}\{u_i(c^R(m_t), m_t) + \delta\left((1-P^{D}-P^{D^*})U_{i,t+1}^R + (P^{D}+P^{D^*})\Omega_i\right)\} \\
&= \max_{m_t}\{u_i(c^R(m_t), m_t) + \delta\left((1-P^{R}-P^{D}-P^{D^*})U_{i,t+1}^R + P^R U_{i,t+1}^R + (P^{D}+P^{D^*})\Omega_i\right)\} \\
&> \max_{m_t}\{u_i(c^R(m_t), m_t) + \delta\left((1-P^{R}-P^{D}-P^{D^*})U_{i,t+1}^I + P^R U_{i,t+1}^R + (P^{D}+P^{D^*})\Omega_i\right)\} \\
&> \max_{m_t}\{u_i(c^I(m_t), m_t) + \delta\left((1-P^{R}-P^{D}-P^{D^*})U_{i,t+1}^I + P^R U_{i,t+1}^R + (P^{D}+P^{D^*})\Omega_i\right)\} \\
&= U_{i,t}^I,
\end{aligned}
$$

where the first inequality uses $U_{i,t}^R > \Omega_i$, the second uses $U_{i,t+1}^R > U_{i,t+1}^I$, and the third uses $c^R(m) > c^I(m)$. This establishes $U_{i,T-1}^R > U_{i,T-1}^I$. Proceeding backward and recursively in a similar fashion for $t \in \{T-2, T-3, \ldots 1\}$ proves the result. **Step 2.** We show that $U_{i,t}^R \geq U_{i,t}^S$ for $t \in \{1, 2, \ldots, T\}$. Proceeding by backward induction, in the final period, T,

$$
\begin{aligned}
U_{i,T}^S &= \max_{m_T}\{u_i(c^S(m_T), m_T) + \delta[(1-P_i^I(m_T, 1-\theta_i-m_T, 0; \mathscr{T}_T) - P^{D^*})U_{i,T+1}^S \\
&\quad + P_i^I(m_T, 1-\theta_i-m_T, 0; \mathscr{T}_T)U_{i,T+1}^I + P^{D^*}\Omega_i]\} \\
&= \max_{m_T}\{u_i(c^S(m_T), m_T) + \delta[(1-P_i^I(m_T, 1-\theta_i-m_T, 0; \mathscr{T}_T) - P^{D^*})U_{i,T+1}^{pre} \\
&\quad + P_i^I(m_T, 1-\theta_i-m_T, 0; \mathscr{T}_T)U_{i,T+1}^{pre} + P^{D^*}\Omega_i]\} \\
&= \max_{m_T}\{u_i(c^R(m_T), m_T) + \delta[(1-P^{D^*})U_{i,T+1}^{pre} + P^{D^*}\Omega_i]\} \\
&= U_{i,T}^R,
\end{aligned}
$$

since $c^S(m) = c^R(m)$ for all $m \in [0, \bar{m}]$. Accordingly, we have that $U_{i,T}^S = U_{i,T}^R > U_{i,T}^I$.

Proceeding backward and recursively, note that in $T-1$,

$$\begin{aligned}
U^R_{i,T-1} &= \max_{m_{T-1}}\{u_i(c^R(m_{T-1}),m_{T-1}) + \delta\left((1-P^{D^*})U^R_{i,T} + P^{D^*}\Omega_i\right)\} \\
&= \max_{m_{T-1}}\{u_i(c^S(m_{T-1}),m_{T-1}) + \delta\left((1-P^{D^*})U^S_{i,T} + P^{D^*}\Omega_i\right)\} \\
&= \max_{m_{T-1}}\{u_i(c^S(m_{T-1}),m_{T-1}) + \delta[(1-P^I_i(m_{T-1},1-\theta_i-m_{T-1},0;\mathscr{T}_{T-1}) \\
&\qquad - P^{D^*})U^S_{i,T} + P^I_i(m_{T-1},1-\theta_i-m_{T-1},0;\mathscr{T}_{T-1})U^S_{i,T} + P^{D^*}\Omega_i]\} \\
&> \max_{m_{T-1}}\{u_i(c^S(m_{T-1}),m_{T-1}) + \delta[(1-P^I_i(m_{T-1},1-\theta_i-m_{T-1},0;\mathscr{T}_{T-1}) \\
&\qquad - P^{D^*})U^S_{i,T} + P^I_i(m_{T-1},1-\theta_i-m_{T-1},0;\mathscr{T}_{T-1})U^I_{i,T} + P^{D^*}\Omega_i]\} \\
&= U^S_{i,T-1},
\end{aligned}$$

where the inequality follows from $U^S_{i,T} = U^R_{i,T} > U^I_{i,T}$. Next, consider $t = T-2$. Then,

$$\begin{aligned}
U^R_{i,t} &= \max_{m_t}\{u_i(c^R(m_t),m_t) + \delta\left((1-P^{D^*})U^R_{i,t+1} + P^{D^*}\Omega_i\right)\} \\
&= \max_{m_t}\{u_i(c^S(m_t),m_t) + \delta[(1-P^I_i(m_t,1-\theta_i-m_t,0;\mathscr{T}_t) - P^{D^*})U^R_{i,t+1} \\
&\qquad + P^I_i(m_t,1-\theta_i-m_t,0;\mathscr{T}_t)U^R_{i,t+1} + P^{D^*}\Omega_i]\} \\
&> \max_{m_t}\{u_i(c^S(m_t),m_t) + \delta[(1-P^I_i(m_t,1-\theta_i-m_t,0;\mathscr{T}_t) - P^{D^*})U^S_{i,t+1} \\
&\qquad + P^I_i(m_t,1-\theta_i-m_t,0;\mathscr{T}_t)U^I_{i,t+1} + P^{D^*}\Omega_i]\} \\
&= U^S_{i,t},
\end{aligned}$$

where the inequality follows since $U^S_{i,t+1} < U^R_{i,t+1}$ and $U^I_{i,t+1} < U^R_{i,t+1}$. This establishes $U^R_{i,T-2} > U^S_{i,T-2}$. Proceeding backward and recursively in a similar fashion for $t \in \{T-3,\dots 1\}$ proves the result.

Step 3. We show that $U^S_{i,t} > U^I_{i,t}$ for $t \in \{1,2,\dots,T\}$. Under the conditions of Lemma 1, we have the following inequality:

$$\left(u_i(c^S(m),m) - u^I_i(c^I(m),m)\right) - \delta(1-P^D)(U^R_{i,t} - \Omega_i) \geq 0, \qquad \forall m,t,$$

since $c^S(m) = c^R(m)\ \forall m$. With a slight abuse of notation, let $U^S_{i,t}(m)$, $U^I_{i,t}(m)$ denote

the objective function of the susceptible and infectious, respectively, evaluated at a given m (not necessarily the optimum). In the last period of the pandemic, we have $U^S_{i,T} = U^R_{i,T} > U^I_{i,T}$. Proceeding backward and recursively, let $t = T-1$. The difference $U^S_{i,t}(m) - U^I_{i,t}(m)$ is given by

$$\begin{aligned}
U^S_{i,t}(m) - U^I_{i,t}(m) &= u_i(c^S(m_t), m_t) - u^I_i(c^I(m_t), m_t) + \delta[(1 - P^I_i(m_t, 1-\theta_i - m_t, 0; \mathscr{T}_t) - P^{D^*})U^S_{i,t+1} \\
&\quad + P^I_i(m_t, 1-\theta_i - m_t, 0; \mathscr{T}_t)U^I_{i,t+1} - (1 - P^R - P^D - P^{D^*})U^I_{i,t+1} - P^R U^R_{i,t+1} - P^D \Omega_i] \\
&> u_i(c^S(m_t), m_t) - u^I_i(c^I(m_t), m_t) + \delta[(1 - P^I_i(m_t, 1-\theta_i - m_t, 0; \mathscr{T}_t) - P^{D^*})U^S_{i,t+1} \\
&\quad + P^I_i(m_t, 1-\theta_i - m_t, 0; \mathscr{T}_t)U^I_{i,t+1} - (1 - P^R - P^D - P^{D^*})U^R_{i,t+1} - P^R U^R_{i,t+1} - P^D \Omega_i] \\
&= u_i(c^S(m_t), m_t) - u^I_i(c^I(m_t), m_t) + \delta[(1 - P^I_i(m_t, 1-\theta_i - m_t, 0; \mathscr{T}_t) - P^{D^*})U^S_{i,t+1} \\
&\quad + P^I_i(m_t, 1-\theta_i - m_t, 0; \mathscr{T}_t)U^I_{i,t+1} - (1 - P^D - P^{D^*})U^R_{i,t+1} - P^D \Omega_i] \\
&> u_i(c^S(m_t), m_t) - u^I_i(c^I(m_t), m_t) + \delta[(1 - P^I_i(m_t, 1-\theta_i - m_t, 0; \mathscr{T}_t) - P^{D^*})U^I_{i,t+1} \\
&\quad + P^I_i(m_t, 1-\theta_i - m_t, 0; \mathscr{T}_t)U^I_{i,t+1} - (1 - P^D - P^{D^*})U^R_{i,t+1} - P^D \Omega_i] \\
&= u_i(c^S(m_t), m_t) - u^I_i(c^I(m_t), m_t) + \delta[(1 - P^{D^*})U^I_{i,t+1} - (1 - P^D - P^{D^*})U^R_{i,t+1} - P^D \Omega_i] \\
&> u_i(c^S(m_t), m_t) - u^I_i(c^I(m_t), m_t) + \delta[(1 - P^{D^*})\Omega_i - (1 - P^D - P^{D^*})U^R_{i,t+1} - P^D \Omega_i] \\
&= u_i(c^S(m_t), m_t) - u^I_i(c^I(m_t), m_t) - \delta[(1 - P^D - P^{D^*})(U^R_{i,t+1} - \Omega_i)] \\
&> u_i(c^S(m_t), m_t) - u^I_i(c^I(m_t), m_t) - \delta[(1 - P^D)(U^R_{i,t+1} - \Omega_i)] \\
&\geq 0,
\end{aligned}$$

where the first inequality follows from $U^R_{i,t+1} > U^I_{i,t+1}$, the second from $U^S_{i,t+1} > U^I_{i,t+1}$, the third from $U^I_{i,t+1} > \Omega_i$, the fourth from $U^R_{i,t+1} > \Omega_i$, and the fifth by assumption. Since this holds for all m and the feasible set $[0, \bar{m}]$ is the same for both disease types, $m^S_{i,t}, m^I_{i,t} \in [0, \bar{m}]$, the inequality must also hold in the max, $U^S_{i,t} = \max_m U^S_{i,t}(m) > \max_m U^I_{i,t}(m) = U^I_{i,t}$. This establishes $U^S_{i,T-1} > U^I_{i,T-1}$. Proceeding backward and recursively in a similar fashion for $t \in \{T-2, \ldots 1\}$ proves the result.

A.2 Proof of Proposition 1

A.2.1 Case 1: Utility benefits from travel

Consider first the case where agents receive direct utility benefits from travel, $\frac{\partial u_i}{\partial m} > 0$. By Inada conditions, travel choices are strictly positive, $m > 0$. In an interior

solution, the first order condition (FOC) for the susceptible agent is

$$\frac{\partial u_i}{\partial m} = -\frac{\partial u_i}{\partial c}\cdot\frac{\partial c}{\partial m} + \delta(U^S_{i,t+1} - U^I_{i,t+1})\frac{\partial P^I_{i,t}}{\partial m}. \tag{27}$$

Uniqueness. Define the continuous function

$$E(m) \equiv \frac{\partial u_i(c(m),m)}{\partial m} + \frac{\partial u_i(c(m),m)}{\partial c(m)}\cdot\frac{\partial c(m)}{\partial m} - \delta(U^S_{i,t+1} - U^I_{i,t+1})\frac{\partial P^I_{i,t}(m)}{\partial m},$$

where $c(m) \equiv w_t\bar{l}(1-\theta_i-m)$ is defined from the Susceptible's budget constraint in (6) and

$$P^I_{i,t}(m) \equiv 1 - \left[\left(\frac{1-\theta_i-m}{1-\theta_i}\right)\left(1-\tau\cdot\frac{(I_{i,t}-M^I_{i,t}+M^I_{j,t})}{N_{i,t}}\right)^{\mathscr{C}^l_{i,t}} + \left(\frac{m}{1-\theta_i}\right)\left(1-\tau\cdot\frac{(I_{j,t}-M^I_{j,t}+M^I_{i,t})}{N_{j,t}}\right)^{\mathscr{C}^m_{i,t}}\right],$$

provides the probability of infection in the absence of home isolation. We then have $E(m) = 0$ at an optimum. Notice

$$\begin{aligned}\frac{dE(m)}{dm} &= \frac{\partial^2 u_i(c(m),m)}{\partial m\partial c(m)}\cdot\frac{\partial c(m)}{\partial m} + \frac{\partial^2 u_i(c(m),m)}{\partial m^2} + \left[\frac{\partial^2 u_i(c(m),m)}{\partial c(m)^2}\cdot\frac{\partial c(m)}{\partial m} + \right.\\ &\left.\frac{\partial^2 u_i(c(m),m)}{\partial c(m)\partial m}\right]\frac{\partial c(m)}{\partial m} + \frac{\partial u_i(c(m),m)}{\partial c(m)}\cdot\underbrace{\frac{\partial^2 c(m)}{\partial m^2}}_{=0} - \delta(U^S_{i,t+1} - U^I_{i,t+1})\underbrace{\frac{\partial^2 P^I_{i,t}}{\partial m^2}}_{=0}\\ &= \underbrace{\frac{\partial c(m)}{\partial m}}_{<0}\left[2\cdot\underbrace{\frac{\partial^2 u_i(c(m),m)}{\partial m\partial c(m)}}_{\geq 0} + \underbrace{\frac{\partial^2 u_i(c(m),m)}{\partial c(m)^2}\cdot\frac{\partial c(m)}{\partial m}}_{\geq 0}\right] + \underbrace{\frac{\partial^2 u_i(c(m),m)}{\partial m^2}}_{\leq 0} < 0\end{aligned}$$

where the inequalities follow from the susceptible's budget constraint and by assumptions on the functional form of utility. It follows that $E(m)$ is strictly decreasing in m.

Now note that by Inada conditions on u_i

$$\lim_{m\to 0} E(m) = \infty, \qquad \lim_{m\to(1-\theta_i)} E(m) = -\infty,$$

$E(m)$ is therefore a continuous strictly decreasing monotonic function of m between $(0, 1-\theta)$ that goes from $+\infty$ to $-\infty$. Then by application of the Intermediate Value Theorem to Monotonic Functions in an open set, the solution $E(m) = 0$ is unique.

The susceptible's optimal travel choice m is decreasing in B. Let $B \equiv \delta(U^S_{i,t+1} - U^I_{i,t+1})\frac{\partial P^I_{i,t}}{\partial m}$, which does not depend on m. By the implicit function theorem, from (27) we have,

$$\frac{\partial^2 u_i(c(m),m)}{\partial m \partial c(m)} \cdot \frac{\partial c(m)}{\partial m} \cdot \frac{\partial m}{\partial B} + \frac{\partial^2 u_i(c(m),m)}{\partial m^2} \cdot \frac{\partial m}{\partial B} =$$
$$- \left[\frac{\partial^2 u_i(c(m),m)}{\partial c(m)^2} \cdot \frac{\partial c(m)}{\partial m} \cdot \frac{\partial m}{\partial B} + \frac{\partial^2 u_i(c(m),m)}{\partial c(m) \partial m} \frac{\partial m}{\partial B} \right] \frac{\partial c(m)}{\partial m} - \frac{\partial u_i(c(m),m)}{\partial c(m)} \cdot \underbrace{\frac{\partial^2 c(m)}{\partial m^2}}_{=0} \cdot \frac{\partial m}{\partial B} + 1$$

Simple algebra shows that

$$\frac{\partial m}{\partial B} = \frac{1}{\underbrace{\frac{\partial c(m)}{\partial m}}_{<0} \left[2 \cdot \underbrace{\frac{\partial^2 u_i(c(m),m)}{\partial m \partial c(m)}}_{\geq 0} + \underbrace{\frac{\partial^2 u_i(c(m),m)}{\partial c(m)^2} \cdot \frac{\partial c(m)}{\partial m}}_{\geq 0} \right] + \underbrace{\frac{\partial^2 u_i(c(m),m)}{\partial m^2}}_{\leq 0}} < 0.$$

The susceptibles' optimal travel choice m converges to the recovered when $B \to 0$. As $B \to 0$ the FOC of the susceptible (27) reduces to FOC of the recovered,

$$\frac{\partial u_i}{\partial m} = \frac{\partial u_i}{\partial c} w \bar{l}.$$

Thus for $B < 0$, $m^S_{i,t} > m^R_{i,t}$ since $m^S_{i,t}$ decreases in B. Likewise, for $B > 0$, we have $m^S_{i,t} < m^R_{i,t}$.

Relative travel by susceptible depends on travel as infection avoidance asset or liability. Under the conditions of Lemma 1, $B < 0$ if and only if $\partial P^I_i / \partial m < 0$ (infection avoidance asset). In this case, $m^S_{i,t} > m^R_{i,t}$. Conversely if $\partial P^I_i / \partial m > 0$, then $B > 0$. Consequently $m^S_{i,t} < m^R_{i,t}$.

A.2.2 Case 2: No utility benefits from travel

Consider now the case where agents do not receive any direct utility benefits from travel, $u_i(c,m) = u_i(c)$. In this environment recovered agents do not travel (unless travel is costless). The susceptible's first order and Kuhn-Tucker conditions imply

$$\frac{\partial u_i}{\partial c} \cdot \frac{\partial c}{\partial m} - \delta(U^S_{i,t+1} - U^I_{i,t+1}) \frac{\partial P^I_{i,t}}{\partial m} \leq 0, \tag{28}$$

with equality if $m^S_{i,t} > 0$.

Uniqueness. Define the continuous function

$$F(m) \equiv -\delta(U^S_{i,t+1} - U^I_{i,t+1}) \frac{\partial P^I_{i,t}(m)}{\partial m} + \frac{\partial u_i(c(m))}{\partial c(m)} \cdot \frac{\partial c(m)}{\partial m}$$

such that $F(m) = 0$ at an interior solution. Differentiating with respect to m gives,

$$\begin{aligned} \frac{dF(m)}{dm} &= -\delta(U^S_{i,t+1} - U^I_{i,t+1}) \underbrace{\frac{\partial^2 P^I_{i,t}}{\partial m^2}}_{=0} + \frac{\partial^2 u_i(c(m))}{\partial c(m)^2} \cdot \left(\frac{\partial c(m)}{\partial m} \right)^2 + \frac{\partial u_i(c(m))}{\partial c(m)} \cdot \underbrace{\frac{\partial^2 c(m)}{\partial m^2}}_{=0} \\ &= \underbrace{\frac{\partial^2 u_i(c(m))}{\partial c(m)^2}}_{\leq 0} \cdot \left(\frac{\partial c(m)}{\partial m} \right)^2 \leq 0 \end{aligned}$$

where the inequality follow from the assumptions on the functional form of utility. By Inada conditions on u_i, we have that

$$\lim_{m \to (1-\theta_i)} F(m) = -\infty.$$

Notice $F(0) < \infty$. If $F(0) > 0$, there is a unique $m^S_{i,t} > 0$. Otherwise $m^S_{i,t} = 0$.

The susceptible travels more than recovered only if B<0. From (28),

$$-\frac{\partial u_i}{\partial c}(w\bar{l}) - \underbrace{\delta(U^S_{i,t+1} - U^I_{i,t+1}) \frac{\partial P^I_{i,t}}{\partial m}}_{=B} \leq 0.$$

Since $\partial u_i/\partial c > 0$, a necessary condition for $m^S_{i,t} > 0$ (and (28) to hold with equality) is $B < 0$. Equivalently, $m^S_{i,t} > 0$ implies $\partial P^I_{i,t}/\partial m < 0$. Thus when travel is an infection avoidance asset ($\partial P^I_{i,t}/\partial m < 0$), $m^S_{i,t} \geq 0$. Otherwise travel is an infection avoidance liability and the susceptible's traveling choice mimics the one of the recovered $m^S_{i,t} = m^R_{i,t} = 0$.

A.3 Proof of Proposition 2

We first prove Proposition 2.(a). First note that by definition,

$$\frac{\partial P^I_i}{\partial h} \equiv \frac{1}{1-\theta_i}\left[\underbrace{\left(1-\tau\cdot\underbrace{\frac{(I_{i,t}-M^I_{i,t}+M^I_{j,t})}{N_{i,t}}}_{\text{Home Exposure}}\right)^{\mathscr{C}^l_{i,t}} - \left(1-\tau\cdot\underbrace{\frac{(I_{i,t}-M^I_{i,t}+M^I_{j,t})}{N_{i,t}}}_{\text{Home Exposure}}\right)^{\mathscr{C}^h_{i,t}}}_{\text{Effectiveness of home isolation in reducing home-infection exposure }(-)}\right] \leq 0$$

where the inequality arises by inspection of the contact rates (exponents). When $\frac{\partial P^I_i}{\partial h} = 0$ home isolation is ineffective in reducing the likelihood of getting infected, and we are back in the environment of Proposition 1. For the rest of this analysis, let us focus on the interesting case where $\frac{\partial P^I_i}{\partial h} < 0$.

In the absence of direct utility benefits from travels, the first order and Kuhn-Tucker conditions for the susceptibles are

$$-\frac{du_i}{dc}w\bar{l} + \delta(U^{I'}_i - U^{S'}_i)\frac{\partial P^I_i}{\partial m} + \mu^{lo}_m - \mu^{hi}_m = 0, \tag{29}$$

$$-\frac{du_i}{dc}w\bar{l} + \delta(U^{I'}_i - U^{S'}_i)\frac{\partial P^I_i}{\partial h} + \mu^{lo}_h - \mu^{hi}_h = 0, \tag{30}$$

$$m\mu^{lo}_m = 0, \tag{31}$$

$$(\bar{m}-m)\mu^{hi}_m = 0, \tag{32}$$

$$h\mu^{lo}_h = 0, \tag{33}$$

$$(\bar{h}-h)\mu^{hi}_h = 0, \tag{34}$$

$$m, h, \mu^{lo}_m, \mu^{hi}_m, \mu^{lo}_h, \mu^{hi}_h \geq 0. \tag{35}$$

Assume an interior solution exists for both $h \in (0, \bar{h})$ and $m \in (0, \bar{m})$. By complementarity slackness conditions, $\mu_h^{hi} = \mu_h^{lo} = \mu_m^{hi} = \mu_h^{lo} = 0$. Then by combining (29) and (30) we get $\partial P_i^I / \partial m = \partial P_i^I / \partial h < 0$. In this edge case, there is a continuum of solutions, so assume without loss of generality that the agent chooses $m > 0$ and $h = 0$.

Let us now consider the case where $\partial P_i^I / \partial m < \partial P_i^I / \partial h < 0$. Simple manipulations yield

$$\frac{\partial P_i^I}{\partial m} - \frac{\partial P_i^I}{\partial h} = \frac{1}{1-\theta_i} \left[\left(1 - \tau \cdot \frac{(I_{i,t} - M_{i,t}^I + M_{j,t}^I)}{N_{i,t}} \right)^{\mathscr{C}_{i,t}^h} - \left(1 - \tau \cdot \frac{(I_{j,t} - M_{j,t}^I + M_{i,t}^I)}{N_{j,t}} \right)^{\mathscr{C}_{i,t}^m} \right] < 0,$$

By combining (29) and (30) we have:

$$\delta \underbrace{(U_i^{I'} - U_i^{S'})}_{\leq 0} \left(\frac{\partial P_i^I}{\partial m} - \frac{\partial P_i^I}{\partial h} \right) = \mu_m^{hi} + \mu_h^{lo} - \mu_h^{hi} - \mu_m^{lo}.$$

Since $U_i^{I'} < U_i^{S'}$ (Lemma 1) and $\partial P_i^I / \partial m < \partial P_i^I / \partial h < 0$, the left hand side is positive. Then we have the following cases:

- $h \in (0, \bar{h}]$ and $m = \bar{m} > 0$: i.e. $\mu_h^{lo} = 0$, $\mu_h^{hi} \geq 0$, $\mu_m^{lo} = 0$, $\mu_m^{hi} > 0$; $\mu_m^{hi} > \mu_h^{hi}$;
- $h = 0$ and $m \in (0, \bar{m}]$: i.e. $\mu_h^{lo} > 0$, $\mu_h^{hi} = 0$, $\mu_m^{lo} = 0$, $\mu_m^{hi} \geq 0$;
- $h = 0$ and $m = 0$: i.e. $\mu_h^{lo} > 0$, $\mu_m^{lo} \geq 0$, $\mu_h^{lo} > \mu_m^{lo}$;

which identify situations in which susceptibles weakly prefer travel to isolation as an infection avoidance mechanism. A similar reasoning can be applied to show that the reverse is true when $\partial P_i^I / \partial m < \partial P_i^I / \partial h < 0$.

Next we prove Proposition 2.(b). The proposition explores conditions under which the lagrange multiplier associated with the lower bound of home isolation is strictly positive ($\mu_h^{lo} > 0$), and, accordingly, agents do not isolate for infection avoidance purposes. First, independently of the presence of direct utility benefits

from travels, inspection of equation (30),

$$\mu_h^{lo} = \frac{du_i}{dc} w\bar{l} + \frac{\delta(U_i^{S'} - U_i^{I'})}{1-\theta_i} \left[\underbrace{\left(1 - \tau \cdot \frac{(I_{i,t} - M_{i,t}^I + M_{j,t}^I)}{N_{i,t}}\right)^{\mathscr{C}_{i,t}^l} - \left(1 - \tau \cdot \frac{(I_{i,t} - M_{i,t}^I + M_{j,t}^I)}{N_{i,t}}\right)^{\mathscr{C}_{i,t}^h}}_{\to \quad 0 \quad \text{as home infection rates go to zero}} \right]$$

shows that as infection rate in the home region goes to zero, the term in brackets on the right-hand-size goes to zero, and the multiplier converges to the marginal utility benefits of working, which is strictly positive.

Second, we explore how the relative benefits of travel choices affect the attractiveness of home isolation. To do so, in presence of direct utility benefits of travel we replace (29) with

$$\frac{du_i}{dm} - \frac{du_i}{dc} w\bar{l} + \delta(U_i^{I'} - U_i^{S'}) \frac{\partial P_i^I}{\partial m} + \mu_m^{lo} - \mu_m^{hi} = 0$$

Subtracting this expression from (30), and manipulating yields

$$\mu_h^{lo} = \frac{du_i}{dm} - \mu_m^{hi} + \frac{\delta(U_i^{S'} - U_i^{I'})}{1-\theta} \left[\underbrace{\left(1 - \tau \cdot \frac{(I_{j,t} - M_{j,t}^I + M_{i,t}^I)}{N_{j,t}}\right)^{\mathscr{C}_{i,t}^m} - \left(1 - \tau \cdot \frac{(I_{i,t} - M_{i,t}^I + M_{j,t}^I)}{N_{i,t}}\right)^{\mathscr{C}_{i,t}^h}}_{\text{Effectiveness of Travel relative to Isolation in reducing infection exposure}} \right]$$

Suppose: *(i)* home and foreign infection rates are sufficiently small (term in squared brackets goes to zero) or travel is more effective than home isolation in reducing the likelihood of infection (term in squared brackets is positive); *(ii)* marginal utility benefits of travel are sufficiently large, $\partial u / \partial m$; and *(iii)* the shadow value of relaxing the upper bound constraint on travel, μ_m^{hi}, is not too large. Under *(i)-(iii)* the lagrange multiplier μ_h^{lo} is positive, agents do not isolate and prefer travel for infection avoidance purposes.

A.4 Proof of Proposition 3

Pre-pandemic problem. The solution to the pre-pandemic agents' problem (5) satisfies the following FOC:

$$\frac{\beta_i}{m_{i,t}^{pre}} = \frac{(1-\beta_i)}{1-m_{i,t}^{pre}},$$

which implies $m_{i,t}^{pre} = \beta_i$.

Infectious and recovered problems. Likewise, the infectious and recovered FOCs are, respectively,

$$\frac{\beta_i^I}{m_{i,t}^I} = \frac{(1-\beta_i^I)}{(1-\theta_i)-m_{i,t}^I},$$
$$\frac{\beta_i}{m_{i,t}^R} = \frac{(1-\beta_i)}{(1-\theta_i)-m_{i,t}^R},$$

which imply $m_{i,t}^I = \beta_i^I(1-\theta_i)$ and $m_{i,t}^R = \beta_i(1-\theta_i)$.

Susceptible Problem. The FOC for the susceptible is:

$$\frac{\beta_i}{m_{i,t}^S} + \delta(U_{i,t+1}^I - U_{i,t+1}^S)\frac{\partial P_{i,t}^I}{\partial m_{i,t}^S} = \frac{(1-\beta_i)}{(1-\theta_i)-m_{i,t}^S},$$

where $\frac{\partial P_{i,t}^I}{\partial m}$ is given by (18).

Let $B \equiv \delta(U_{i,t+1}^S - U_{i,t+1}^I)\frac{\partial P_{i,t}^I}{\partial m}$, and rearrange the susceptibles' first order condition.

$$\frac{\beta_i}{m_{i,t}^S} = \frac{(1-\beta_i)+B(1-\theta_i)-Bm_{i,t}^S}{(1-\theta_i)-m_{i,t}^S},$$

The marginal benefits of travel in the left-hand-side is an hyperbolic function with a vertical asymptote at 0, strictly decreasing in the feasible set $m_{i,t}^S \in [0,\bar{m}]$. The right-hand-side is an hyperbolic function with vertical asymptote at $(1-\theta_i)$ and strictly increasing in the feasible set $m_{i,t}^S \in [0,\min\{\bar{m},1-\theta_i\}]$. Accordingly, given $B \equiv \delta(U_{i,t+1}^S - U_{i,t+1}^I)\frac{\partial P_{i,t}^I}{\partial m}$, there exists a unique real interior solution to the susceptible problem for $m \in [0,1-\theta]$. (Note, the upper-bound $\bar{m}$ may still be binding.)

Characterization of the solution. The solution to the susceptible problem consists of one of the roots $(\hat{m}^S_+, \hat{m}^S_-)$ that solve the quadratic equation

$$(m^S_{it})^2 - \left(\frac{1}{B} + (1-\theta_i)\right) m^S_{it} + \frac{\beta_i(1-\theta_i)}{B} = 0, \tag{36}$$

where

$$\hat{m}^S_+ \equiv \frac{1}{2}\left((1/B + (1-\theta_i)) + \sqrt{(1/B + (1-\theta_i))^2 - 4\beta_i(1-\theta_i)/B}\right),$$
$$\hat{m}^S_- \equiv \frac{1}{2}\left((1/B + (1-\theta_i)) - \sqrt{(1/B + (1-\theta_i))^2 - 4\beta_i(1-\theta_i)/B}\right),$$

From Proposition 1 we know that the sign of $\frac{\partial P^I_{i,t}}{\partial m}$ distinguishes the two cases of travel as infection avoidance asset (< 0) or liability (> 0), and in turn determins whether agents travel more or less than recovered, $m^R_{i,t} = (1-\theta_i)\beta_i$.

When $\frac{\partial P^I_{i,t}}{\partial m} < 0$, we have that $-4\beta_i(1-\theta_i)/B > 0$. Accordingly,

$$\sqrt{(1/B + (1-\theta_i))^2 - 4\beta_i(1-\theta_i)/B} > \sqrt{(1/B + (1-\theta_i))^2} = |\frac{1}{B} + (1-\theta_i)| \geq \frac{1}{B} + (1-\theta_i)$$

Accordingly, $\hat{m}^S_-$ is negative and not feasible. The unique solution in the case of travel as infectious avoidance asset is therefore $\hat{m}^S_+ > 0$

Let us now consider the case of travel as infectious avoidance liability, $\frac{\partial P^I_{i,t}}{\partial m} > 0$. From 1 we know that for any B the solution is lower than $m^R_{i,t} = (1-\theta_i)\beta_i$. By contradiction, let us suppose that the solution is the $\hat{m}^S_+$ root. Then

$$\left((1/B + (1-\theta_i)) + \sqrt{(1/B + (1-\theta_i))^2 - 4\beta_i(1-\theta_i)/B}\right) \leq 2(1-\theta_i)\beta_i$$

We also know that traveling decreases in B. Accordingly, let us focus on the case where $B \to \infty$, which gives the minimum of the left-hand-side for $B \in \mathbb{R}_+$ (travel as

infectious avoidance liability),

$$(1-\theta_i)+\sqrt{((1-\theta_i))^2} \leq 2(1-\theta_i)\beta_i$$
$$2(1-\theta_i) \leq 2(1-\theta_i)\beta_i$$

which reaches a contradiction, since $\beta_i < 1$ ($\perp$).

Since a unique solution exists, it follows that when $\frac{\partial P^I_{i,t}}{\partial m} > 0$, the susceptible optimal travel choice is the left-root,

$$\hat{m}^S_- \equiv \frac{1}{2}\left((1/B+(1-\theta_i)) - \sqrt{(1/B+(1-\theta_i))^2 - 4\beta_i(1-\theta_i)/B}\right) \leq m^R_{i,t}.$$

Accordingly, under Assumption 1, absent isolation choices, susceptible choose to travel more when traveling reduces the likelihood of becoming infectious $\left(\frac{\partial P^I_{i,t}}{\partial m^S_{i,t}} < 0\right)$ and less otherwise,

$$m^S_{i,t} = \begin{cases} \frac{(1+B(1-\theta_i))+\sqrt{(1+B(1-\theta_i))^2-4B\beta_i(1-\theta_i)}}{2B}, & \frac{\partial P^I_{i,t}}{\partial m^S_{i,t}} < 0 \quad \text{Inf. Avoidance Asset} \\ \frac{(1+B(1-\theta_i))-\sqrt{(1+B(1-\theta_i))^2-4B\beta_i(1-\theta_i)}}{2B}, & \frac{\partial P^I_{i,t}}{\partial m^S_{i,t}} > 0 \quad \text{Inf. Avoidance Liability} \end{cases}$$

Finally, we show the equality in (21). Define $\tilde{B} \equiv B(1-\theta_i)$. From (36) we have

$$B(m^S_{it})^2 - \left(1+(1-\theta_i)B\right)m^S_{it} + \beta_i(1-\theta_i) = 0.$$

This implies,

$$\begin{aligned}
m^S_{i,t} &= \frac{\left(1+(1-\theta_i)B\right) \pm \sqrt{\left(1+(1-\theta_i)B\right)^2 - 4B\beta_i(1-\theta_i)}}{2B} \\
&= \frac{1}{2B} + \frac{(1-\theta_i)}{2} \pm \frac{\sqrt{\left(1+(1-\theta_i)B\right)^2 - 4B\beta_i(1-\theta_i)}}{2B} \\
&= \frac{(1-\theta_i)}{2}\left(1+\frac{1}{\tilde{B}}\right) \pm \frac{(1-\theta_i)}{2\tilde{B}}\sqrt{\left(1+\tilde{B}\right)^2 - 4\beta_i\tilde{B}} \\
&= \frac{m^R_{i,t}}{2\beta_i}\left(1+\frac{1}{\tilde{B}}\right) \pm \frac{m^R_{i,t}}{2\tilde{B}\beta_i}\sqrt{1+\tilde{B}(\tilde{B}+2(1-2\beta_i))} \\
&= m^R_{i,t}\left[\frac{1}{2\beta_i} + \frac{1}{2\beta_i\tilde{B}}\left(1 \pm \sqrt{1+\tilde{B}(\tilde{B}+2(1-2\beta_i))}\right)\right].
\end{aligned}$$

Thus,

$$\begin{aligned}
\frac{m^S_{i,t}}{m^R_{i,t}} &= \frac{1}{2\beta_i} + \frac{1}{2\beta_i\tilde{B}}\left(1 \pm \sqrt{1+\tilde{B}(\tilde{B}+2(1-2\beta_i))}\right) \\
&= \frac{1}{2\beta_i} + \frac{2\beta_i - 1}{2\beta_i} + \left[\frac{1-2\beta_i}{2\beta_i} + \frac{1}{2\beta_i\tilde{B}}\left(1 \pm \sqrt{1+\tilde{B}(\tilde{B}+2(1-2\beta_i))}\right)\right] \\
&= 1 + \left[\frac{1-2\beta_i}{2\beta_i} + \frac{1}{2\beta_i\tilde{B}}\left(1 \pm \sqrt{1+\tilde{B}(\tilde{B}+2(1-2\beta_i))}\right)\right].
\end{aligned}$$

Now, to prove (22), note that for an interior solution with $h^S_{i,t} > 0$, the susceptible agent's FOCs imply

$$\frac{\beta_i}{m^S_{i,t}} + \delta(U^I_{i,t+1} - U^S_{i,t+1})\frac{\partial P^I_{i,t}}{\partial m^S_{i,t}} = \delta(U^I_{i,t+1} - U^S_{i,t+1})\frac{\partial P^I_{i,t}}{\partial h^S_{i,t}}.$$

Thus,

$$
\begin{aligned}
m^S_{i,t} &= \frac{\beta_i}{\delta(U^I_{i,t+1} - U^S_{i,t+1})(\frac{\partial P^I_{i,t}}{\partial h^S_{i,t}} - \frac{\partial P^I_{i,t}}{\partial m^S_{i,t}})} \\
&= \frac{(1-\theta_i)\beta_i}{\delta(U^I_{i,t+1} - U^S_{i,t+1})\left(\left(1-\tau\cdot\frac{(I_{j,t}-M^I_{j,t}+M^I_{i,t})}{N_{j,t}}\right)^{\mathscr{C}^m_{i,t}} - \left(1-\tau\cdot\frac{(I_{i,t}-M^I_{i,t}+M^I_{j,t})}{N_{i,t}}\right)^{\mathscr{C}^h_{i,t}}\right)} \\
&= \frac{m^R_{i,t}}{\delta(U^S_{i,t+1} - U^I_{i,t+1})\left(\left(1-\tau\cdot\frac{(I_{i,t}-M^I_{i,t}+M^I_{j,t})}{N_{i,t}}\right)^{\mathscr{C}^h_{i,t}} - \left(1-\tau\cdot\frac{(I_{j,t}-M^I_{j,t}+M^I_{i,t})}{N_{j,t}}\right)^{\mathscr{C}^m_{i,t}}\right)}.
\end{aligned}
$$

B Solution Algorithm

We introduce a solution algorithm to recover the sequence of probabilities that satisfy (10). The algorithm iterates between the epidemiological and economic model until the two are consistent.[53] The algorithm follows these steps:

1. **Initialize the Aggregate Disease State**: Start with an initial aggregate disease state of the economy, $\mathscr{T}_{i,0}$, where a small portion of the population is infectious to initiate the pandemic.

2. **Guess Infection Probabilities and Travel Choices**: Guess the region-specific time series of infection probabilities, $\{\mathscr{P}^{SI}_{i,t}\}_{t=1}^{T}$, and aggregate susceptibles' travels and consumption, $\{\hat{M}^{S}_{i,t}, \hat{C}^{S}_{i,t}\}_{t=1}^{T}$

3. **Simulate the Pandemic Evolution Forward**: Given $\{\mathscr{P}^{SI}_{i,t}\}_{t=1}^{T}$, simulate the evolution of the pandemic according to equations (1) through (4). Collect the aggregate disease state for each period, $\mathscr{T}_{i,t} = (S_{i,t}, I_{i,t}, R_{i,t}, D_{i,t})$.

4. **Compute Regional Populations**: Determine the population in each region and period using the sequence of aggregate disease states and equation (12).

5. **Solve the Agents Problem Backward**: Given $\{\mathscr{T}_{i,t}\}$, solve the susceptible agent's problem described in (6). Solve backward from the last period, $t = T$, to the beginning of the pandemic, $t = 0$.[54] Collect choices of infectious and recovered individuals, which are independent of the aggregate disease state, $\mathscr{T}_{i,t}$.

6. **Re-Simulate the Pandemic Forward**: Simulate the pandemic forward from $t = 0$ to T using the endogenous choices together with (11) to compute the share of susceptible which become infectious in each period $\{\tilde{P}^{I}_{i,t}\}_{t=1}^{T}$.

[53] In Appendix F.3, we verify the accuracy of the algorithm by comparing to another approach which uses the Fischer-Burmeister function to solve the equilibrium equations directly.

[54] We assume the pandemic ends with certainty at time T (e.g., due to the introduction of a vaccine). Thus, at time $T+1$, the remaining S, I, and R types become identical, all policy restrictions are lifted, and the continuation value for each type at time T is derived from the solution to (5).

7. **Compare and Update Guesses**: Compare the aggregate disease states generated from the initial guesses $\{\hat{P}^I_{i,t}\}^T_{t=1}$ with those derived from the endogenous choices $\{\tilde{P}^I_{i,t}\}^T_{t=1}$. If the sequences are sufficiently far, update the guesses and repeat steps 2-7 until convergence.

C More on Quantitative Analysis

C.1 Endogenous Travel and Isolation Choices

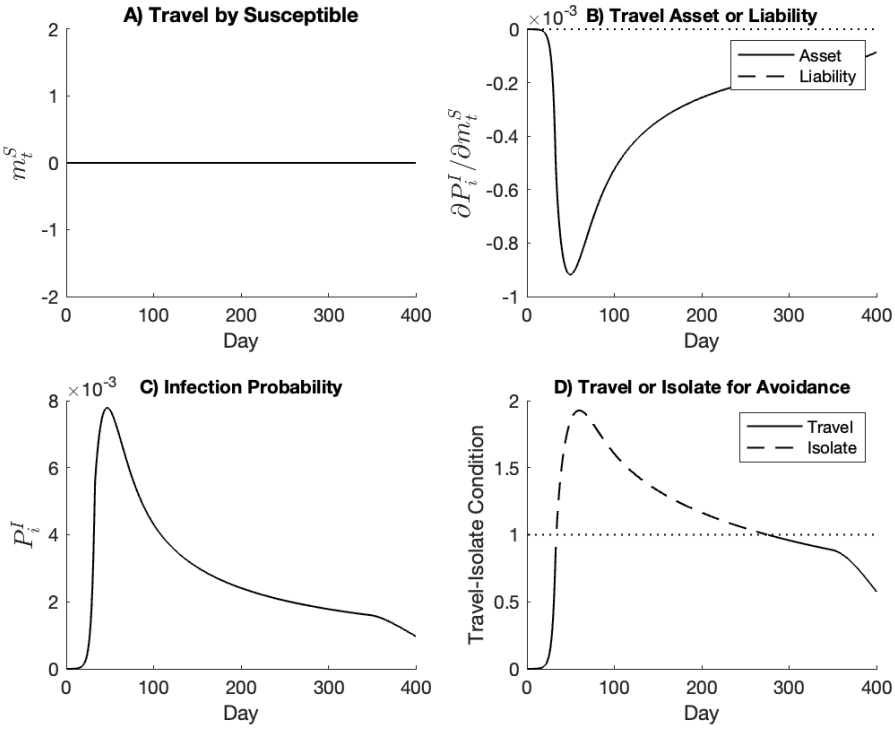

Figure 4: Symmetric regions with no utility from travel.

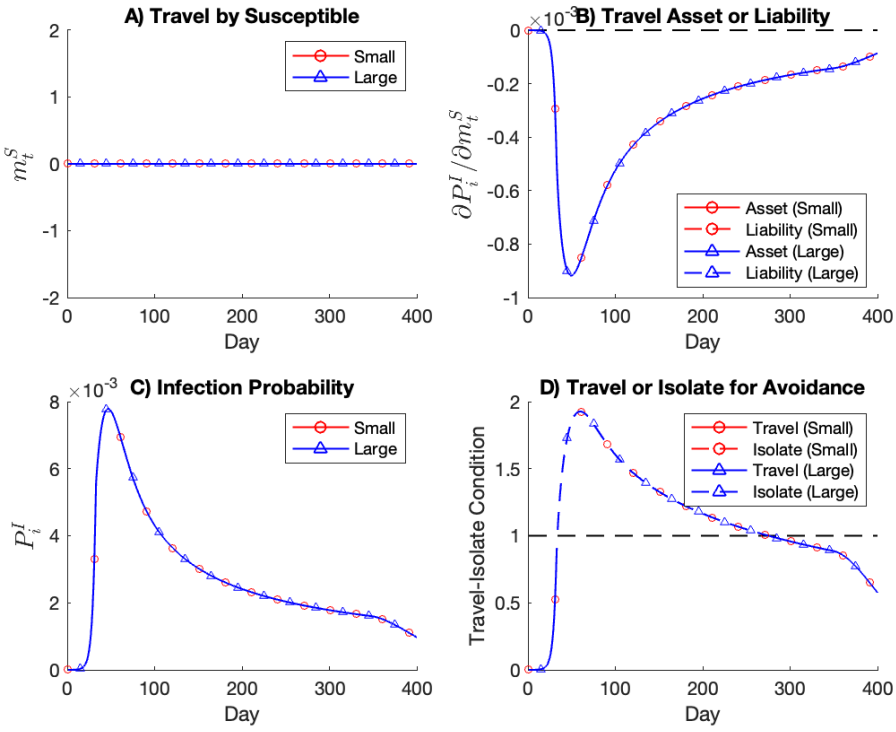

Figure 5: Asymmetric size regions with no utility from travel.

C.2 Disease Dynamics and Behavioral Responses

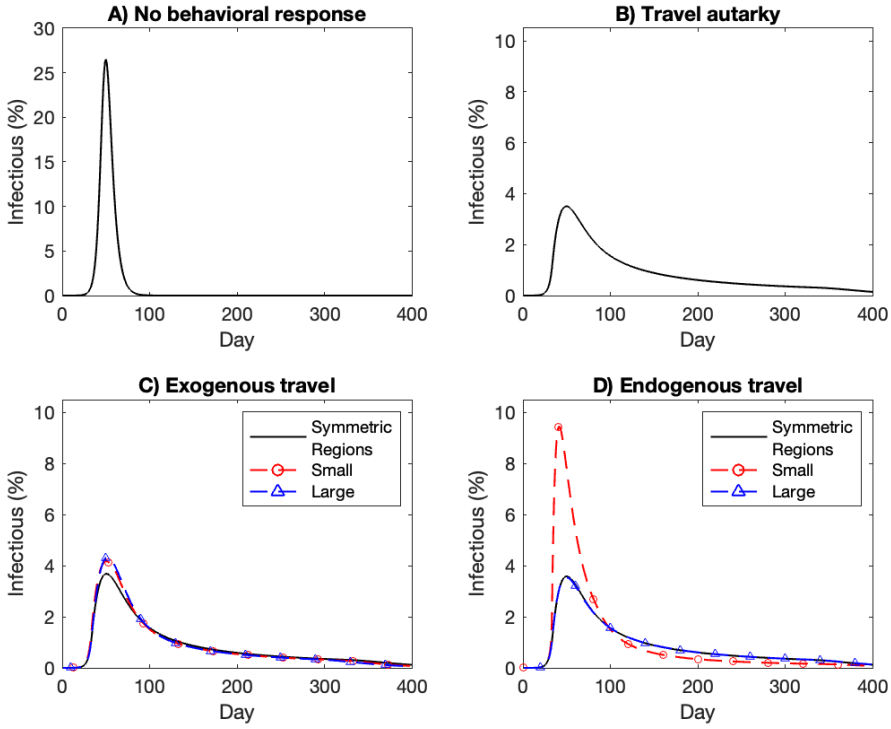

Figure 6: Infectious under no behavioral response, home isolation autarky, exogenous, and endogenous travel (benchmark) model specifications with identical home (small) and foreign (large) infectious seeds.

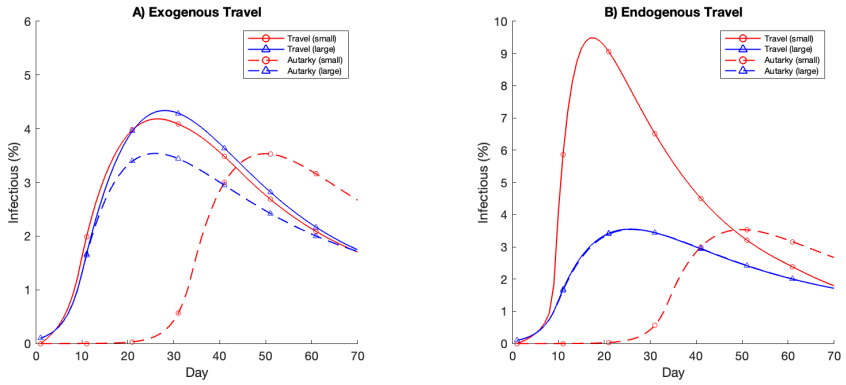

Figure 7: Infectious under alternate model specifications, contrasting home isolation autarky with exogenous (Panel A) or endogenous (Panel B) travel. In all cases, home (small) infectious seed is less than foreign (large) infectious seed $I_{0,H} < I_{0,F}$.

C.2.1 Asymmetric Autarky Economies

Table 5: Peak Infectious and Days Between Peaks under Travel Autarky

	Peak Infectious (%)		Days Between Peaks	
	$I_{0,H} = I_{0,F}$	$I_{0,H} < I_{0,F}$	$I_{0,H} = I_{0,F}$	$I_{0,H} < I_{0,F}$
Symmetric Size				
No Behavioral Response	26.52	26.52	0	24
Home Isolation	3.51	3.51	0	24
Asymmetric Size				
No Behavioral Response	26.46	26.46	0	24
Home Isolation	3.53	3.53	0	24

C.2.2 No Home Isolation

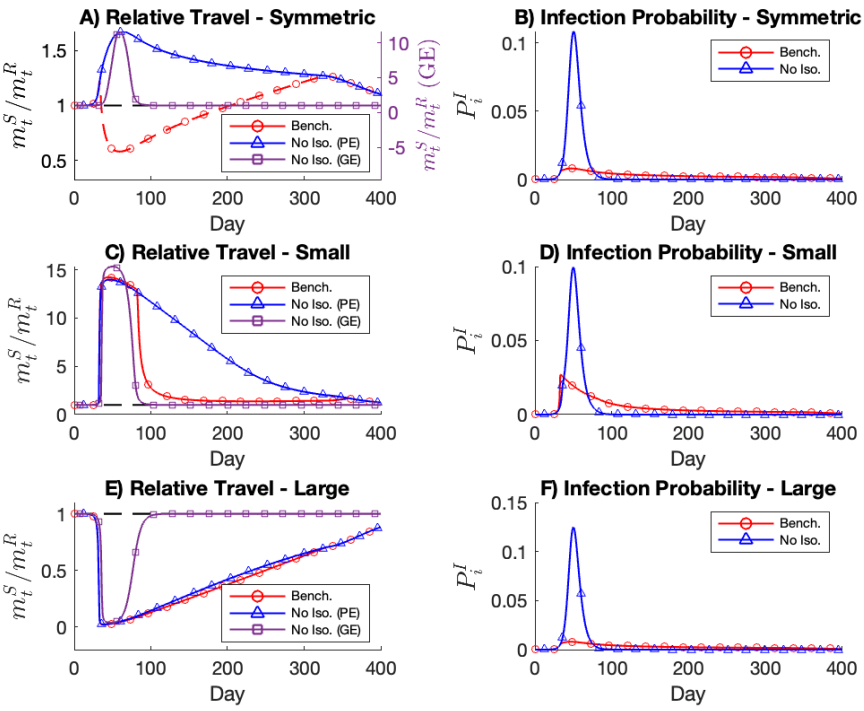

Figure 8: Susceptibles' travel relative to recovered (Panels A, C, and E) and infection probability (Panels B, D, and F) under alternative model specifications. Under the benchmark model (Bench.), agents can isolate. Under the no-isolation partial equilibrium (PE) model, agents cannot isolate and disease dynamics are generated by the benchmark model. Under the no-isolation general equilibrium (GE) model agents cannot isolate and disease dynamics are consistent with agents' choices.

This section compares susceptibles' travel choices and resulting disease dynamics in economies with and without home isolation. Mirroring the exposition in the text, we analyze both a symmetric and asymmetric economy.

We find that absent home isolation, agents overrely on travel for disease avoidance purposes in both symmetric and asymmetric economies. To establish this point, Panel A of Figure 8 shows the susceptibles' travel choices for: (i) our benchmark economy where susceptibles can isolate (Bench.); (ii) a partial equilibrium economy where agents cannot isolate and the disease dynamics are generated by

the benchmark economy where susceptibles can isolate (PE); and (iii) an economy where agents cannot isolate with its own internally consistent disease dynamics (GE). Panel B reports disease dynamics for both model specifications. We then replicate this analysis for the asymmetric economy and report the associated travel responses and disease dynamics for the small region in Panel C and D and for the large region in Panel E and F, respectively.

Panel A shows that susceptibles faced with the same disease dynamics as the benchmark overrely on travel for infection avoidance purposes in absence of home isolation. This is evidenced by the blue line with triangle marks consistently showing higher susceptibles' travel intensity throughout the pandemic and always above the recovered ones (>1). A similar pattern emerges for susceptibles' travel choices in the small region (Panel C)—where travel is effective for infectious avoidance throughout the pandemic—but not in the large region, where travel is an infection avoidance liability (as discussed in Section 5.1).

Crucially, the coupled general equilibrium (GE) travel responses and disease dynamics show a remarkably different behavior in models with and without home isolation across both symmetric and asymmetric economies. Absent home isolation, susceptibles are unable to meaningfully reduce contacts with infectious, greatly accelerating the pandemic (Panels, B, D, and F, blue lines with marked triangles) both by accentuated traveling and working activities.

Finally, Table 6 shows the absence of home isolation yields a relationship between disease dynamics and travel choices that is inconsistent with the data. See Section 7 for more information.

Table 6: The Avoidance Role of Travel in the Data and Model

	Data		Model without isolation	
	(1)	(2)	(3)	(4)
log relative infectious$_{i,t}$	-0.337^{***}	-0.489^{***}	0.021^{**}	0.027^{***}
	(0.027)	(0.034)	(0.009)	(0.010)
log relative infectious$_{i,t} \cdot d_t^{high}$		0.376^{***}		-0.023^{***}
		(0.037)		(0.008)
County FE	Yes	Yes	No	No
Day FE	Yes	Yes	No	No
N	298,373	298,373	729	729
R^2	0.971	0.971	0.015	0.038

Note: OLS estimates of the effect of the log relative infectious share in county i on the log of inbound travel to region i, multiplied by 100. Columns (1)-(2) report estimates using the PlaceIQ cellphone data and Coronavirus Resource Center data, covering the period from March 11, 2020 to August 21, 2021. Columns (3)-(4) report estimates using data generated by the model without home isolation. Robust standard errors are in parenthesis.

C.3 Public Policy under Pandemic Federalism

C.3.1 Welfare Calculation

We report welfare effects in consumption equivalent units. The value for an economy with no pandemic is

$$U^{\text{no pandemic}} = \sum_{t=0}^{\infty} \delta^t \sum_i \lambda_i \left(u(c_{i,t}, m_{i,t}) + P^{D^*} \Omega_i \right), \tag{37}$$

where $c_{i,t}, m_{i,t}$ solve (5). The value for the economy that experiences the pandemic is

$$\begin{aligned} U^{\text{pandemic}} = &\sum_{t=0}^{T} \delta^t \sum_i \left(\sum_{z \in \{S,I,R\}} z_{i,t} u^z(c_{i,t}^z, m_{i,t}^z) + D_{i,t}^* \Omega_i \right) \\ &+ \sum_{t=T+1}^{\infty} \delta^t \sum_i \lambda_i^{post} \left(u(c_{i,t}, m_{i,t}) + P^{D^*} \Omega_i \right), \end{aligned} \tag{38}$$

where $D^*_{i,t}$ are new deaths from either the virus or other causes and λ_i^{post} is the population share of i post-pandemic (i.e. the population share pre-pandemic less those that die from the virus). Define $U(\xi)$ welfare under no pandemic when consumption is adjusted by ξ,

$$U(\xi) \equiv \sum_{t=0}^{\infty} \delta^t \sum_i \lambda_i \left(u\left(c_{i,t}(1+\xi), m_{i,t}\right) + P^{D^*} \Omega_i \right) \tag{39}$$

Under each pandemic scenario, we report the value ξ (in percentage points) that makes welfare in the absence of a pandemic equal to that under the pandemic, $U(\xi) = U^{\text{pandemic}}$. A negative ξ indicates a welfare *loss* relative to the no-pandemic economy.

C.3.2 Exogenous Social Distancing Policies

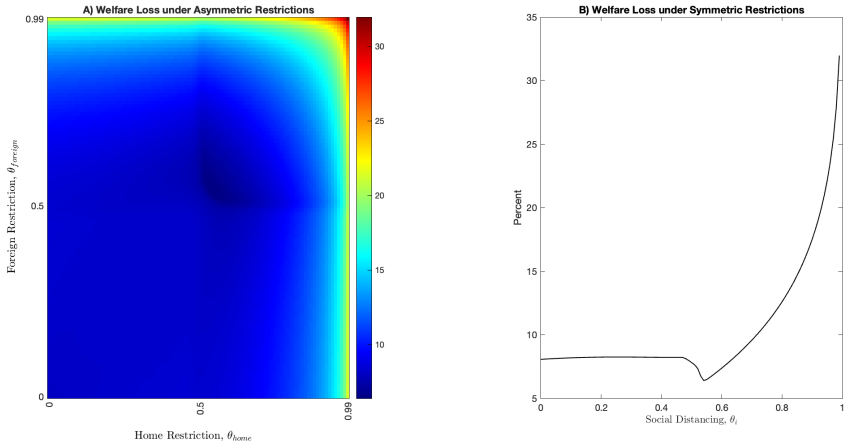

Figure 9: Welfare under different social distancing requirements - Symmetric Economy

C.3.3 Exogenous Travel Bans

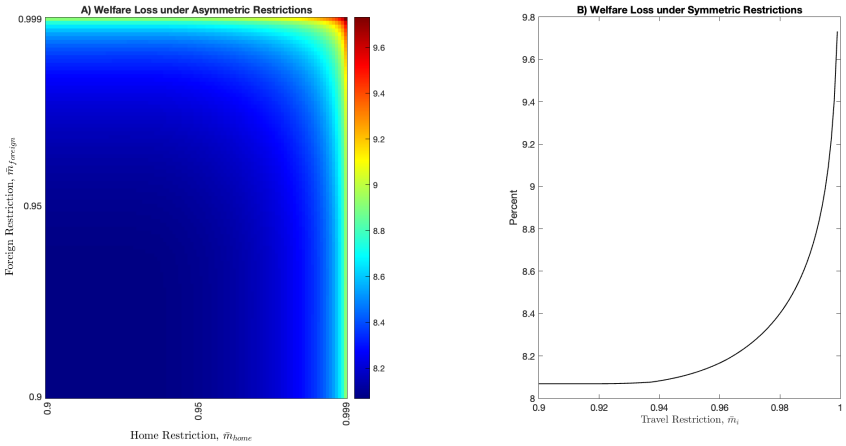

Figure 10: Welfare under different travel restrictions - Symmetric Economy

Table 7: Optimal Travel Bans

	Fixed Travel restriction	Infections-Guided Travel restriction	Infections-Guided Threshold (%)
Symmetric	None	None	0
Asymmetric Small	0.25	0.5	0
Asymmetric Large	None	0.75	2

Note: Optimal travel bans (aggregate-welfare maximizing) for symmetric and asymmetric regions, with both fixed and infections-guided rules. Travel restriction denotes the relative reduction of travel as a share of the pre-pandemic level; for example a value of x implies that travel is limited to at most a $(1-x)$ share of the pre-pandemic travel level. "None" indicates no restriction on travel. Infections-guided restrictions are active only when the global infectious share is above the threshold value.

C.3.4 Nash Solution to Optimal Public Policies

Travel restriction game. We study the Nash equilibrium of the travel restriction game with a fixed policy rule when the foreign region begins with a higher initial infectious share, $I_{foreign,0} = 0.1\%$, $I_{home,0} = 0.0001\%$. In all cases, the prisoners dilemma outcome with $\bar{m}_{home} = \bar{m}_{foreign} = 99\%$ is the unique Nash equilibrium outcome. Table 8 displays equilibrium outcomes.

Table 8: Nash equilibrium outcomes under alternate infection seeding

	Peak Infectious	Welfare
Symmetric Size	3.59	-23.35
Asymmetric Size - Small	4.22	-5.03
Asymmetric Size - Large	3.53	-21.54

Social distancing game. Consider a game where local policymakers choose social distancing requirements for their own region θ_i, taking the policy of the other region as given. We allow policymakers to choose from the grid $\theta_i \in \{0, 0.25, 0.5, 0.75, 0.99\}$. That is, a reduction of time spent on economic activities of 25%, 50%, 75%, or 99%, or no restriction. In all cases, the unique Nash equilibrium is that with *no* social distancing restrictions, $\theta_i = 0$, which lead to identical outcomes to those presented in Section 5.2 under endogenous travel.

D Surrogate Models

Consider a vector $\underline{\mathbf{x}} \in \mathbb{X} \subset \mathbb{R}^n$ which summarizes the state of the economy; this vector may include the aggregate disease states (S, I, R, D) as well as model parameters (or "pseudo-states"). Now, let $y \in \mathbb{R}^m$ be a vector of outcomes of our epi-econ model associated with a particular input vector $\underline{\mathbf{x}}$; for example, these outcomes could be the cumulative welfare losses reported in the last column of Table 3. The key intuition behind the surrogate model approach is to find an estimate,

$$\hat{f} : \mathbb{X} \to \mathbb{R}^m$$

of the unknown mapping $f : \mathbb{X} \to \mathbb{R}^m$ between the input space $\mathbb{X}$ and epi-econ model outcomes $y = f(\underline{\mathbf{x}})$.

To do so, we proceed as follows. As it is not feasible to evaluate the unknown function f over the entire domain $\mathbb{X}$, we solve the epi-econ model at finitely many points, $\underline{\mathbf{x}} \in \mathbb{X}$, to construct a rich training sample of $(f(\underline{\mathbf{x}}), \underline{\mathbf{x}})$ (Subsection D.1). We then use this training sample to estimate our surrogate model, $\hat{f} : \mathbb{X} \to \mathbb{R}^m$, that is an estimator of the epi-econ vector-valued outcomes $f(\mathbb{X})$ (Subsection D.2). For our purposes, we choose different specification of our surrogate models for each outcome (Subsection D.3). In our quantitative analysis, we then leverage the estimated (trained) surrogate model, to generate predictions and conduct sensitivity analysis without the need to solve the epi-econ model additional times.

D.1 Generating the Training Sample

We study the following model parameters: infectious productivity ϕ, reproductive number R_0, duration of infectiousness d, case fatality rate μ, time 0 infectious seeds $I_{home,0}, I_{foreign,0}$, and the home population share λ_{home}.

First we use estimates of disease characteristics from the epidemiological literature collected in Table 9 to determine the boundaries of our grids. For R_0, we choose a lower bound of 1.01 ($\mathrm{R}_0 > 1$ is necessary to start a pandemic), and an upper bound of 18, corresponding to estimates for the highly infectious measles. We set the duration of infectiousness, d, within a range of 5 days (COVID-19)

Table 9: Estimates of epidemiological parameters across diseases

Disease	R_0	d	μ
Ebola	1.51-2.53 (Michigan)	6 (CDC)	0.5 (WHO)
H1N1	1.46-1.48 (Michigan)	∼8 (De Serres et al., 2010)	0.0002 (CDC)
Seasonal flu	0.9-2.1 (Michigan)	8 (CDC)	0.0001 (CDC)
Measles	12-18 (Michigan)	8 (WHO)	0.0003 (CDC)
MERS	1 (Michigan)	10+ (CA Public Health)	<0.35 (WHO)
Polio	5-7 (Michigan)	20 (ECDC)	0.05-0.15 (ECDC)
SARS	<1-2.75 (Michigan)	10+ (IL Public Health)	0.03 (WHO)
Smallpox	5-7 (Michigan)	21 (CDC)	0.3 (WHO)

Table 10: Parameter ranges for surrogate model training sample

	ϕ	R_0	d	μ	$I_{i,0}$	λ_{home}
Lower bound	0.29	1.01	5	0.0001	1e-9	1e-5
Upper bound	1	18	21	0.5	1e-5	0.5

to 21 days (smallpox). The case fatality rate μ varies from 0.0001 (seasonal flu) to 0.5 (Ebola). As noted by Ash et al., 2022, the infectious productivity ϕ must lie in the range $[d_a/d_h, 1]$, where d_a is the duration of asymptomatic and d_h is the average duration of infection conditional on being hospitalized.[55] We use Ebola, which has particularly severe symptoms, to construct the lower bound for ϕ. This implies $\phi \in [0.29, 1]$.[56] Finally, we set the bounds for the initial infectious shares to $I_{i,0} \in [1e-9, 1e-5]$ ($i \in \{home, foreign\}$), and the home population share to $\lambda_{home} \in [1e-5, 0.5]$.

Second, we use a Sobol sequence (Sobol', 1967), a low-discrepancy, quasi-random sequence, to generate the training sample on the parameter space $\mathbb{X}$ defined by Table 10.[57] Our fast solution algorithm enables us to solve the 1,000,000 in a

[55] Infectious productivity is estimated as a weighted average of the (population) share of time spent in different degrees of disease severity (asymptomatic, minor sufferers, hospitalized). The restriction $\phi \in [d_a/d_h, 1]$ ensures the relevant population shares are non-negative. See Supporting Information 2.1.1 of Ash et al., 2022 for a discussion.

[56] Per the CDC, Ebola symptoms appear 2 - 21 days after exposure. Qureshi et al., 2015 report a mean hospitalization duration for Ebola patients of 7 days. From these, we assign a lower bound for ϕ of 2/7.

[57] Low-discrepancy sequences fill the sample space more evenly than does drawing points from a uniform distribution, and have been shown to work well in high-dimensional problems (see, e.g., Kucherenko and Sytsko, 2005). In addition, they improve over a grid-based approach by providing

reasonable timeframe—approximately 24 hours for the laissez-faire economies—by parallelizing across 64 (x86_64 AMD Milan) CPU cores on the CU Boulder Alpine Supercomputer.[58]

For each model economy (parameter vector), we collect results for both the laissez-faire equilibrium (Section 5.1) and the Nash equilibrium outcome to the travel restriction game (Section 5.3).

D.2 Training of the Surrogate Models

We train surrogate models to estimate time-invariant equilibrium outcomes, such as the peak infection in region i. The surrogate models are trained as function of the seven parameters $\underline{\mathbf{x}}^{params} = [\phi, R_0, d, \mu, I_{home,0}, I_{foreign,0}, \lambda_{home}]$, and are used to make predictions for the time-invariant outcomes,

$$\widehat{\text{Time-invariant Outcome}}_i = \hat{f}_i(\underline{\mathbf{x}}^{params}).$$

D.3 Surrogate Models Specifications

Following the approach in Chen, Didisheim, and Scheidegger (2023), we employ "deep surrogates" (i.e. surrogates constructed using deep neural networks). In the construction of any neural network, the user must specify the network "hyper-parameters" such as the number of hidden layers and nodes per hidden layer. We use K-fold cross-validation to select the model architecture.[59] We compare performance across networks with two or three hidden layers, and 10, 50, or 100 nodes per layer. We also choose the regularization parameter (L2 regularization) from the set

the surrogate information on the behavior of outcomes over the entire parameter space, rather than only on specific hyperplanes.

[58] We choose the full set of 1,000,000 parameter combinations before training the surrogate model. An alternate approach involves estimating the surrogate on an initial training sample, and subsequently choosing additional sample points in regions of the parameter space where the surrogate performs poorly (see e.g. Chen, Didisheim, and Scheidegger, 2023).

[59] K-fold cross-validation proceeds as follows. For each hyperparmeter combination under consideration, the data is split into K subsets (i.e. folds), with the model trained on $K-1$ folds, and evaluated on the remaining fold. This process is repeated K times for each hyperparameter set. Those hyperparameters which minimize the (average) loss during cross-validation are chosen.

$\{1e-1, 1e-2, ..., 1e-6\}$. The ReLU activation function is used to introduce non-linearity to the network, and we train using mini-batch stochastic gradient descent (Robbins and Monro, 1951; Bengio, 2012; Azinovic, Gaegauf, and Scheidegger, 2022) and the Adam optimization algorithm (Kingma, 2014).[60]

D.4 Travel as an Effective Asset

We define travel to be an effective asset when it reduces the infection probability and is preferred to isolation as an avoidance mechanism. Formally, travel is an effective asset if:

(a) $\partial P^I_{i,t}/\partial m^S_{i,t} < 0$ and $h^S_{i,t} = 0$ OR

(b) $\partial P^I_{i,t}/\partial m^S_{i,t} < 0$ and $h^S_{i,t} > 0$ and the denominator of (22) is less than one,

$$\delta(U^S_{i,t+1} - U^I_{i,t+1}) \left[\left(1 - \tau \cdot \frac{(I_{i,t} - M^I_{i,t} + M^I_{j,t})}{N_{i,t}} \right)^{\mathscr{C}^h_{i,t}} - \left(1 - \tau \cdot \frac{(I_{j,t} - M^I_{j,t} + M^I_{i,t})}{N_{j,t}} \right)^{\mathscr{C}^m_{i,t}} \right] < 1.$$

We report the average share of time for which travel is an effective asset, conditional on global infection rates being at least one in one million (the infection seed used in Section 5). For J economies, the statistic is given by

$$X^{\text{eff. asset}} \equiv \frac{1}{J} \sum_{j=1}^{J} \frac{1}{T^*_j} \sum_{t=1}^{T} \mathbb{I}(m^S_{home,t,j} \text{ is effective}) \cdot \mathbb{I} \left(\sum_i I_{i,t} \geq 1e-6 \right),$$

where $T^*_j \leq T$ denotes the number of periods with infection rates above one in one million for economy j, the first indicator function is equal to one when travel is an effective asset as defined by conditions (a) and (b) above, and the second indicator function is equal to one if global infection rates are above the cutoff.

[60] We use mini-batches of size 512 and a learning rate of 10^{-3}. We use early stopping which withholds a subset of the training data (5%) for validation during each epoch, and ends the training process when the model performance on the validation set stops improving. This helps to prevent overfitting.

We also report the average share of time for which travel is effective, conditional on global infection rates being at least one in one million and no more than 1%. The statistic is calculated

$$X^{\text{eff. asset low inf.}} \equiv \frac{1}{J}\sum_{j=1}^{J}\frac{1}{T_j^{**}}\sum_{t=1}^{T}\left[\mathbb{I}(m^S_{home,t,j} \text{ is effective})\cdot\mathbb{I}\left(\sum_i I_{i,t}\geq 1e-6\right)\right.$$
$$\left.\cdot\mathbb{I}\left(\sum_i I_{i,t}\leq 0.01\right)\right],$$

where $T_j^{**}\leq T$ denotes the number of periods with infection rates above one in one million and below 1% for economy j.

D.5 Permutation Feature Importance

The permutation feature importance is a methodology used to evaluate the relative importance of model parameters. This model inspection technique proceeds as follows. For each of the n parameters (features) $\underline{\mathbf{x}}\in\mathbb{X}\subset\mathbb{R}^n$, the column of the dataset corresponding to parameter (feature) d is randomly shuffled. Predictions are then made using the corrupted data. The permutation importance is then

$$\text{Permutation feature importance}(d) = S(f(\underline{\mathbf{x}}),\hat{f}(\underline{\mathbf{x}})) + \left[\underbrace{-\frac{1}{K}\sum_{k=1}^{K}S(f(\underline{\mathbf{x}}),\hat{f}(\underline{\mathbf{x}}_{k,d}))}_{\text{Permutations}}\right],$$

where $\underline{\mathbf{x}}_{k,d}$ is the corrupted data and the score $S(\cdot)$ denotes the prediction accuracy of the surrogate model (higher values of the score are associated with better accuracy of $\hat{f}(\underline{\mathbf{x}})$). We select as score function the negative of the mean absolute error, the same score function used to train our surrogate model. The first term reports the score before the shuffling. The second term (in squared brackets) reports the average score across the K permutations of the d parameter (feature). If a parameter d is irrelevant (for the model outcome), its permutations do not affect its score; in this case, the Permutation feature invariance gets close to 0. Conversely, permutations of

a relevant parameter would reduce the accuracy of the surrogate model fit, reducing (on average) its score, generating a positive second term in brackets. Accordingly, a more relevant parameter is associated with larger values of its Permutation feature importance.[61]

For comparability, Table 11 lists the permutation feature importance for each outcome in Figure 3, after normalizing each row to sum to one.

Table 11: Permutation Feature Importance

	ϕ	R_0	d	μ	$I_{home,0}$	$I_{foreign,0}$	λ_{home}
Endo. Travel and Isolation							
Travel Effective	0.15	0.36	0.06	0.2	0.04	0.03	0.16
Travel Effective ($I > 1\%$)	0.13	0.37	0.07	0.21	0.04	0.04	0.15
Disease Dynamics and Behavior							
Peak Sync. - Exogenous	0.1	0.25	0.13	0.18	0.11	0.11	0.11
Peak Sync. - Endogenous	0.18	0.32	0.07	0.2	0.01	0.02	0.2
Peak Inf. - Exogenous	0.09	0.41	0.06	0.16	0.02	0.03	0.22
Peak Inf. - Endogenous	0.27	0.26	0.05	0.14	0.05	0.04	0.18
Public Policy							
Peak Infection - Nash	0.04	0.45	0.02	0.05	0.0	0.0	0.44
Welfare Loss - Nash	0.19	0.38	0.02	0.21	0.02	0.02	0.17

D.6 Partial Dependence Plot

Partial dependence plots are used to illustrate the effect of an input (epi-econ parameter) on some output generated by a "black box" algorithm (Hastie et al., 2009). Let $\underline{\mathbf{x}} \in \mathbb{X} = \mathbb{X}_1 \times \mathbb{X}_2 \times \ldots \times \mathbb{X}_d \times \ldots \times \mathbb{X}_n \subset \mathbb{R}^n$. The Partial dependence plot reports for an arbitrary level of the parameter $x_d \in \mathbb{X}_d \subset \mathbb{R}$ (horizontal axis) an estimate of

[61] Permutation feature importance may take negative values when a model is overfit to noise or the model permutations accidentally disrupt misleading patterns learned by the model. Large negative values are therefore symptoms of problems in the surrogate model estimation. For irrelevant parameters, permutation feature importance may be negative due to numerical rounding factors. When Permutation feature importance$(d) < 0$ and $|\text{Permutation feature importance}(d)| < 1e-6 \cdot \sum_k |\text{Permutation feature importance}(k)|$, we set the permutation feature importance for parameter d to zero for computing the normalized values in Table 11.

the partial dependence of the model outcomes $f(x_d, \underline{\mathbf{x}}^C)$ on x_d,

$$\text{Partial dependence}(x_d) \equiv E\left[f(x_d, \underline{\mathbf{x}}^C)\right],$$

where the expectation is taken with respect to the complement parameter inputs, $\underline{\mathbf{x}}^C$, $\underline{\mathbf{x}}^C \equiv [x_1, ..., x_{d-1}, x_{d+1}, ..., x_n]$. This expectation is estimated for each value of x_d by

$$\widehat{\text{Partial dependence}}(x_d) \equiv \frac{1}{J}\sum_{j=1}^{J} \hat{f}(x_d, \underline{\mathbf{x}}_j^C),$$

where J is the number of economies, $\hat{f}(x_d, \underline{\mathbf{x}}_j^C)$ is the value of the estimated surrogate model at (an arbitrary) $x_d \in \mathbb{X}_d$ and $\underline{\mathbf{x}}_j^C$, where j indexes all occurrences of $\underline{\mathbf{x}}^C$ in the training data. The Partial dependence then measures the effect of parameter x_d on the model outcome, taking into account the average effect of all other parameters, $\underline{\mathbf{x}}^C$.

E More on Empirical Validation

This appendix provides supplemental information to Section 7.

E.1 Constructing the Stock of Infectious and Relative Infectious Share

We use data on new daily cases in region i on day t to construct a time series describing the evolution of the stock of infectious in i, $\{I_{i,t}\}_{t=0}^{T}$, where $t = 0$ and $t = T$ correspond to the start and end dates of the Johns Hopkins data. We assume the economy begins with no infectious in the initial period (corresponding to January 22, 2020), $I_{i,0} = 0$ for all i. Next, for all periods $t > 0$, we compute the stock of infectious using equation (2) in the main text, taking the new infections in region i on day t, $\mathscr{P}_i^{SI}(\mathscr{A}_t, \mathscr{T}_t)S_{i,t}$, from the Johns Hopkins data.

We compute the relative infectious rate, $X_{i,t}$, as the infectious share in i relative to the weighted average infectious share in all other US counties ($j \neq i$), weighted

by the county j population share,

$$X_{i,t} = \frac{\frac{I_{i,t}}{Pop_i}}{\sum_{j \neq i} \frac{I_{j,t}}{Pop_j} \cdot \frac{Pop_j}{\sum_{k \neq i} Pop_k}}.$$

E.2 Model Data

This section details the model-generated data used in Section 7. We assume the population of the home region is 1/3000th of the total population, and initialize the pandemic in the foreign region. The initial infectious seed is chosen so that the measure of new infectious in the first period matches the number of new cases on March 11, 2020 divided by the U.S. population. We calculate travel into the small region using the sum of travel by those in each disease state relative to the total measure of agents in the small region on day t,

$$Y_{home,t} = \frac{\sum_{Z \in \{S,I,R\}} M^Z_{foreign,t}}{N_{home,t}}.$$

The relative infectious in the home region is,

$$X_{home,t} = \frac{\frac{I_{home,t}}{S_{home,t}+I_{home,t}+R_{home,t}}}{\frac{I_{foreign,t}}{S_{foreign,t}+I_{foreign,t}+R_{foreign,t}}}.$$

F Further Robustness

This section provides further robustness tests.

F.1 Exposed disease state

We consider an extension of the model by adding a fifth disease state, "exposed," to the SIRD model. These exposed agents are pre-symptomatic and do not realize they have become exposed. They therefore make decisions as though they were susceptible. Following an incubation period, exposed individuals will then develop symptoms and become infectious. The SEIRD system governing the transitions

across disease states becomes:

$$
\begin{aligned}
S_{i,t+1} &= \left(1 - \mathscr{P}_i^{SI}(\mathscr{A}_t, \mathscr{T}_t) - P^{D^*}\right) S_{i,t} + \gamma\left(S_{i,t} + E_{i,t} + I_{i,t} + R_{i,t}\right), \\
E_{i,t+1} &= \left(1 - P^{D^*} - P^I\right) E_{i,t} + \mathscr{P}_i^{SI}(\mathscr{A}_t, \mathscr{T}_t) S_{i,t}, \\
I_{i,t+1} &= \left(1 - P^{D^*} - P^R - P^D\right) I_{i,t} + P^I E_{i,t}, \\
R_{i,t+1} &= \left(1 - P^{D^*}\right) R_{i,t} + P^R I_{i,t}, \\
D_{i,t+1} &= D_{i,t} + P^D I_{i,t} + P^{D^*}\left(S_{i,t} + E_{i,t} + I_{i,t} + R_{i,t}\right),
\end{aligned}
$$

where P^I is the share of exposed agents who become infectious each period, given by $P^I = 1/d_a$, and d_a is the average duration an agent spends pre-symptomatic. Following Ash et al., 2022, we set $d_a = 5.2$.

The presence of exposed agents creates a delay in the timing of peak infections and lowers the peak infection rate, though the qualitative results are otherwise similar. To illustrate, we recreate Table 2 for a model including the exposed disease state. Results are shown in Table 12.

Table 12: Peak Infectious and Days Between Peaks for Models with Exposed Disease State

	Peak Infectious - Home (%)		Days Between Peaks	
	$I_{0,H} = I_{0,F}$	$I_{0,H} < I_{0,F}$	$I_{0,H} = I_{0,F}$	$I_{0,H} < I_{0,F}$
Autarky				
No Behavioral Response	12.95	12.95	0	58
Home Isolation	3.14	3.14	0	58
Symmetric Size				
Exogenous Travel	3.24	3.28	0	4
Endogenous Travel	3.19	3.18	0	8
Asymmetric Size				
Exogenous Travel	3.60	3.61	4	4
Endogenous Travel	8.35	8.39	11	11

F.2 Alternative home exposure risk

We consider an alternative formulation for the exposure probability under which susceptible agents do not meet tourists when isolating. Under the alternate specification, (11) is replaced by

$$P_i^E(m_t^S, l_t^S, h_t^S; \mathscr{T}_t) \equiv 1 - \Bigg[\underbrace{\left(\frac{l_t^S}{1-\theta_i} \right)}_{\text{Work share}} \left(1 - \underbrace{\tau \cdot \frac{(I_{i,t} - M_{i,t}^I + M_{j,t}^I)}{N_{i,t}}}_{\text{Home Exposure}} \right)^{\mathscr{C}_{i,t}^l}$$

$$+ \underbrace{\left(\frac{m_t^S}{1-\theta_i} \right)}_{\text{Travel share}} \left(1 - \underbrace{\tau \cdot \frac{(I_{j,t} - M_{j,t}^I + M_{i,t}^I)}{N_{j,t}}}_{\text{Foreign Exposure}} \right)^{\mathscr{C}_{i,t}^m} + \underbrace{\left(\frac{h_t^S}{1-\theta_i} \right)}_{\text{Isolation share}} \left(1 - \underbrace{\tau \cdot \frac{(I_{i,t} - M_{i,t}^I)}{N_{i,t}^*}}_{\text{Home Exposure}} \right)^{\mathscr{C}_{i,t}^h} \Bigg].$$

The relevant i populations become

$$N_{i,t} = \sum_{Z \in \{S,I,R\}} Z_{i,t} - M_{i,t}^Z - H_{i,t}^Z + M_{j,t}^Z, \tag{40}$$

$$N_{i,t}^* = \sum_{Z \in \{S,I,R\}} Z_{i,t} - M_{i,t}^Z, \tag{41}$$

where $H_{i,t}^Z = h_{i,t}^Z Z_{i,t}$ denotes the population isolating. Finally, average consumption (14) becomes

$$C_{i,t}^* \equiv \sum_{Z \in \{S,I,R\}} \left(\underbrace{c_{i,t}^Z \frac{Z_{i,t} - M_{i,t}^Z - H_{i,t}^Z}{N_{i,t}}}_{\text{Consumption by } i \text{ agents}} + \underbrace{\kappa \frac{M_{j,t}^Z}{N_{i,t}}}_{\text{Consumption by } j \text{ agents}} \right).$$

Table 13 recreates the results presented in Section 5.2 under the alternative home exposure risk.

Table 13: Peak Infection and Days Between Peaks for Models with Alternative Home Exposure Risk

	Peak Infectious - Home (%)		Days Between Peaks	
	$I_{0,H} = I_{0,F}$	$I_{0,H} < I_{0,F}$	$I_{0,H} = I_{0,F}$	$I_{0,H} < I_{0,F}$
Autarky				
No Behavioral Response	26.52	26.52	0	24
Home Isolation	7.47	7.47	0	24
Symmetric Size				
Exogenous Travel	9.21	9.36	0	0
Endogenous Travel	8.26	6.94	0	7
Asymmetric Size				
Exogenous Travel	6.93	6.97	2	2
Endogenous Travel	8.45	8.49	7	7

F.3 Solving with the Fischer-Burmeister function

The first order and Kuhn-Tucker conditions for the susceptible problem are

$$\frac{-(1-\beta_i)}{1-\theta_i-m-h} + \frac{\beta_i}{m} + \delta(U^{I'} - U^{S'})\frac{\partial P_i^I}{\partial m} - \mu_m^{hi} = 0, \tag{42}$$

$$\frac{-(1-\beta_i)}{1-\theta_i-m-h} + \delta(U^{I'} - U^{S'})\frac{\partial P_i^I}{\partial h} + \mu_h^{lo} - \mu_h^{hi} = 0, \tag{43}$$

$$\mu_m^{hi}(\bar{m} - m) = 0, \tag{44}$$

$$\mu_h^{lo} h = 0, \tag{45}$$

$$\mu_h^{hi}(\bar{h} - h) = 0. \tag{46}$$

Our solution algorithm solves for the endogenous choices directly using the FOCs. To verify the solution accuracy (especially close to the constraints), we implement an alternate routine which solves the above system of equations and compare results. In particular, we replace (44)-(46) with their equivalent representations using

the Fischer-Burmeister function (see e.g. Maliar, Maliar, and Winant, 2021):

$$\left(\mu_m^{hi} + (\bar{m} - m) - \sqrt{(\mu_m^{hi})^2 + (\bar{m} - m)^2}\right)^2 = 0,$$
$$\left(\mu_h^{lo} + h - \sqrt{(\mu_h^{lo})^2 + h^2}\right)^2 = 0,$$
$$\left(\mu_h^{hi} + (\bar{h} - h) - \sqrt{(\mu_h^{hi})^2 + (\bar{h} - h)^2}\right)^2 = 0.$$

The latter have an advantage in that they are smooth approximations of the Kuhn-Tucker conditions, useful when using a nonlinear solver (especially one which does not allow constraints).

We solve the modified system of equations using the Matlab function fsolve. The two algorithms obtain a maximum difference in the aggregate disease states (share of the population) of 0.0000003.

F.4 Restricted Range on R_0

We confirm the robustness of our results in Section 6 for a restricted range of the reproductive number, R_0. Specifically, we generate one million new parameter combinations (training sample), with $R_0 \in [1.01, 6]$ (the other parameter ranges are left according to the bounds in Table 10). We then train surrogate models on the new (restricted) data. Figure 11 uses these trained surrogates to recreate Figure 3 in the main text under the restricted range on R_0.

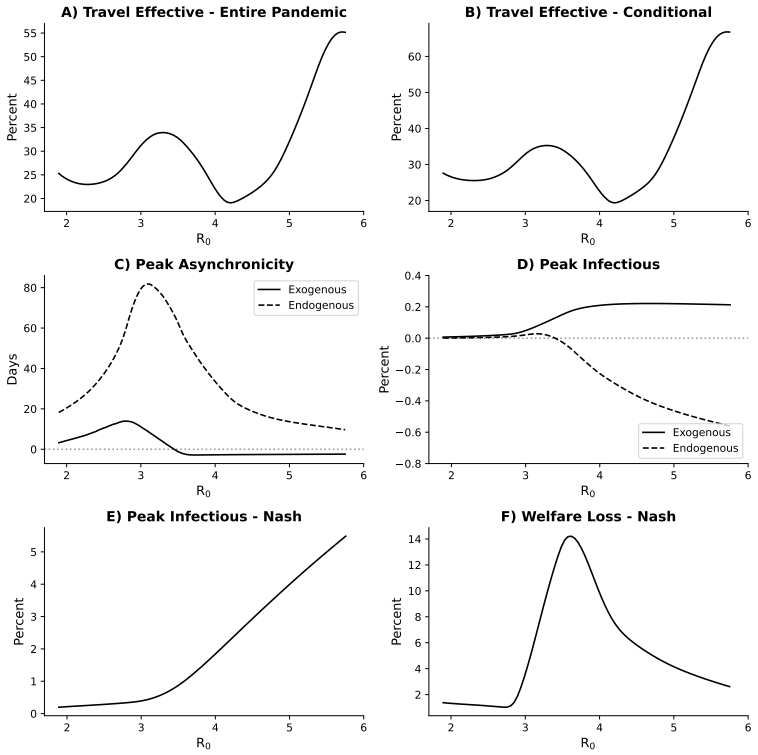

Figure 11: Partial dependence plot of model outcomes (vertical axis) on R_0 (horizontal axis) for $R_0 \in [1.01, 6]$. A) Average percent of days travel is an effective avoidance asset. B) Average percent of days travel is an effective avoidance asset when the infectious population share is above 1%. C) Change in the time between home and foreign peaks from a home isolation autarky model to models with exogenous (solid line) or endogenous (dashed line) travel. D) Percentage point change in peak infectious (percent of population) from a home isolation autarky model to models with exogenous (solid line) or endogenous (dashed line) travel. E) Peak infectious under the 'worst' (aggregate-welfare-minimizing) Prisoner's Dilemma. F) Change in welfare (consumption equivalent units) from the aggregate-welfare-maximizing coordinated solution to the aggregate-welfare-minimizing Prisoner's Dilemma.